NOVEL UWB ANTENNA SYSTEM FOR BREAST CANCER DETECTION

By

Muhammad Zahid Akram

A thesis submitted to the Faculty of Electrical Engineering Department, Military College of Signals, National University of Sciences & Technology, Pakistan in partial fulfillment of the requirements for the degree of MS in Electrical (Telecom)

August, 2022

THESIS ACCEPTANCE CERTIFICATE

Certified that final copy of MS/MPhil thesis written by Mr. **Muhammad Zahid Akram, MSEE-24 Course**, Registration No **NUST00000274218** of **Military College of Signals** has been vetted by undersigned, found complete in all respect as per NUST Statutes/Regulations, is free of plagiarism, errors and mistakes and is accepted as partial, fulfillment for award of MS/MPhil degree. It is further certified that necessary amendments as pointed out by GEC members of the student have been also incorporated in the said thesis.

Signature: _____

Name of Supervisor: Assoc Prof Farooq Ahmed Bhatti, PhD

Date: _____

Signature (HoD): _____

Date: _____

Signature (Dean): _____

Date: _____

ABSTRACT

Breast cancer is an uncontrolled growth of epithelial cells in the breast. It is a 2nd more common cancer in women after lung. Early detection is the only way to combating it and ensuring effective treatment. The examination of any breast pathology should include a "triple assessment": clinical assessment, imaging, and cytology. Mammography X-rays, computed tomography (CT), ultrasound, and MRI are often used as diagnostic tools for detecting breast cancer, but for early cancer diagnosis these devices do not much support. Additionally, various downsides were frequently caused by the aforementioned gadgets. the uncomfortable scanning, ionizing radiation, misleading effects, and false-negative effects, for instance. On the other hand, microwave imaging is a different technique for detecting breast cancer early. Patients now require efficient antennas that deliver improved imaging, diagnosis, and therapy because to advancements in medical research. The suggested research project also offers UWB antennas as a potential remedy for this issue.

The thesis presents a unique ultra-wideband Microstrip Patch antenna system that operates in the C, X, and some portion of S bands, to have an early detection of breast cancer. The cupper ground plane and a slotted loaded over the patch of the microstrip patch antenna will serve as the conducting materials. A FR-4 Lossy with the thickness of 1 mm and dielectric constant 4.3 is used to develop the antenna. A coaxial feed line is selected for the antenna with dimensions of 31x31 mm, that antenna operate in wide range 3.4 GHz to 10 GHz. An innovative ultra-wideband Microstrip Patch antenna is created to operate at frequencies between 3.34 GHz and 10 GHz, to achieve the return losses less than -10 dB at all of the aforementioned frequencies, and with a fractional bandwidth more than 6 GHz. In addition, 4-element antenna array has also been developed. Breast phantom has also been developed and Ground penetrating radar technique has been implemented on the phantom for the detection of the cancer tumor. An excellent result has been achieved using Ground penetrating radar technique.

DEDICATION

Dedicated to my parents, my family and my dear ones for their continuing support and encouragement throughout my master's course work and research.

DECLARATION

No content of work presented in this thesis has been submitted in support of another award of qualification or degree either in this institution or anywhere else.

ACKNOWLEDGEMENT

First of all, I would like to say thanks to my supervisor Associate Professor Dr. Farooq Ahmad Bhatti and co-supervisor madam Maryam Rasool, who helped me and assisted me during my research work. His kindness and encouragements had always been a morale booster whenever I had problems during my research phase. I am impressed by his humble and kind nature. Besides, I would also like to say thanks to my thesis committee members respected Dr Imran Rashid, Dr Adil Masood, and Dr. Zeeshan Zahid.

I can never forget the efforts of my parents and especially my elder brother, Hafiz Muhammad Tahir Akram who brought up me to this stage of my life and without their prayers and support I could never have so much success in my life. I would like to say thanks to all my friends who helped me in my research work and especially to Ghulam Qadir, Iqrar Haider, Sohaib Tariq and Ahsan Javid for their continuous encouragement, motivation, and support.

And above all, Thanks to Allah Almighty for everything.

Table of Contents

List of ACRONYMS

NCBI	International Telecommunication Union
PTA	Pakistan Telecommunication Authority
CST	Computer Simulation Technology
MRI	Magnetic Resonance Imaging
MIMO	Multiple Input Multiple Output
SAR	Specific Absorption Rate
US	Ultrasound
FDTD	Finite-Difference Time-Domain
ISL	Inter Satellite Link
UBW	Ultra-Wide Band
EBG	Electromagnetic Band Gap
DGS	Defective Ground Surface
CT	Computed Tomography
FSS	Frequency Selective Surface
VNA	Vector Network Analyzer
MIST	Imaging through reference body
NBCC	National Breast Cancer Coalition
MPA	Microstrip Patch Antenna

List of Figures

List of Tables

Chapter 1

INTRODUCTION

1.1 Background:

Breast cancer is the most frequent cancer among women, aside from skin and liver cancer. It has turned into a significant concern to women. Breast cancer deaths have increase over the years, Currently Pakistan has the highest prevalence of pancreatic cancer across Asian countries, with one in every nine women at risk of developing the disease throughout their lifespan [1]. As per a recent survey, 40.7 % of Pakistani women wasted their time trying alternative medications, 17.1 % ignored mild lumps, and 10.6 % presented late because they regarded the breast a private organ. The latest study was carried out to assess the function of several risk factors in the development of breast cancer[2]. The average age of cases of breast cancer in the current research was 44.3 years, and most of them have been premenopausal. Cases identified at a younger age showed aggressive clinicopathological traits as well as a distinct biological entity. Obesity was a very well risk factor for the development of breast cancer, especially in postmenopausal women[3].

Cancer is produced by alterations in genes, which have been the basic physical elements of heredity. Genes are organized into chromosomes, which are lengthy strands of closely packed DNA [4]. Tumor is a genetic disease, which means that it is caused by abnormalities in the genes that regulate how our cells behave, particularly how they develop and multiply.

There are two type of breast cancer.

- Invasive ductal carcinoma
- Invasive lobular carcinoma

Each of these diagnostic techniques compliments the others and enhances diagnostic performance when used. Mammography X-rays, CT scan, ultrasonography, and magnetic resonance imaging (MRI) are frequently employed as diagnostic techniques for identifying breast cancer, These approaches have some disadvantages, including false positive and missed detection, due to low-resolution scanning we cannot find-out clear image of tumor, due to high costs mostly women cannot bear its cost of testing and not easy to chase it out , unpleasant compression and ionizing, performance decrease for deep-lying or solid tumors, and a time-consuming diagnostic procedure, because of existing clinical imaging has limitations, a researcher is exploring for alternative techniques to detect breast tumors at an early stage[5]. however, these procedures have a few limitations and undesirable qualities when utilized for early cancer detection. The point is that each approach has certain flaws that make it hard to use from current techniques, therefore we need a novel approach or technique that is highly effective and can help us identify cancer at an early stage [6]. Microwave imaging is one of the simplest techniques for detecting cancer tissue at an early stage; with this approach, we examine the dielectric constant at different frequencies and the body's specific absorption rate SAR. We know that each organ of the body has a different specific absorption rate SAR. Like that, the dielectric constant of each portion of the body is distinct, and each organ, such as the breast, liver, or brain, whatever you want to check has its own dielectric constant of normal tissue and malignant tissue. The microwave imaging technique depend on the dielectric characteristic of the tumor and the healthy tissue around it. The tumor and healthy tissue reflect the microwave frequencies differently that is a concept which we are use in practical method for identifying Malignant cells[7].

We can use a single antenna or array of antenna to send the signals to the specific area of human tissue where the signals are reflected through backscattering and receive by the

array. After receiving the signal, we evaluated it using a suitable computing system to determine the presence of a tumor. To produce high resolution and accurate pictures, compact antennas must be able to emit signals over a large frequency range while retaining waveform fidelity over a wide range of angles in such MWI systems utilizing the ultra-wideband. Dielectric constant of tumor tissue is six time greater than the dielectric constant of a normal tissue; the reason is water abnormal tissue contain more water than the normal tissue [8].

Microwave breast imaging is presently being studied in various methods. The first approach, known as microwave radar scanning, involves illuminating the breast with an ultrawideband (UWB) electromagnetic pulse. The second option is microwave tomography. Unlike microwave radar imaging, tomographic methods employ a narrower frequency range of radiation [7,8].

Early identification has been highlighted as the most significant component in increasing the survival rate to reduce and eliminate this disease. In addition, there is a tremendous need to study dependable, comfortable, and highly successful technological solutions for early breast cancer detection with and without tumor. The proposed study is carried out by designing. Ultra-wideband devices that run from 3.34 GHz to more than,12 GHz.

1.2 Research Methodology:

1.2.1 Motivation:

Globally, breast cancer is becoming one of the leading causes of mortality for women. Over the years, a number of methods for diagnosing breast cancer have been explored, but none have been successful in identifying the right treatment and medicine to remove the breast cancer tumor from the woman. The cause was the early diagnosis of abnormal tissue when it was still very difficult to cure the disease since it had spread to neighboring tissues and body components. Therefore, the only option to deliver a quick and effective

therapy is by early diagnosis of this malignant tissue. The sole method for the early identification of malignant tissue is microwave imaging, which is discussed extensively in literature. Antennas are crucial in this process.

Engineering professionals with an interest in the literature sought to benefit mankind by using the suggested UWB antenna to medical equipment, particularly to the early identification of malignant tissue using microwave imaging techniques.

1.2.2 Problem statement:

There is a lot of data in the literature that highlights the need of identifying malignant tissue in a woman's breast as soon as possible in order to receive the right therapy at the right time and limit the tumor's growth. Different antennas have been designed, and researchers have presented their work, enabling microwave imaging of cancerous tumors. Additionally, we wanted to create a novel antenna for use in microwave imaging of malignant tissue. We developed following problem statement for our MS thesis after doing a thorough literature review:

Novel UWB Antenna System For Breast Cancer Detection

1.2.3 Aims and Objectives:

1.2.3.1 A novel design Microstrip Patch antenna operating at UWB:

A develop a novel design of Ultrawide band antenna that could work in the broad range of 3.3 to 10 GHz is presented. The antennas produce efficient effects with very low losses at many frequencies. For the suggested antenna, a co-axial feeding strategy is selected, which increases the antenna's overall performance [18]. For the frequency range of 3.3 GHz to 10 GHz, the developed antennas provide efficient gain and very low losses and also very comfortable with the patient’s measurements.

1.2.3.2 A novel design Array of antenna operating at UWB:

As a result, this thesis proposes a unique layout of UWB Microstrip Patch antenna for Breast cancer detection that operates at wide band frequencies ranging from simulated 3.14 GHz to 12 GHz and has a high gain and minimal return losses.

After developing the UWB antenna, developed the 4-element array of microstrip patch antenna. All 4-elements works independently in the design, simulated results of antenna array shows that the good return losses, important factor is mutual coupling between antenna, Mutual coupling amongst exceptional antennas demonstrates that at the target frequency, the most issue of S21, S31, and S41 is considerably less than -20 dB, indicating that this antenna array is well-suited for microwave breast imaging [15]. Furthermore, the developed antennas' frequencies are specifically suited to the scientific popular and PTA frequency allocation board for breast cancer diagnosis.

1.2.3.3 Development of Breast Phantom and tumor:

A list of literature is available about the development of the phantom. A realistic model of the phantom has been developing on CST where is equivalent to the theoretical developed phantom. A realistic breast model has been tested using Microwave imaging base on ground penetrating radar imaging. The breast phantom has been embedded with cancer tumor. The electrical permittivity and dielectric constant of phantom and tumor has been verified [7]. A microstrip patch antenna array consisting of four elements of antenna has been developed and used to have detection tumor on the developed phantom.

The results show that there is a strong link between normal and cancerous tissues. Because of the literature, they behave in the same way. As a result, we used those phantoms to compare the results of our antennas with and without malignancies.

1.3 Applications:

Antennas designed at ultra-wide band frequencies can be used for lot of applications due to the better performance of it in adverse conditions.

The main purpose of designing a phased array Microstrip Patch antenna at wideband is a proposal for its usage in Breast Cancer detection because wide band is most important band for tumor detection all over the body. The selected frequencies are highly matched to the NCBI standard and PTA Frequency Allocation Board assigned frequencies for medical application Breast Cancer detection.

Wearable Antenna is one of the most important developing technologies, with multiple uses in fitness, navy, navigation, and recreation. WBAN technologies, particularly wearable antennas, offer low-cost options for remote sensing and monitoring of a variety of physiological data in the human body. While considering the advantages of WBAN and wearable antennas, one should also consider their impact on the human body. Antenna designers must keep in mind the suitable RF generation for wearable systems, while ensuring that electromagnetic immersion in human tissue has the least impact on performance and benefit. Among scientific gadgets and external equipment, antennas with these frequencies can be utilized for radar-based applications and Bio-conversation systems for brief-range biotelemetry applications.

Chapter 2

LITERATURE REVIEW

2.1 Microstrip Patch antenna:

2.1.1 Introduction:

"An antenna is a sensor or transition device that transforms electromagnetically emitted energy to electric signals." A patch antenna is an antenna that is created by etching away a patch of conductive material on a dielectric surface. The dielectric material is put atop a ground plane, which supports the entire system. Excitation to the antenna is also given through feed lines linked through the patch [32]. Because it is made using a microstrip technology on a PCB, it is also known as a Microstrip or printed antenna. Basically, these kinds of antennas are low-profile antennas that are suited for microwave frequency purposes with frequencies larger than 0.100 GHz

In this thesis we have Ultra-wideband antennas accessible in the literature. A common form of printed antenna is the microstrip antenna. As seen in Figure 2.1, a typical microstrip antenna consists metallic conductor surfaces insulating dielectric medium. Typically, one-layer functions as a radiator and the other as a ground. Microstrip technology is becoming increasingly used in metallic devices because to its compactness and compliance.

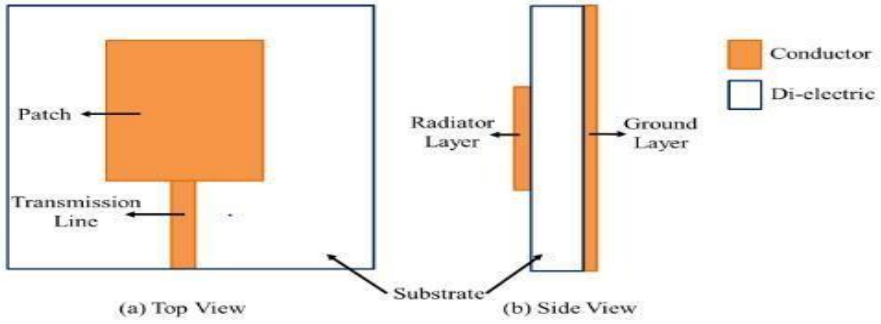

Figure 2.1 Microstrip Patch antenna

The Microstrip Patch antenna has many applications that work in different areas of life, but now the Microstrip Patch antenna will be selected in stages by biomedical scientific processes because of its amazing features. Different shapes of Microstrip Patch antennas are proposed that can be used for detection of anything by using phased arrays [1].

2.2 Microstrip Patch antenna proposed for cancer detection:

In this part, the principal types of Microstrip Patch antennas that well be deployed for Breast Cancer detection in various bands will be given. All the performance criteria of these antennas, including as return loss, gain, radiation qualities, and size, are covered.

2.2.1 UWB Antenna with circular patch for early breast cancer detection

In this paper circular patch antenna is proposed for C and X band for breast cancer detection shown in figure 2.2. It covers 3.1 GHz from C band to 10.2 GHz in X band. FR4 epoxy substrate is used which dielectric permittivity is 4.4 and its loss tangent tan δ is 0.02 and microstrip feeding is used for power up the antenna [9]. The size is 28×37.5 mm^2. We have a maximum gain of 8.28 dB at 2.83 GHz and a gain greater than 3.83 dB over the whole [2.83 - 10.42] GHz band. The results are quite good for biological applications.

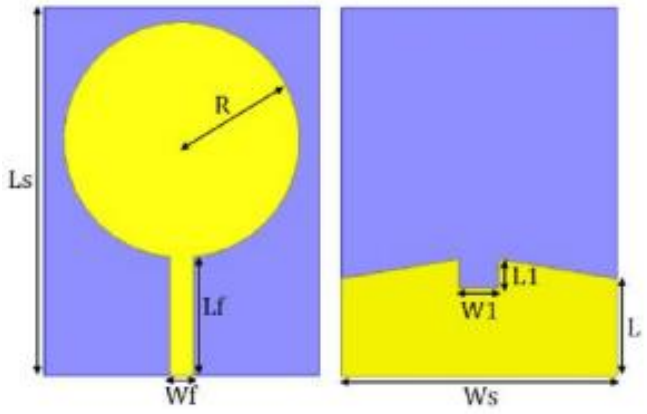

Figure 2.2 UWB antenna with circular patch [9]

2.2.2 Smart UWB Antenna for early Breast Cancer Detection

In this paper smart UWB antenna is design for early stage breast cancer detection shown in figure 2.3. It covers 2.96–10.68 GHz. FR4 with thickness of 1.58 mm substrate is used which dielectric permittivity is 4.3 and the loss tangent tan δ of the substrate is 0.02 [10]. The size is 23×21 mm^2. We have a maximum gain of 4.41 dBi at 11 GHz and a gain is between 1.5 – 4.41 dBi over the whole [2.96 - 10.68] GHz band. , This antenna has a wider impedance spectrum, making it an appealing choice for medical imaging systems used to detect breast cancer. Smart UWB T-shaped patch of the antenna is shown in figure 2.3.

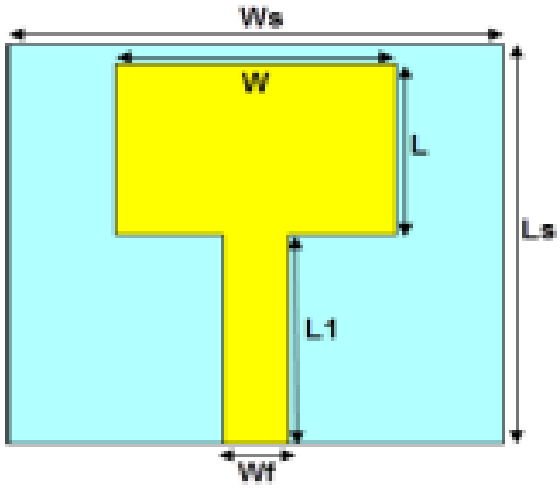

Figure 2.3 Patch of T -shaped Antenna [10]

This antenna had three different grounds mounted on substrate, which are shown in Figure 2.4. It provides maximum return losses 55dB if we used ground shown in figure 24a, 36.5dB if used ground shown in figure 24b and 26.945 dB if used ground shown in figure 2.4c

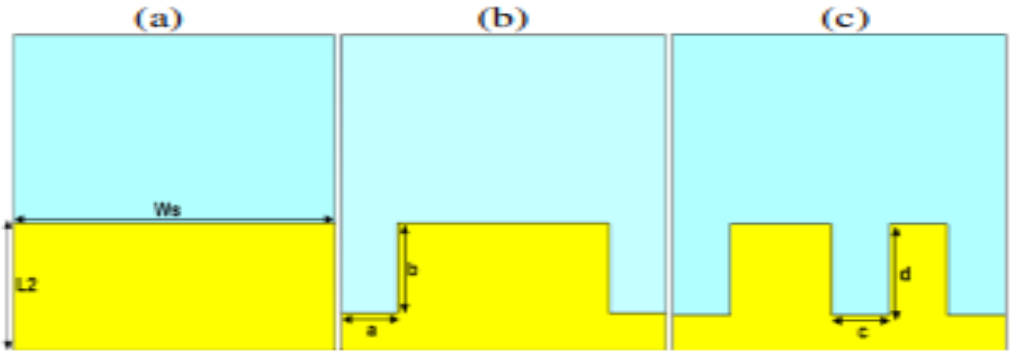

Figure 2.4 T-shaped Microstrip Patch antenna

2.2.3 Breast Tumor Detection System Based on a Compact UWB Antenna Design

The author claims in this study effort to depict a has a square ring shape, with a compact size of 35 mm x 20 mm, ground plane dimensions 8 mm x 20 mm, and a uniform strip width W_f = 1.8 mm giving an impedance matching for 50 Ω and feed the antenna is offset from the center. The antenna is printed on a 1.6 mm thick FR-4 substrate with a relative permittivity r = 4.4 and micro strip feedline used to excite the antenna [11].

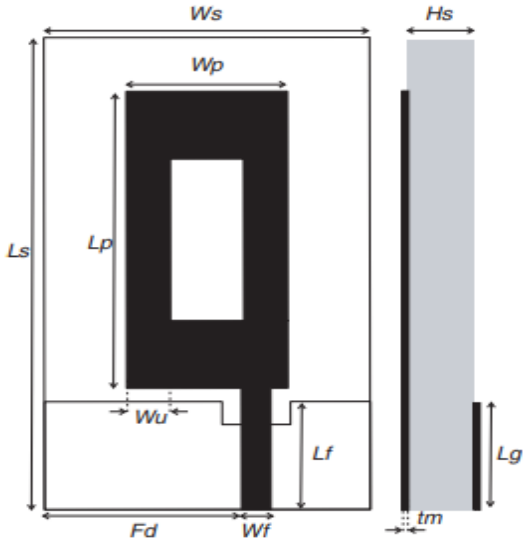

Figure 2.5 Square shape UWB Patch Antenna [11]

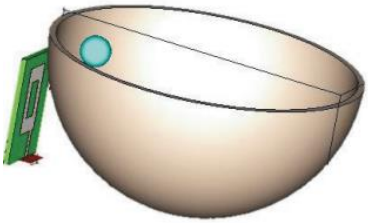

Figure 2.5a antenna place on phantom with tumor

The antenna is designed using CST software. Design provides the return loss of -32 dB and gain of 5.2 dBi for single element [3]. It creates a Heterogeneous breast model with 5 mm tumor of our abnormal breast shown in figure Above.

2.2.4 Novel Ultra-Wideband Directional Antennas for Microwave Breast Cancer Detection

In this research work an elliptical shaped UWB patch antenna with two different design of ground is proposed for Breast Cancer detection [12]. It consists elliptical shaped patch with partial ground as shown in figure 2.6. Width size is 28mm and length is 30mm for single element defected ground plane. The antenna is designed using software of HFSS at solution frequency is 4.2 GHz. Design provides the return loss of -28 dB at 6 GHz

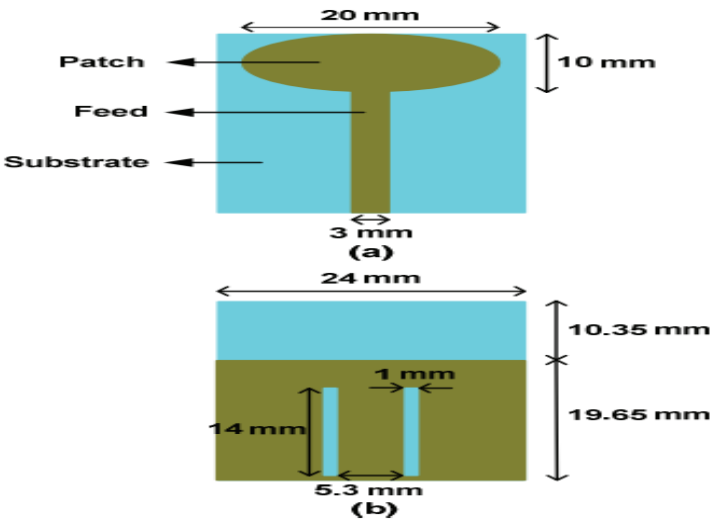

Figure 2.6 Elliptical shaped Patch Antenna and figure a and b show ground [12]

and gain between 7.4 dBi to 8.81dBi for first design and 24 dB at 14 GHz and gain

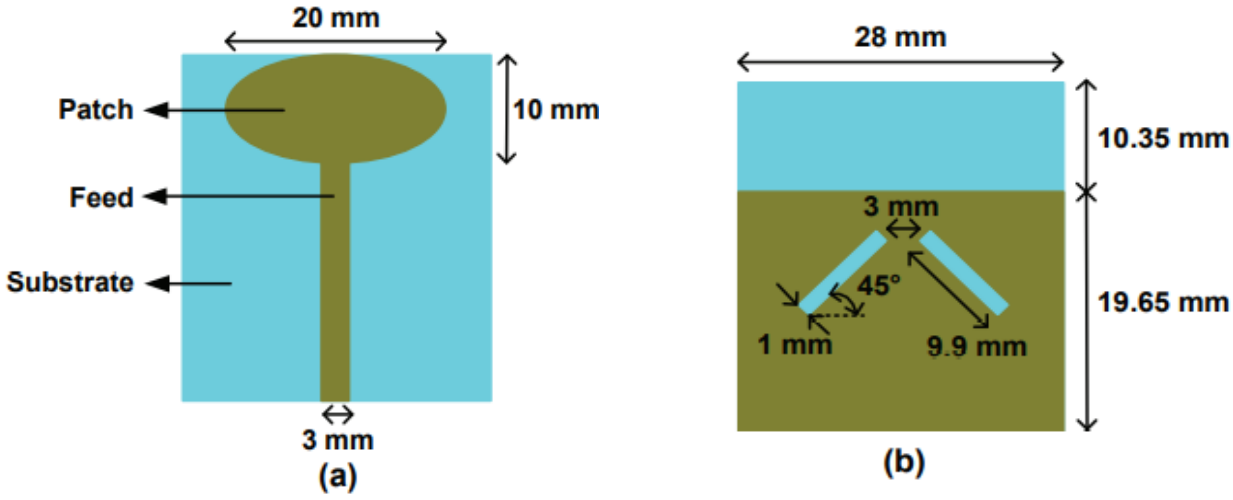

Figure 2.6a Elliptical shaped Patch Antenna and figure a and b show ground [12]

regulates between 7.15 dBi to 9.08 dBi. FR4 substrate is used with a relative permittivity of 3.9 and a thickness of 1.6 mm and micro strip feedline used for the powered the antenna. The author did not make the array of antenna, he just used one single antenna with different ground. Design parameters and all the used parameters are shown in figure 2.6

2.2.5 Directive Low-Band UWB Antenna for In-body Medical Communications:

In this study presents a novel antenna construction. The antenna is designed in the Ultra-wideband (UWB) band, 3.75-4.25 GHz, which was first established in the Body Area Networks (BAN) portion of the IEEE 802.15.6 standard [13]. The antenna is 89 mm60 mm21 mm. The antenna is a directional with a reported gain of 8 dBi at 4 GHz center frequency. The final geometry obtained is shown in figure 2.7.

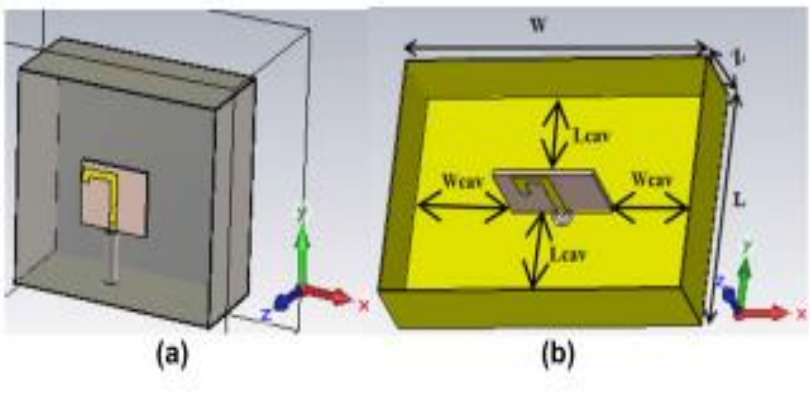

Figure 2.7 Overall view of the low-band UWB antenna in (a) ‘‘Floated’’ and (b) ‘‘Grounded’’ approaches

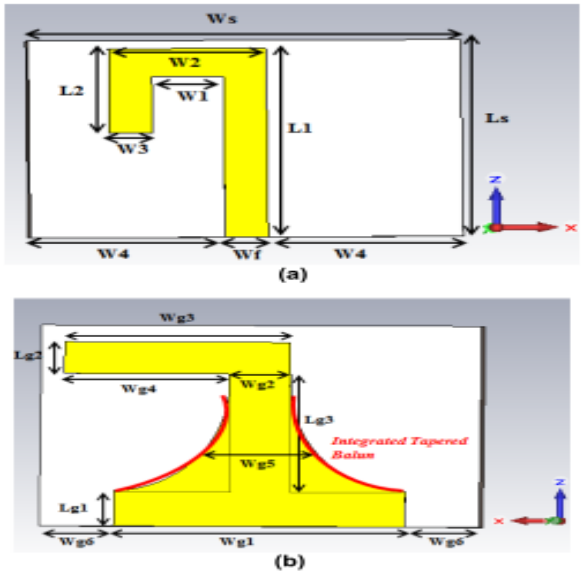

Figure 2.7a. Structure of the ‘‘Grounded’’ UWB antenna in (a) Front and (b) Back views [13]

This is the multilayer model, which is low ultra- wideband and gives us low gain of antenna and reflection coefficient is start from 3.72 GHz frequency to 4.5 GHz. Antenna design provides the gain of 7.2 dBi and 7.22 dBi at these frequencies.

2.2.6 Wearable Microstrip Patch Ultra-Wide Band Antenna for Breast Cancer Detection:

The proposed design antenna is novel, and the ultra-wideband antenna is made of microstrip and has an increased bandwidth design for application in breast cancer diagnosis. Its size is 30mm x 36mm x 1.6mm and 100% pure cotton is used for it. Design

of antenna is shown in figure 2.8-1 (a), (b), (c), (d).

The antenna gives the best performance when you used pure cotton. Here is the reflection coefficient of different substrate used in design like other than pure cotton with permittivity is 1.6 F/m and height is 1.6 mm is panama fabric with permittivity 2.2 F/m and width is 1.6mm Fleece with permittivity 2.22 F/m and height is 1.524 mm and Dacron with 3 F/m permittivity and height of substrate is 1.524 mm. S1,1 shown in Figure 2.8a below.

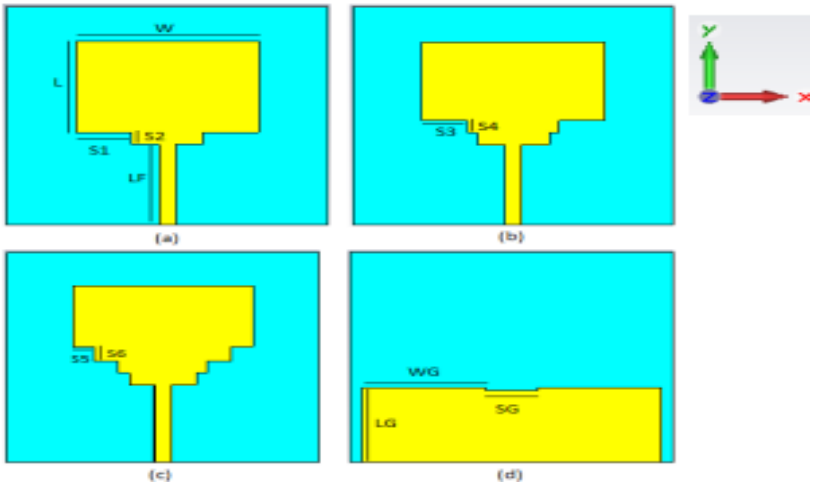

Figure 2.8 Geometry of the proposed antenna **(a)** Structure 1, **(b)** Structure 2, **(c)** Structure 3, **(d)** Ground plane is the same for all structures [14]

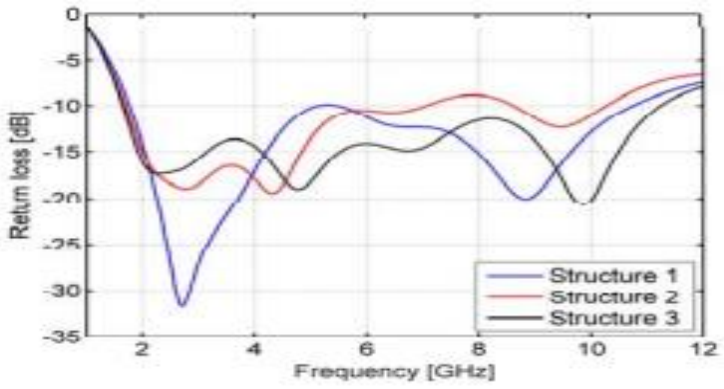

Figure 2.8a Simulated return loss of the various structures

2.2.7 A Compact Flexible UWB Antenna for Biomedical Applications: Especially for Breast Cancer Detection

In this paper author tell us that the best way to detect the Breast cancer tissue is UWB antenna. The design of UWB antennas for biomedical applications is a thrilling venture that needs more observe to enhance the health care machine.

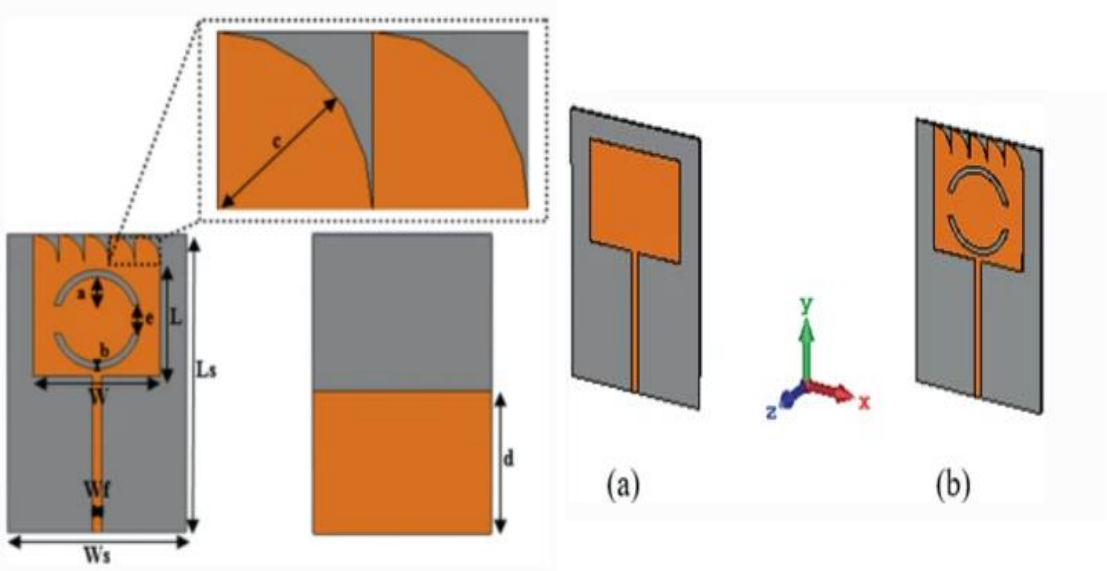

Figure 2.9. Comparison of simple rectangular shape and arc cut shape rectangular antenna [15]

This work presents a UWB antenna published on a flexible substrate with a thickness of 0.254 mm and a relative permittivity of r = 2.2 that operates in the 3.64–12.11 GHz frequency band. Gain of that antenna is vary from 1dBi to 6dBi [15].

The size of antenna is much not bigger. Return losses -10dB are start from 4.3 GHz for structure A and ends in 13.5 GHz and return losses for sturcture B is starts from 3.9 GHz to 12 GHz. The Author invastigates radiation petterns and returns losses of the antenna to find out the tumor tissue in normal tissue.

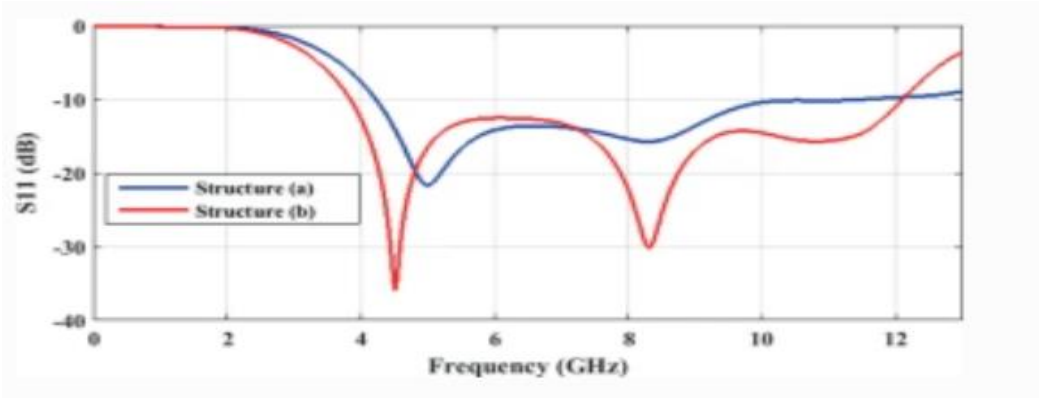

Figure 2.9a Return Loss comparison of two patches

The antenna gives good results using CST software. It provides better gain at given frequencies. Cut in patch technique is used to improve the results like return losses.

2.2.8 Design of Ultra-Wideband MIMO Antenna for Breast Tumor Detection

In this research paper the researcher explains his work regarding cancer detection through antenna. His antenna is used in ultra-wideband microwave imaging systems intended for the early detection of breast cancer. FR-4 substrate with relative permittivity 4.4 and thickness of 1 mm used for printed antenna on it. The antenna is made to function in the air's ultra-wideband frequency band. He makes MIMO of antenna. His antenna operates at frequency from 2.3 GHz to 12.2 GHz. The shape of antenna is circle [16]. Author claim that his antenna works well and provide better results. Gain of that antenna is vary from 1dBi to 4.5dBi. The size of antenna is 70 x 35 mm^2. CST software used for the simulate the results.

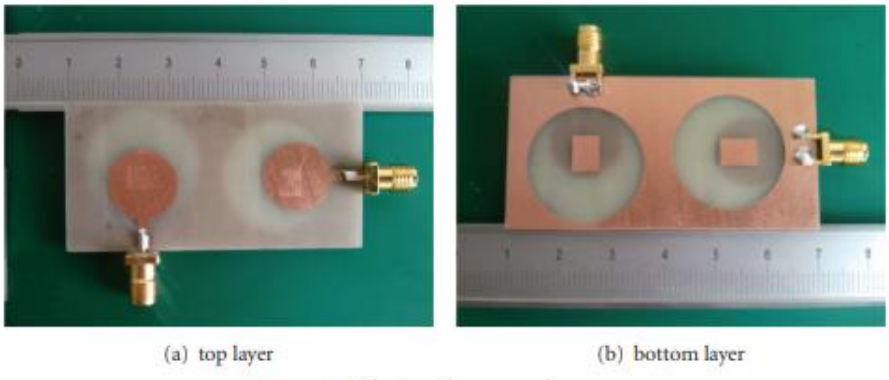

Figure 2.10. Fabricated proposed antenna [16]

2.2.9 Directive Tumor Detection via Specific Absorption Rate Technique Using Ultra-Wideband Antenna

The author of this paper used low gain ultra-huge band (UWB) projector array antenna for human breast most cancers detection in a microwave detection system the use of the unique absorption rate (SAR) method [17]. The addition of a copper reflector at an ultimate distance allows to boom the meant antenna benefit. An excessive gain antenna is required in HMD (human microwave detection) structures to penetrate multilayer structures by increasing the focus of electromagnetic radiation into the target shape.

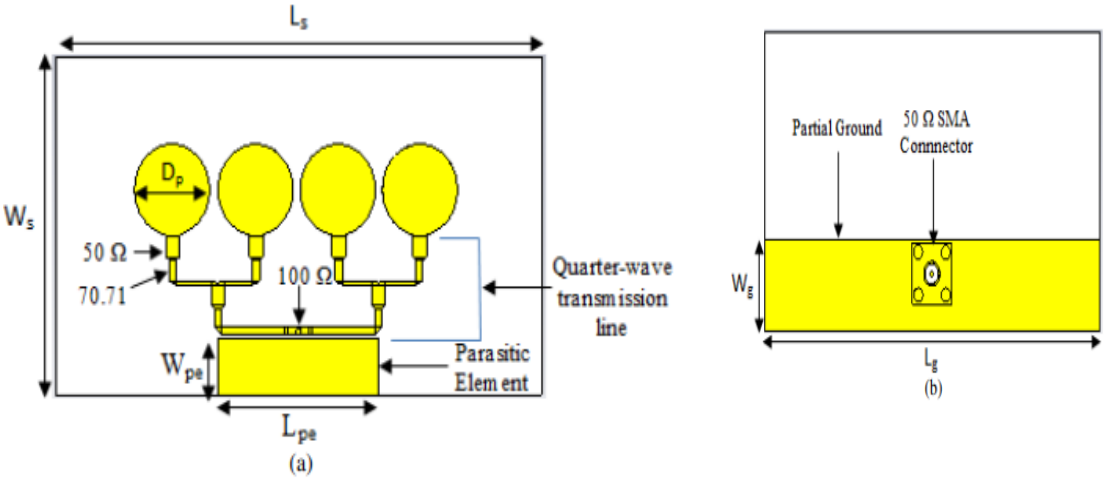

Frequency range without reflector is 2.2 GHz to 10.8 GHz and gain vary from 2.1dBi to

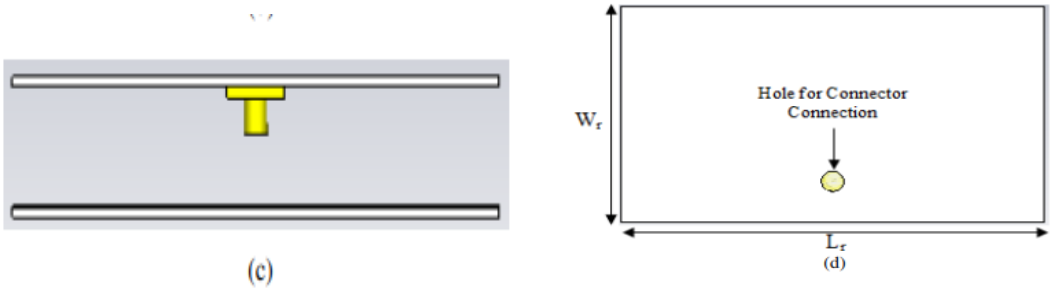

10.2dBi throughout frequency, frequency range with reflector starts from 1.8 GHz to 10.4 GHz and gain vary from 3.2dBi to 14.1dBi.

Fig 2.11 The simulated geometry of the proposed UWB array antenna, **a)** front view, **b)** transparent back view (without reflector) **c)** top view **d)** back view [17]

For powering up antenna the researcher used coxial feed. You can see it in figure and he makes array of it with different reference impedance of 50 ohm and 70.71 ohm and 100 ohm.

2.3 Comparison

The main task of proposed antenna for Breast Cancer detection or any other application of C band communication is that you must maintain efficient gain and minimum losses. For this purpose, different design engineers design different shape antennas to obtain efficient results. Moreover, different techniques are used for the enhancement of gain to fulfill the criteria of satellite communication. That's why I have chosen different research papers in my literature survey for the implementation of any appropriate technique for the improvement of gain and efficient shape for the design of antenna. Comparison of the different techniques used in different research papers for the improvement of gain and many other required parameters are discussed in table 2.1. Table shows the comparison of gain and return losses of the proposed Microstrip Patch antennas used for satellite communication.

2.4 Development of Breast Phantom:

The first request for detection of tumor is phantom which is used for cancer detection. Breast phantom is constructed for the detection of the tumor in female body. That's phantom has properties nearly equal to the real tissues. In this way we can checked our antenna by place it on phantom. We need to construct the two types of phantoms; first type is made of normal or ideal tissue and second phantom is consist of tumor tissues. First, we need to know how to create a realistic breast model. A realistic model is one that is accurate in terms of containing relevant tissues, is physically dependent to resemble true breast architecture, and has tissue attributes that match those measured on actual tissue samples.

Table 2.1 Comparison of gain, return loss and techniques used in proposed Patch Antennas

Sr No	Name of Paper	Substrate /Heigth	Operating Freq. (GHz)	Size (in mm)	Return Loss (S11)	Gain (in dBi)	Feeding	Array /MIMO
1	UWB circular patch [4]	FR4 epoxy substrate /1.6	3.1 - 10.3	28×37.5	< -35 dB	3.82 - 8.28	Microstrip feed	No
2	Smart UWB antenna [5]	FR4 epoxy substrate /1.6	2.96-10.68	23×21	< -36 dB	1.5 - 4.41	Microstrip feed	No
3	Compact UWB Antenna [6]	FR4 epoxy substrate /1.6	3.3-11	35×20	< -32 dB	2.5 - 5.2	Microstrip feed	No
4	UWB Directional Antennas [7]	FR4 epoxy substrate /1.6	3.9-14.4	28x30	< -24 dB	7.15-9.08	Microstrip feed	No
5	UWB Directive Low-Band [8]	FR4 epoxy substrate /1.6	3.72-4.25	89x60	<-34 dB	7.22-8	Microstrip feed	Array
6	Wearable UWB Antenna for cancer detection [9]	pure cotton/1.6	1.6-11.2	30x36	< -34	6.72	Microstrip feed	No
7	A Compact flexible UWB antenna [10]	Roger/ 0.254	3.64-12.11	33x36	<-36	1-6	Microstrip feed	No
8	UWB MIMO antenna [11]	FR4 epoxy substrate /1	2.25-12.5	70x35	< -30 dB	1-4.5	Microstrip feed	MIMO
9	UWB Directive Tumor Detection [12]	Taconic (TLY-5)/1.5748	2.2-10.8	10x15	< -46 dB	3.2-14.1	Coxial feed	Array

Their electrical property are highlighted in Chapter 4. Breast phantoms today have a lot of limitations. This work's phantom blends the flexibility of a mathematical phantom with practical anatomy based on real human data.

Several research institutions throughout the world were researching on tissue-mimicking materials for breast phantoms, looking at simple oil-in-gelatin combinations as well as more complex chemical compositions, maybe for three-D printing. A mixture of gelatin, water, grape seed oil, propylene glycol, and commercial dishwashing solutions, for example, was measured at 1 to 4 GHz. If you wish to replicate low-density (i.e., fatty) tissues, try a mixture of propylene glycol, water, gelatin, grape seed oil, industrial dishwashing liquid, formalin, and glyoxal or glutaraldehyde [37]. They developed an exceptional composition of agar, vegetable oil, dishwashing liquid, and corn-flour for excessive-density tissues, on the other hand. To imitate the dielectric properties of human breast tissues up to twenty GHz, the author recommended combinations consisting of different percentages of kerosene and safflower oil. Unique chances of p-toluic acid, n-propanol, deionized water, 200 Bloom gelatin, formaldehyde, oil, and detergent have been employed to simulate fat, gland, skin, and cancer tissues, and they have been described between 1 and 6 GHz, according to this research. In addition, certain solutions based on 3-D printing generation have been offered [22].

This novel phantom might also be a useful tool for breast imaging researchers to optimize and improve outstanding imaging tactics, as well as to analyses and compare the clinical performance of various breast imaging modalities. The first guidance to address the creation of precise tissue phantoms using the UWB microwave band is the first guide to discuss the creation of accurate tissue phantoms using the UWB microwave band. Because early exams cannot be performed on human participants, a completely realistic breast model is required for microwave imaging evaluation studies. Several oil-in-gelatin combinations are used to simulate dispersive dielectric properties in a variety of human tissues in this picture. From 500 MHz to 20 GHz, the relative permittivity and permeability of combinations formed in 10% increments in oil extent are measured.

The tests were carried out with the help of a vector network analyzer and a closed hardened metal porous ceramic coaxial probe. For every measurement, the probe is immediately put on the phantom region at room temperature. Three measurements are averaged for each phantom. Changing the percent quantity of oil in the mixture can change the dielectric properties of the phantom in a way that makes sense to any tissue type. It can be seen that an 80 % oil phantom practically matches the chosen characteristics for fats, whereas a 25 % oil phantom intensively mirrors the favored habitats for skin by correlating with the Cole-Cole models of genuine tissue measures presented in [19].It's also worth mentioning that a 10% oil aggregation closely reflects the electrical properties of malignant tissue. The recipe and procedures for manufacturing the phantoms are given in [18].

For several reasons, the conclusions of this investigation are broad. A technique for producing realistic permittivity and conductivity tissue phantoms across a broad frequency range has been disclosed. However, what sets this piece apart is that the phantoms are made entirely of low-cost additives and are simple to build. The phantoms solidify with time and may be left in contact with one another without losing their dielectric properties, allowing for heterogeneous phantoms. These discoveries enable the use of real-life breast phantoms to study dielectric properties and shape.

In another paper, the researcher adapts the phantom mixes and suggests a method for producing a dielectrically and physiologically realistic homogeneous breast model. Phantoms for cancers, epidermis, glandular, and fat are mixed with different percentages of oil, such as 10, 20, 30, and so on [27]. The tissue phantom homes are measured using a dielectric probe linked to a VNA throughout a frequency range of 50 MHz to 13.51 GHz. For each phantom, measurements were taken and averaged. Despite the fact that no mathematical comparisons are performed, the dielectric homes of the four mixes are believed to be quite similar to those of genuine tissues. Aside from four phantom compositions, [20] also provides a method for creating a geometrically accurate entire breast

model. To begin, place a liquid skin phantom in a 4.2" diameter pan and squeeze it with a narrower 4" diameter bowl to create a hemispherical replica. Once the pores and skin have hardened, the smaller dish is removed, and liquid fats are injected into the pores and skin. Currently, a cover with cylindrical rods linked is affixed to the top of the bowl, forcing the fats to solidify and develop holes. A syringe is then used to inject the tumor or gland mixture, or each, into the holes. The pores and skin, lipids, and glands of this breast variant are illustrated in this shot [28].

second, it's nice Plastic is used to create an amazing more realistically molded breast model since it is a malleable material with good electrical qualities. pleasant It's not a long hemispheric sphere since it's been shaped into the shape of a breast. The complete model may then be produced in the same way as the hemispheric case after the breast cast has been grown. pleasant Plastic, on the other hand, has the benefit of being able to be used to build glandular systems of any shape or size, perhaps resulting in glands that are more reasonable. The smallest realistic model is 106 x 90 mm, while the largest is 130 x 108 mm. Skin thickness ranges from 2.4 mm to 2.9 mm. Overall, this study demonstrates remarkable progress in the development of realistic breast models. It allows the four tissue phantom types to be combined into a single version. Engineers may also choose the size and density of the gland tissue. Making skin-like fabric that is only a few millimeters thick is tough, but it would result in a more realistic-looking breast phantom. A homogeneous breast phantom inside a tumor inner was created by a researcher in [19, 29, 30]. The sodium chloride (NaCl), distilled water, xanthan gum, polyethene powder, agar powder, and sodium dehydratase monohydrate were all utilized to enhance the phantom's size. The key chemicals that affect the phantom's dielectric steady are NaCl, agar, and distilled water in this case. Because agar powder is a jelly, it keeps the phantom's shape.

2.5 Important parameter of antennas

Gain, bandwidth, radiation pattern, beamwidth, polarization, and impedance are important antenna properties. The antenna sample is the antenna's response to a plane wave that is incident on it from a certain direction or the relative power density of the wave that the antenna transmits in that direction.

Base on the literature survey we are going to study different technique to develop the purpose antenna. We have to focus on size reduction of the patch antenna because of its application for the biomedical side and secondly the we are focus to construct the ultrawide band which is suitable for the medical application and this get the ultrawide band frequency size become larger, so size reduction of the antenna is very important. So the different technique on the base of the literature we have used for the reduction of the patch of the antenna and secondly for further reducing the size of the patch and to optimized the required frequency of ultrawide band we have used the DGS on the ground so that we can achieve the required frequency [31].

Having comfort used for the antenna over location we used coaxial feed structure so that the patient must be comfortable when we go for the real scenario when we do the measurement and try to achieve the depth of the tumor in the breast. So, for that purpose we have used the coaxial feed for excite the antenna.

Chapter 3

UWB MICROSTRIP PATCH ANTENNA FOR EARLY STAGE OF CANCER DETECTION

In this chapter, extremely wideband design and analysis A patch antenna in the shape of an oval is available. Similarly, Antenna-1, Antenna-2, Antenna-3, and Antenna-4 are assigned to each of the remaining three antennas at the frequencies utilized in extremely wideband. For breast cancer detection, all antennas 1 to 4 are used, and they all operate on the same frequency, which is 3.12 GHz to 12 GHz. The antenna design process is broken down into three basic stages. The single detail Microstrip Patch antenna is designed at the first stage. The edges notching strategy is used in the second step to improve gain. The third level is array design, with the primary goal of meeting the requirements of the phased array technique proposed for tumor detection in human body.

3.1 UWB Microstrip Patch Antenna

3.1.1 Selection of material

Base on literature, before developing the model of the purposed antenna, we study different author research paper, what type of material we can used for this type of antenna and fabricating of it. One option is the fabricates of antenna on some cloth like jeans, but in sort of its not much successful in medical science, because cloth becomes wet, easily catches by fire in this way its antenna performance will reduced but people are trying to make it on cloth.

The design procedure began with the selection of FR4 as the dielectric substrate with a dielectric consistency of 4.3. Because of its inexpensive cost, FR-4 with a height of 1.0 mm was employed. FR-4 has the potential to be a very low-cost substrate with no commercial issues [8]. The goal of those antennas is to get normal higher results for breast cancer diagnosis in accordance with NCBI popular while keeping antenna dimensions in a regular range.

Following Microstrip Patch novel the strategy on the design Microstrip Patch antennas are proposed in this research work: for the detection of cancer in human body, radar system and security-based system and many more.

3.1.2 Analytical Design of Antenna:

Whenever you go for design any kind of antenna you must have knowledge for that equations. In this way it's easy to know that what is the size of antenna for particular frequency.

Patch Radius = a = $= \frac{F}{\sqrt{\left\{1+\frac{2h}{\pi\varepsilon_r F}\left[ln\left(\frac{\pi F}{2h}\right)+1.7726\right]\right\}}}$

$$F = \frac{8.791\times10^9}{f_r\times\sqrt{\varepsilon_r}}$$

Patch Width = W= $\frac{1}{2f\left(\sqrt{\varepsilon_0\mu_0}\right)}\times\sqrt{\frac{2}{\varepsilon_r+1}}$

Patch Length Extension = (ΔL) = $0.412h\times\frac{\left(\varepsilon_{reff}+0.3\right)\times\left(\frac{W}{h}+0.264\right)}{\left(\varepsilon_{reff}-0.258\right)\times\left(\frac{W}{h}+0.8\right)}$

Patch Length (L) = $\left(\frac{1}{2f\sqrt{\varepsilon_{reff}}\times\sqrt{\varepsilon_0\mu_0}}\right)-2\Delta L$

Effective Patch Length = Le = L+$2\Delta L$

Location of coaxial feed line:

By using this equation, we can find-out the location of coaxial feed line, Here X_f will tell us the location of feed on x-axis and Y_f will tell the location of feed at y-axis.

$$X_f = \frac{L}{\sqrt{\varepsilon_{eff}}} \qquad\qquad Y_f = \frac{w}{2}$$

W = width of the patch antenna

L = length of the patch antenna

f_0 = resonance frequency

c = speed of light

Ɛr = dielectric constant of the substrate

Leff = effective length

ΔL = length extension

h = thickness of the substrate

Ɛeff = effective dielectric constant of the substrate

3.1.3 Basic Structure

The idea of novel design Microstrip patch antenna is the aim of thesis and it not very difficult to achieve this Microstrip Patch structure. Take two circular patches and place is one circle patch antenna over second circle join them and then reshape it to make is oval. I think you have to put in your mind is that when you go for reshaped any design you can scale only to axis that is x, y axis or you can change only one axis either x axis or y axis. After that I draw an adjust rectangular shaped patch that is slightly smaller than then radius of the circle. Assign a coaxial feed line to the Microstrip Patch. It is simple Microstrip Patch antenna as shown in figure in 3.1

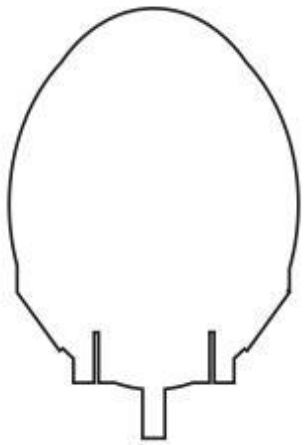

Figure 3.1 Basic Structure of microstrip patch Antenna in Stage 1 of design Process

That Microstrip Patch antenna consists of four different elements, radiating patch,

substrate, ground plane and transmission feed. The design of Microstrip Patch antenna starts with the selection of the shape of radiating patch and the transmission line feed structure. Rectangular patch is selected as radiating element of Microstrip Patch and its size is 31 mm x 31 mm and the band it covers is 3.2 GHz to 12 GHz of frequencies.

The antennas are fed by coaxial feed. The radius of circles for coaxial feed is 0.7 mm radius for inner circle, the radius of outer circle is 2.4 mm and isolation between both circle by donut who inner radius is start is 0.7 which is equal to the radius of feed and outer radius is 2.3mm, you have to design coaxial feed like that its impedance matched to 50-ohm. The Figure 3.1 depicts the antenna's essential structure at this stage. Figure 3.2 depicts level 1 of a simulated Microstrip Patch antenna with a single detail utilizing CST.

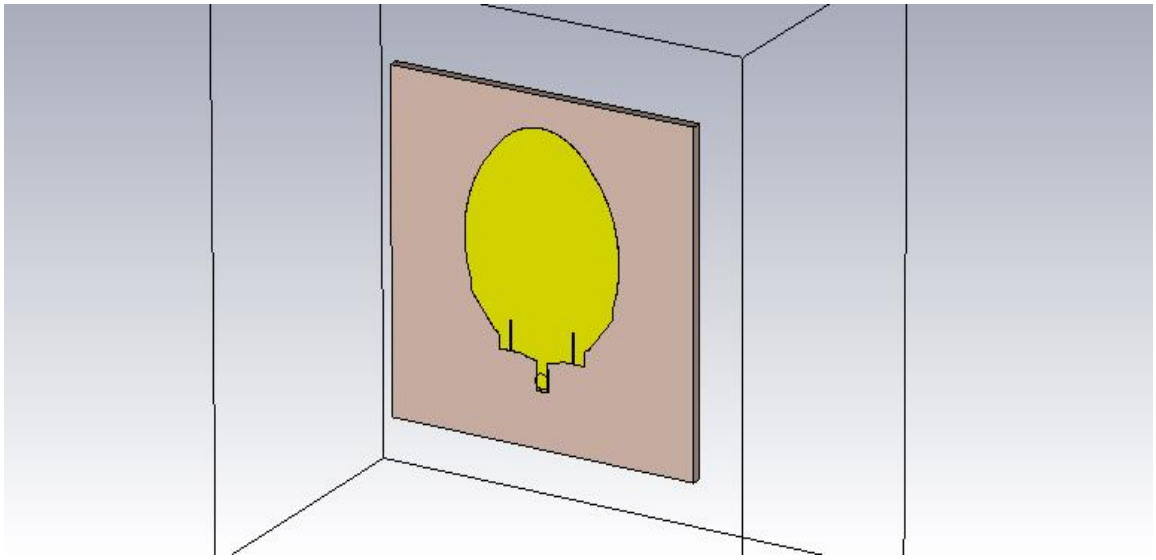

Figure 3.2 Microstrip Patch Antenna model without Notched edges (Simulated)

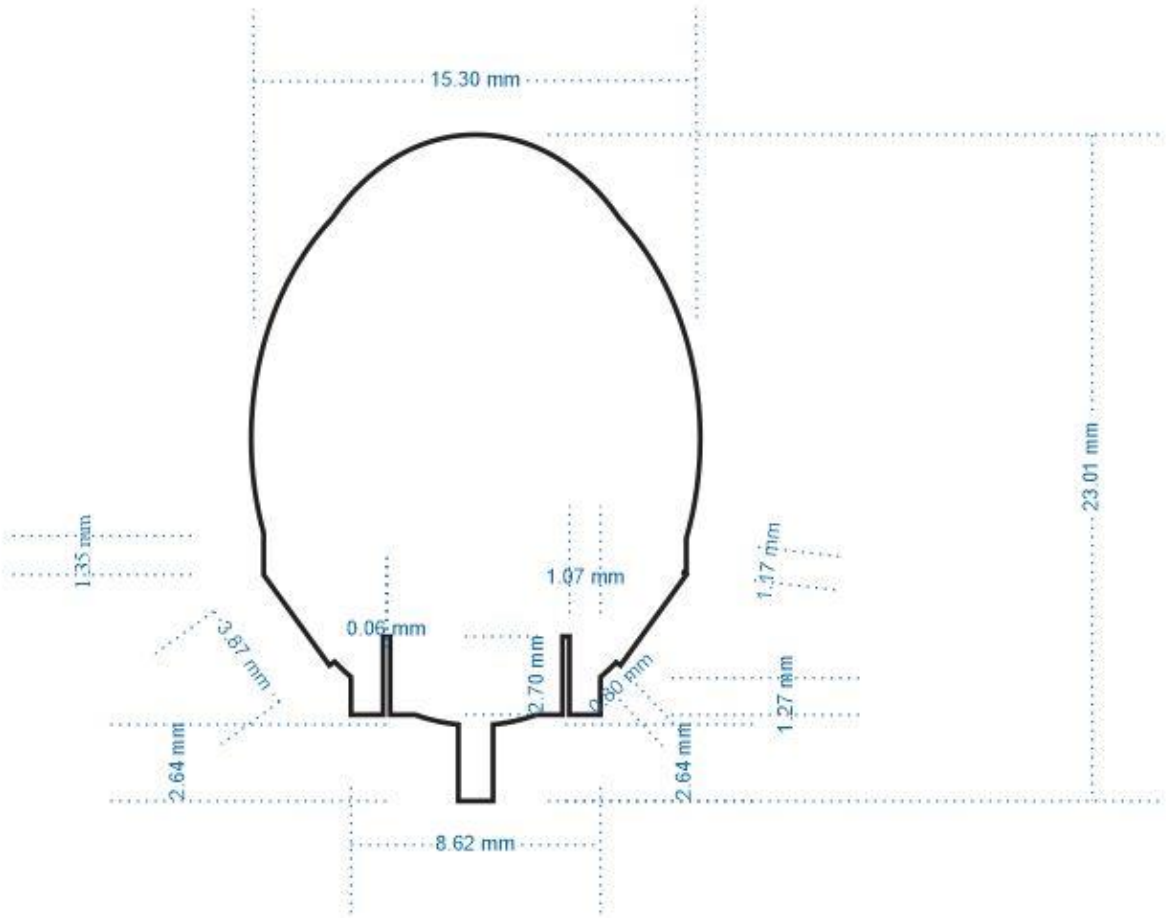

Figure 3.3 dimensions of antenna

3.1.4 Notching Technique:

This strategy is essentially based on the concept of imposing notches of varying sizes at specific spots in an antenna's configuration. The straightforward rationale for using this notching strategy is to improve particular factors such as go back losses, gain, and radiation sample. This approach is used by the majority of UWB antennas to provide extraordinarily broad bandwidth [18]. Notches can be constructed at unusual positions on an antenna patch based on the layout and specifications, however notches towards the edges are beneficial for increasing gain [20].

One of the researchers used a notching approach for a UWB MIMO antenna to get the best of both worlds: maximal UWB and stepped forward gain [21]. To achieve exceptionally broad band and precise isolation, most UWB antenna designers adopted the notching approach. This method is especially beneficial in UWB antennas and UWB MIMO antennas [22].

The notch strategy not only improves effects but also provides more bands for communication. [19] provides an examination of all notching strategies and improvements in outcomes.

3.1.5 Feeding technique:

There are two types of feeding procedures. Contact is the primary option, and non-contact is the secondary [4]. Feeding techniques are classified into four types: coaxial probe, microstrip line, aperture coupled, and proximity coupled. The feeding mechanism used for a Microstrip Patch antenna is crucial because it effects the bandwidth, S_{11}, VSWR, patch size, radiation performance, and impedance matching.

The best directivity is provided by an inset fed antenna, while the lowest is provided by a co-axial fed antenna. The aperture antenna has a moderate directivity. Because of their high directivity, inset fed antennas can be employed as a coupler in MRI packages for long-distance communications.

To meet the utility's standards, the antenna length is kept if possible, for the lower frequency band. To reduce the size of the antenna, several difficulties for antenna architecture were employed, such as employing dielectric substrates with high permittivity and resistive or reactive loading. By adjusting the antenna's shape, the electric period may be increased. Using strategically placed notches on the patch antenna Patch antennas were made shorter by embedding various forms of slots and slits.

For better results you need to exactly equal impedance matching between antenna and port, which is 50 ohms. If you did not match exactly then simulated and measured results did not the same. Its means when you design antenna with other then 50 ohms although you get the simulated desire result but when go for measure result its very much different from simulated results. Here are you can see the comparison between the different feedline.

Type of Feeding	Spurious feed radiation	Reliability	Ease of Fabrication	Impedance matching	Bandwidth
Coaxial Probe Feed	More	Low	Soldering and Drilling required	Easy	2-5%
Microstrip Line Feed	More	Better	Easy	Easy	2-5%
Aperture Coupled Feed	Less	Good	Alignment required	Easy	21%
Proximity Coupled Feed	Minimum	Good	Alignment required	Easy	13%

Table 3.1 Comparison table of feedlines

3.1.6 Notched Edges Microstrip Patch antenna:

Exclusive solutions for shifting the S11 parameter and increasing the antenna's gain can be used, as previously stated in section 2.3. One of them is the process of notching the edges. It is necessary to remember that the gain of the proposed antenna is the most important characteristic, which is why this notching area technique is used in the initial layout stage. After designing the patch, we can increase the antenna gain by employing unique tactics but using the notching area approach in the pattern will be the icing on the cake. Because the size of notching differs for different antennas, it may be stated in the next step of the parametric values conversation.

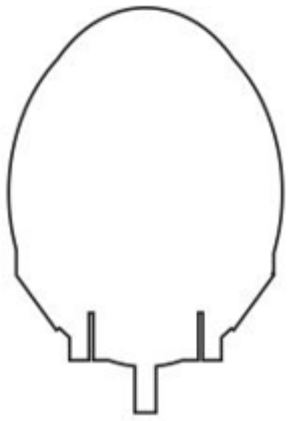

Figure 3.4 Antenna model with Notched edges in Stage 2 of design Process.

Simulated Notched edges Microstrip Patch antenna using CST software is shown in figure 3.4

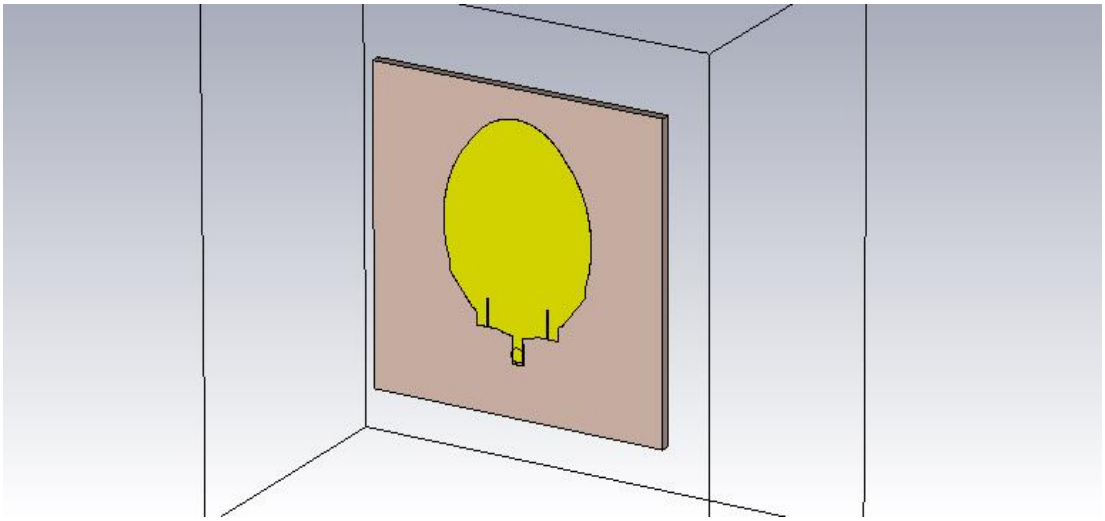

Figure 3.5 Microstrip patch Antenna with Notched edges (Simulated)

3.1.7 Parametric analysis:

3.1.7.1 Impact of the radius of circular patch:

To maximize the radius of a round patch, it has been discovered that increasing the round patch's value results in the lowest resonance frequency. Even when you move the circle upward and downward, you can see the major different in results. S_{11} move from there ideal position to the backward in this way band width reduced. As a result, at the resonant frequency and bandwidth, this factor has the greatest influence.

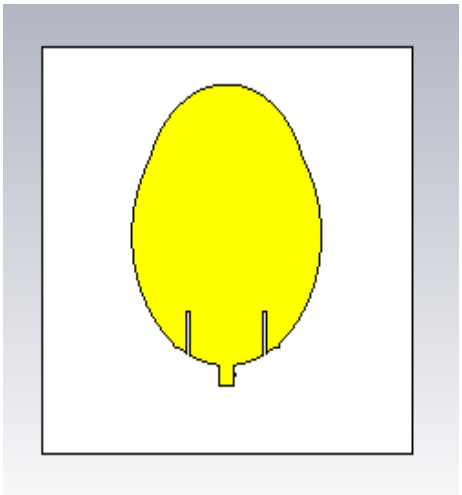

Figure 3.5a MPA with circle moves downward

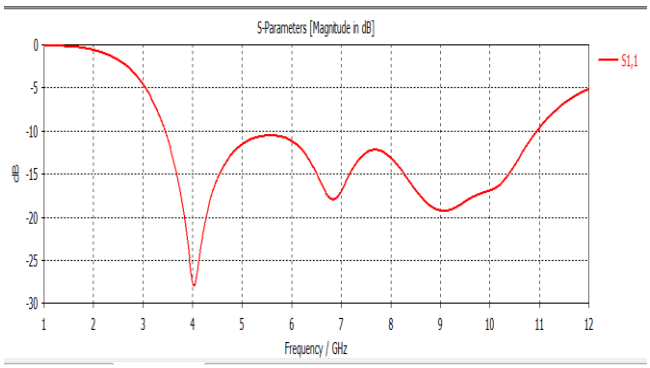

Figure 3.5b S_{11} of microstrip antenna without notched edges

After moving circle downward, you can see what happed with S_{11}, S_{11} peak is reduced. Although when we move circle move upward then we see the same distortion in S_{11}. You can see in figure 3.5(a) and 3.5(b). As a consequence, this strategy is highly advantageous in terms of increasing profits. This method satisfies the low gain antenna's advised criterion for detecting cancerous tumors.

3.1.7.2 Impact of the cuts in Patch on results:

This demonstrates that slotted patch antenna scale reduction is greater than slotted floor plane patch scale reduction. Furthermore, when the slot width grows wider, the resonant frequency shifts to the lower frequency side. Most GPSs employ a patch antenna. They don't have to be square; they may be polarized in a circular shape as well. A slot antenna is an antenna made of a hollow in a flat piece of metal or a different conductor. In that it has a complimentary model, it's similar to a dipole. You can see the effect of cuts in figure.

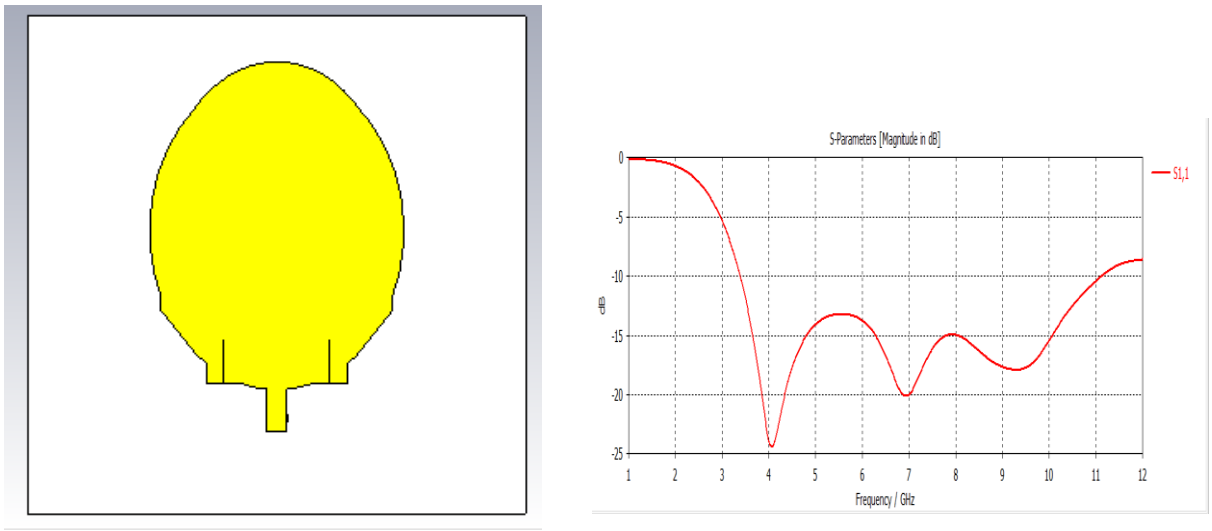

Figure 3.6 Microstrip patch antenna with cut in patch

3.1.7.3 Impact of the defected ground on results:

Ground has major impact on results, cuts in ground put greater effect on gain and S_{11} as well. The development of the antenna performance was aided by research into the ground plane findings and radiator-floor coupling. It has been determined that the width of the floor plane performs the dominant role for the gain enhancement. growth in bandwidth is obtained whilst period of the ground plane is improved. It has been determined that there may be very much less impact of width of the ground aircraft on returned lobe radiation. back lobe radiation decreases as duration of the floor plane increases.

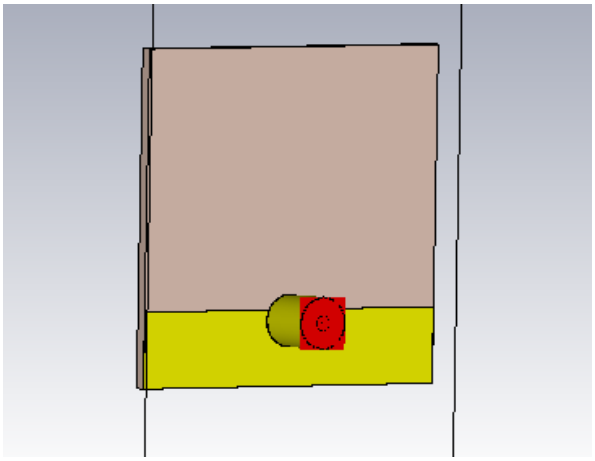

Figure 3.7 (a) Ground shape of MPA (b) return losses

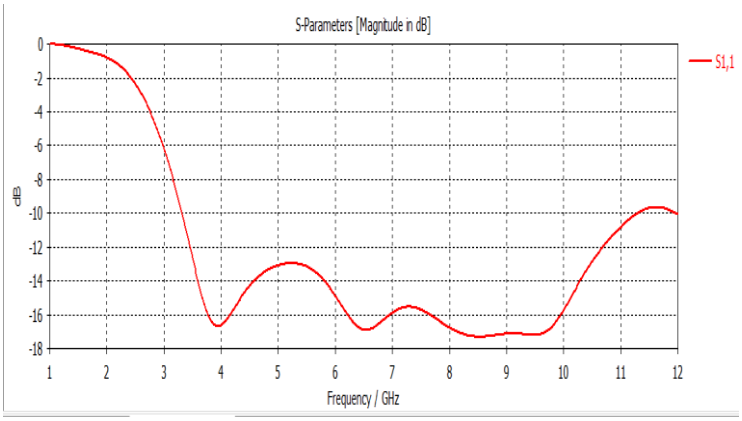

We can see that when we you ground width is to the width of the substrate and when we reduced the width of ground then you can see that the return losses are better than previous one. Here you can see in figure

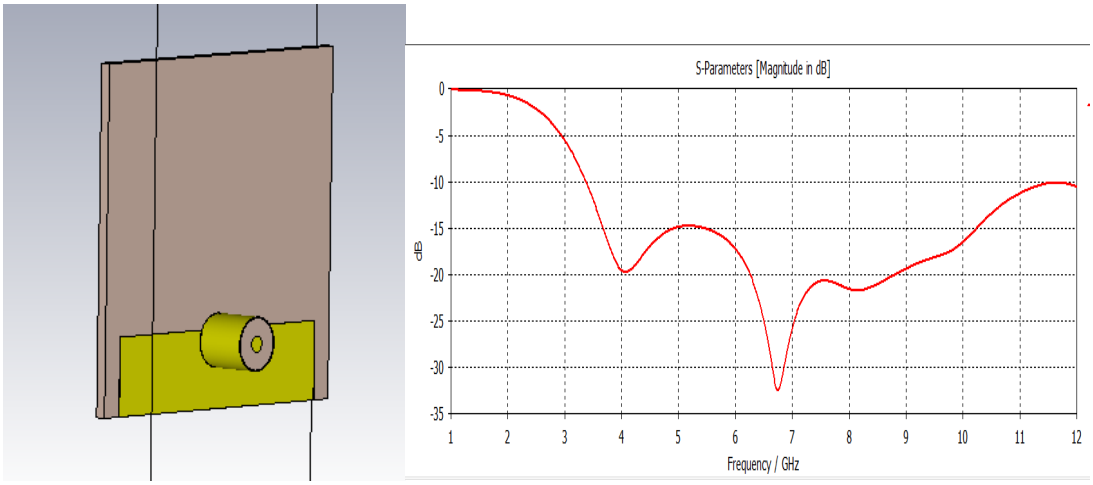

Figure 3.8 Ground Shape (Smaller) **(b)** Return losses

3.1.7.4 Impact of the Feeding on results:

The impacts of coaxial line feed, microstrip line feed, and coplanar beam feed on the overall performance of a rectangular patch antenna are discussed. The findings reveal that impedance matching would be the most important aspect of an antenna's overall performance. In co-axial feed, the placement of the feed factor is also critical. A planer shape is obtained in the case of micro strip feed, and the influence of feed proximity is eliminated. Here you can see if we change the position of feed it makes the big different on results. In my research work during antenna design I preferred Coaxial feed line and because my antenna is UWB when I change the position of coaxial feed line I see the major different in results, sometimes radiation and returns loss becomes a single band and at some position we cannot get returns losses.

3.1.7.5 Improvement in Return Losses with Notched Edges Technique:

The notching edges approach has also been shown to be effective for the reduction of return losses when advantage has grown. This thesis may offer go back loss with and without notched area approach for various antennas. I'd want to compare go back losses using a single Microstrip Patch antenna with and without notched edges throughout 3.3

to 12 GHz. At 4 GHz, a single Microstrip Patch antenna with no notches has a gain of -24.77 dB, at 5 GHz and 6 GHz we get S11 about -13 dB, S11 at 7 GHz is -20 dB and 8 GHz is -15GHz and so on you can see in figure 3.7(a). However, when the notching portion technique is used, the identical antenna with similar settings provides a gain 1.96 dBi.to maximum 4.614. as shown in figure 3.7(b).

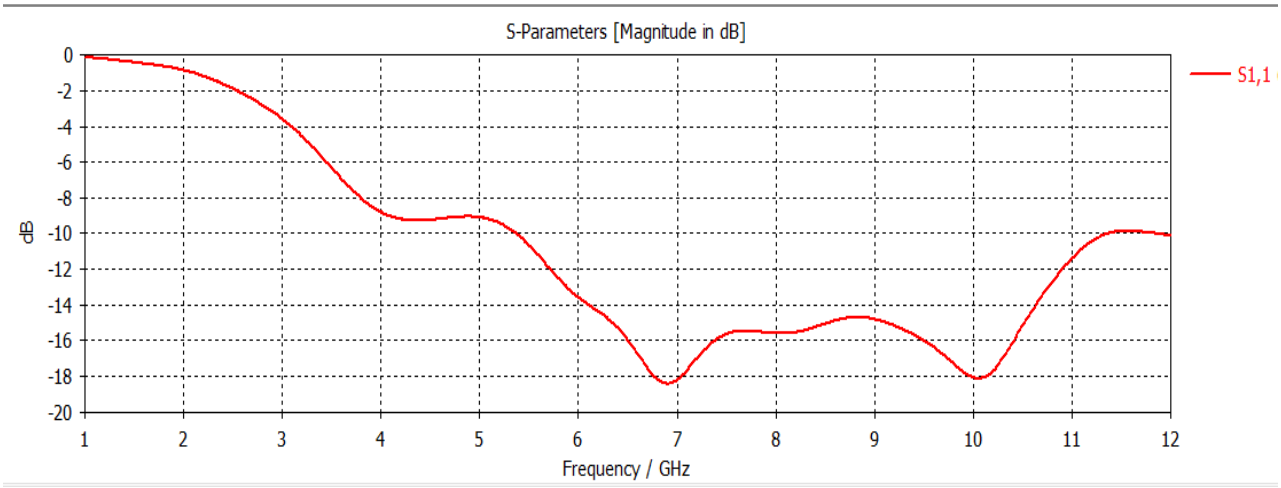

Figure 3.9 S_{11} of Microstrip patch antenna without notched edges

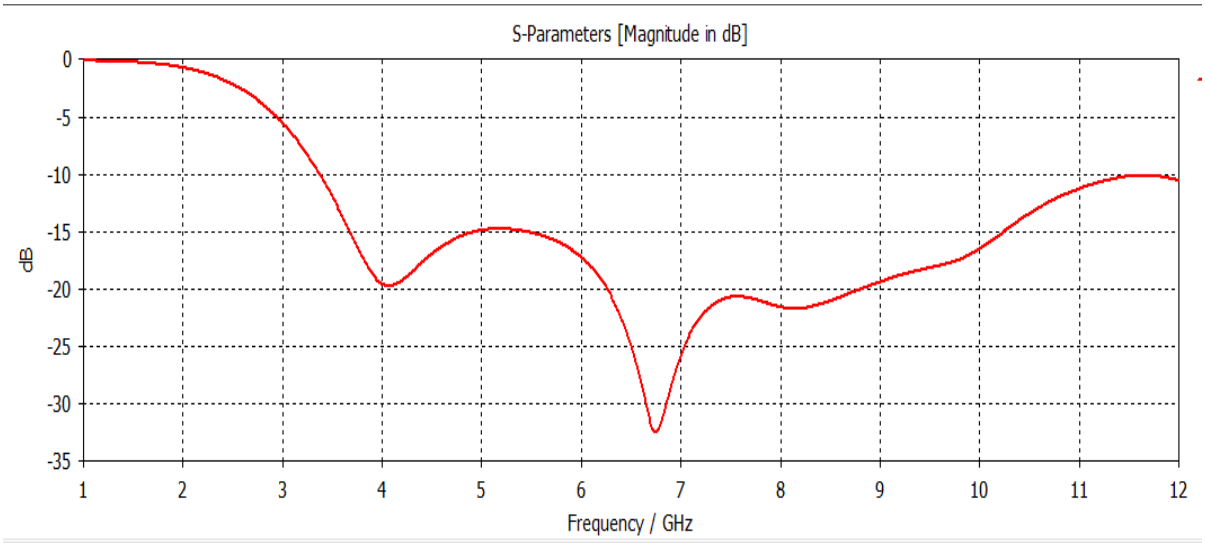

Figure 3.9a S_{11} of Microstrip patch antenna with notched edges

You can see in figure 3.9 (b) the return loss after notched technique is improve throughout the required frequencies but just at 4 GHz frequency is different that is -20 dB and S_{11} and frequency 5 Ghz, 6 GHz, 7 Ghz, 8 GHz, 9 GHz, 10GHz, 11 GHz and 12 GHz is -15 dB, -17 dB, -25 dB, -22 dB, -19 dB, -16.5 dB, -12 dB and 10.5 dB respectively. So, the notching part approach is highly useful in discounting return losses since it increases all

over the frequency return losses.

3.2 Geometry of Microstrip Patch antenna

Patch of Microstrip Patch antenna comprises and scaling of two circles, one rectangular patch add below and 2 rectangular patch added with angle of 45 degree and -45 degree which is 135 degree add in patch and after that we excite that antenna with coaxial feeding. Those values or parameters are denoted by a combination of alphabets. It's critical to make those parameters that are represented by alphabets more challenging.

In a correct cutting facet, these parameters are displayed. In parent 3.8, the antenna has an oval form, and the rationalization of those characteristics is shown in table 3.1.

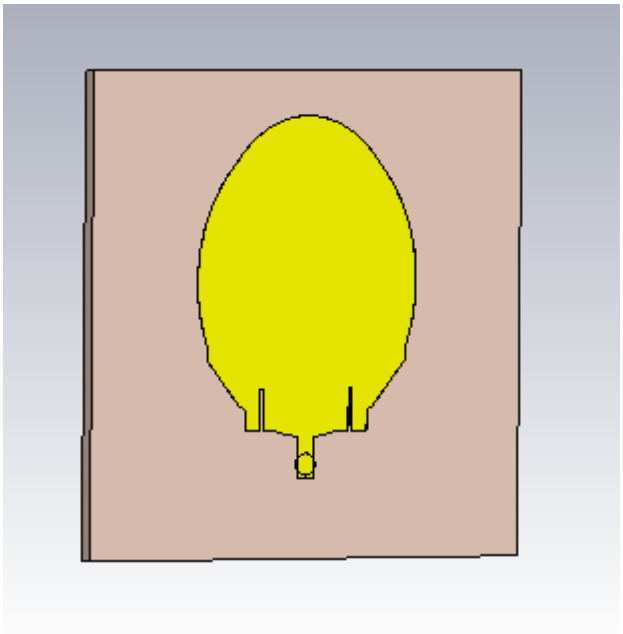

Figure 3.10 Antenna Front side view

Table 3.2 parameters used in Microstrip patch antenna

Sr. No.	Parameter	Description
1	a	Width of Patch
2	b	Length of Patch
3	c	Width of bottom Patch
4	d	length of bottom Patch
5	e	Distance from end to cut
6	f	Width of Cut in patch
7	g	Length of Cut in patch
8	h	Distance between from cut to circle end
9	i	Distance between from circle and bottom patch
10	j	45-degree patch length
11	k	edge of patch
12	l	Distance between 45-degree patch and end of patch
13	m	Width of substrate
14	n	Length of Substrate
15	o	Width of ground
16	p	Length of ground

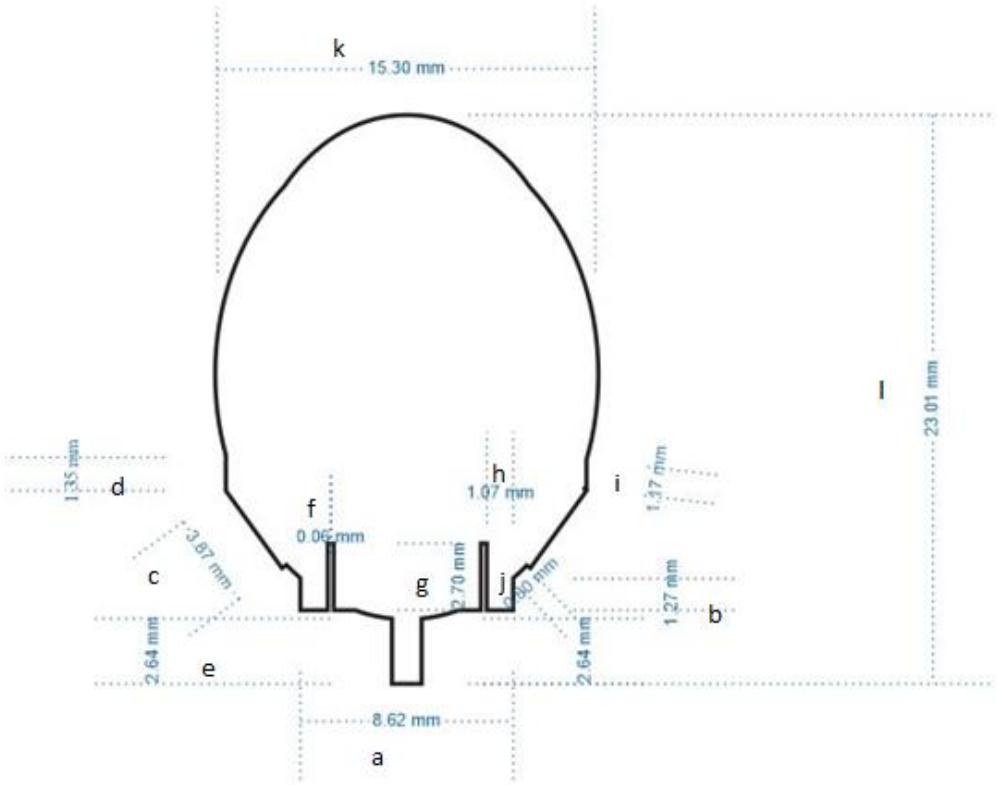

Figure 3.11 parameter of final shape of antenna

The patch's upper area is made up of circles, while the patch's lower section is made up

of three rectangular patches. First part of rectangular patch is a patch with length a and b is the width of that patch below this rectangular patch I draw another small patch with width d and c is the length. Here a, b, c, d is a variable used for identified the parameter. After that for making Microstrip Patch of antenna I draw two circles with radius of m and n from height from reference point is o and p. After draw a circle I have drawn lower part of the patch on both side two rectangular shape with the angle of 42 degree with length of variable j and edge of the patch is k.

The distance between both edge of the patch and end of the patch is equal to the variable l. after that we need to draw cut for get the better results, these cuts put both side of antenna. Size of that cut is f x g. f is the width of the cut and g is the length of these cuts. We employ variables because they aid in the creation of results. We can quickly alter the value of any parameter without having to open the geometry of each antenna and change its own values. As a result, all of the parameters described above are employed with variables and are discussed in depth in Table 3.1

3.2.1 Antenna for breast cancer detection:

Basically, here are many antennas to detect the tumor, some are very big in size and some have high gain another are not good returns losses and not up-to the mark as we need for detection. Some researcher makes antenna by shape of circle, bowtie, spiral shaped, rectangular and many other shapes. Many works on single band and some are work on Ultrawide band. Some researcher makes dual band for that noble work. My design is novel shape. Design of my antenna is oval. Here I used fr-4 lossy substrate for 1 mm thickness with dielectric constant is 4.3 and electric tendency is 0.025(count. Fit) and its thermal conductivity is 0.3 W/K/m. I used coaxial feeding for this excitation. Results on my antenna is better then other. My antenna cover frequency band 3.24 GHz to 12 GHz simulated results and its measure results is about 3.13 GHz to 11.7 GHz.

This change is due to surrounded and atmosphere condition and many other factors which

impact the antenna results.

3.2.2 Optimization in antenna design:

As you already see the design of antenna, the design is novel and its give us best results and that one which are very nearly equal to the required one we need for tumor detection. If you change in size then the band we achieve after change is less than the proposed antenna design as you can see shape and results in figure 3.9.

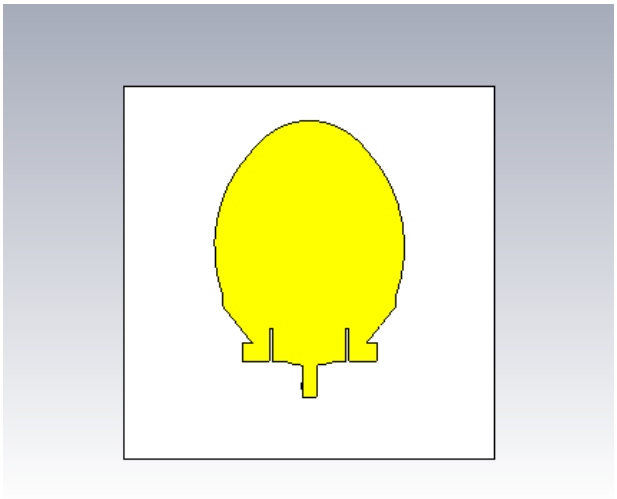

Figure 3.12 Microstrip patch antenna

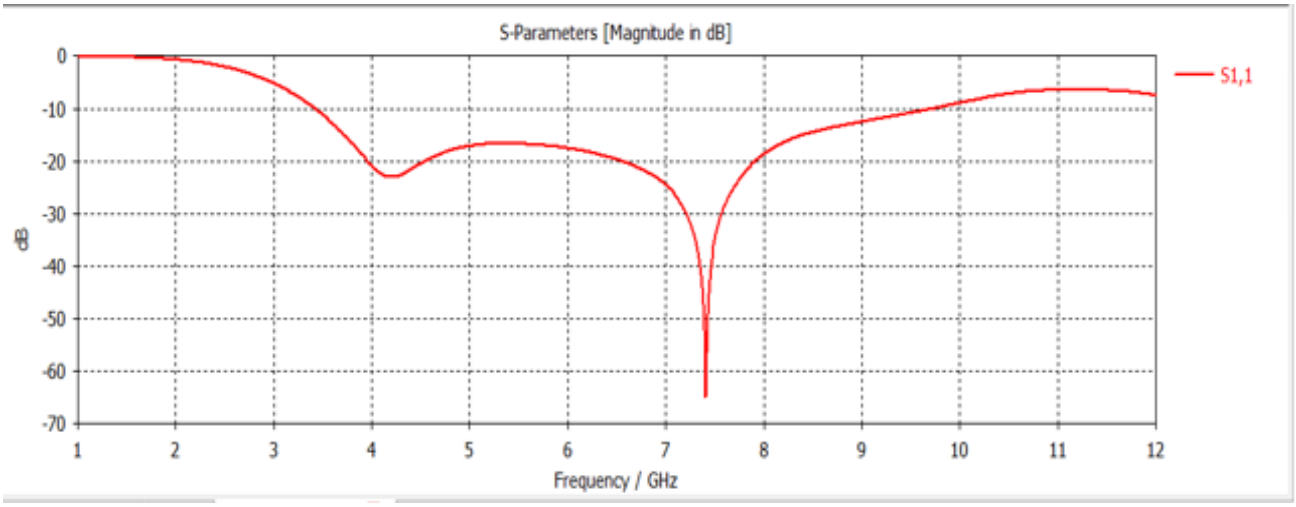

Figure 3.12a Microstrip patch antenna and it's results (Simulated)

Table 3.3 Values of parameters used in microstrip patch antenna

Sr. No.	Parameter	Value (in mm)	Sr. No.	Parameter	Value (in mm)
1	a	10.98	**9**	i	1.60
2	b	1.50	**10**	j	2.57
3	c	3.87	**11**	k	0.12
4	d	1.35	**12**	l	0.39
5	e	1.06	**13**	m	31
6	f	0.24	**14**	n	31
7	g	3.00	**15**	o	27
8	h	0.83	**16**	p	7

3.2.3 Final Shape of antenna

A final shape of antenna is shows in figure, final shape of antenna is like Microstrip Patch and ground is smaller than its substrate. 1mm height of substrate is used and from my final shape of antenna we get better performance from it.

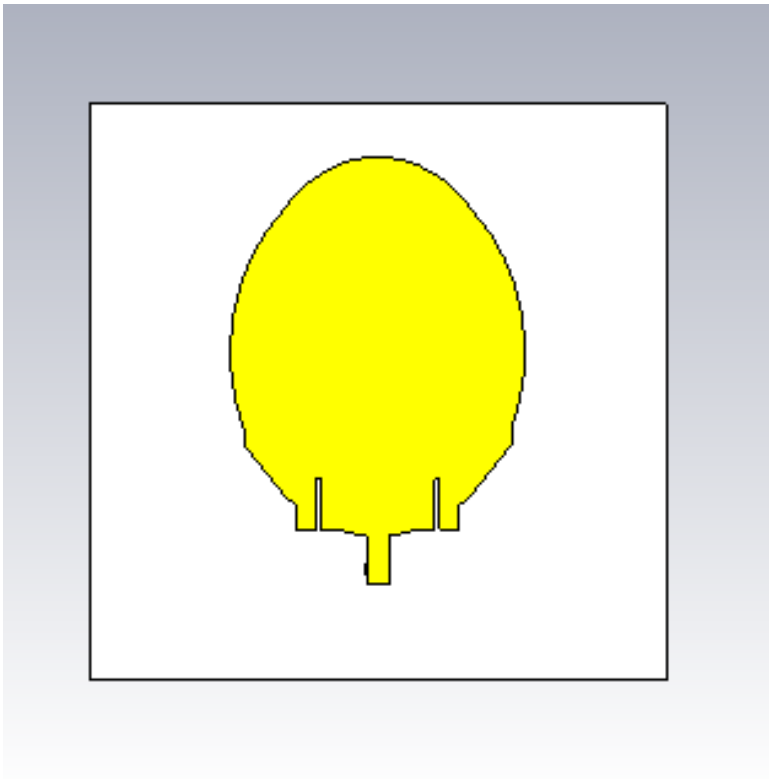

Figure 3.13 Proposed final shape antenna front side (Simulated)

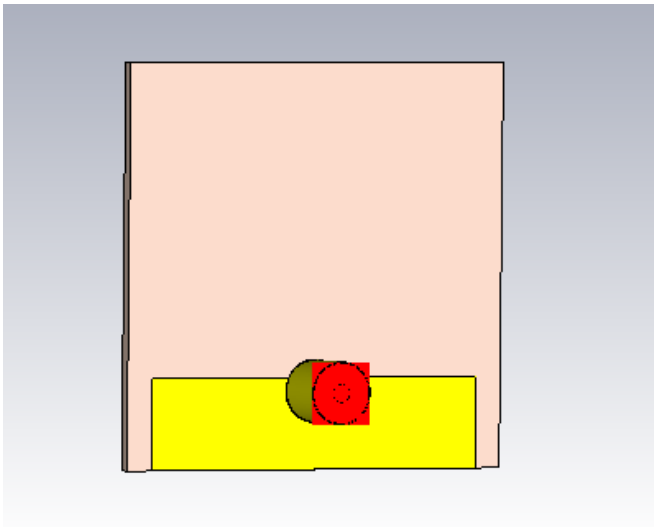

Figure 3.13a Proposed final shape antenna back side (Simulated)

Table 3.4 Values of parameters used in final shape antenna

Sr. No.	Parameter	Value (in mm)	Sr. No.	Parameter	Value (in mm)
1	a	8.62	**9**	i	1.17
2	b	1.27	**10**	j	0.8
3	c	3.87	**11**	k	15.30
4	d	1.35	**12**	l	23
5	e	2.64	**13**	m	31
6	f	0.06	**14**	n	31
7	g	2.70	**15**	o	27
8	h	1.07	**16**	p	7

Microstrip Patch antenna follows the allotted frequencies of the NCBI Frequency allocation table for medical purposed (Breast Cancer detection) [32]

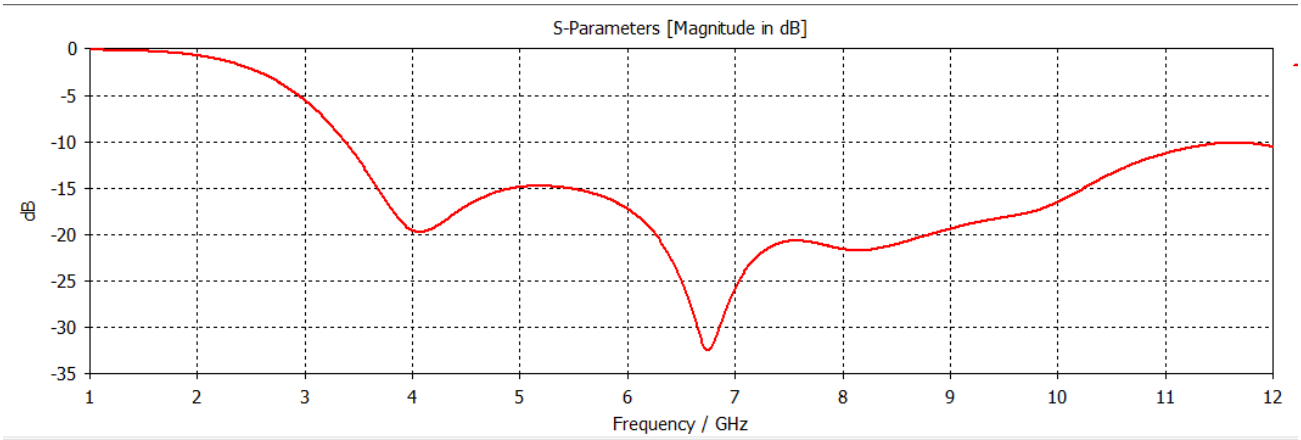

Figure 3.14 Return losses proposed final shape antenna (Simulated)

Now we can check the radiation pattern of antenna at different frequency which are useful for the detection of tumor in breast. We select the frequency at 4.25 GHz 7 GHz and 9 GHz frequency. Figure 3.12a, 3.12b 3.13c are the radiation pattern of antenna at at 4.25 GHz 7 GHz and 9 GHz frequency respectively.

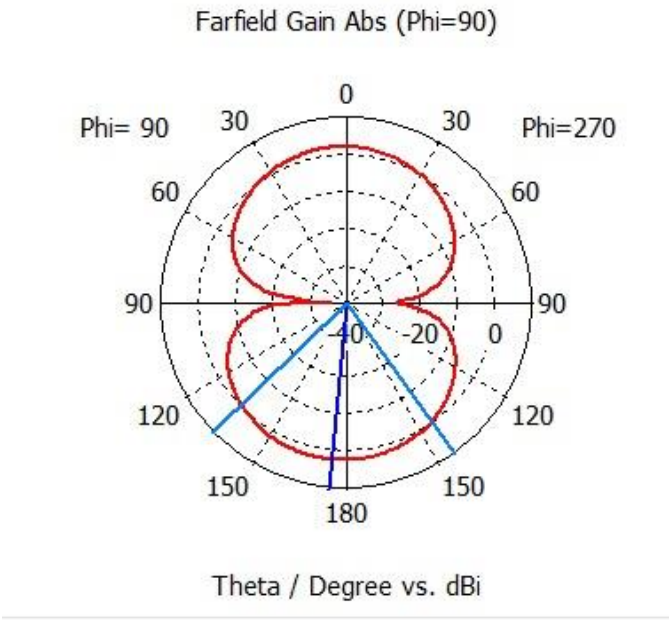

Figure 3.14 a

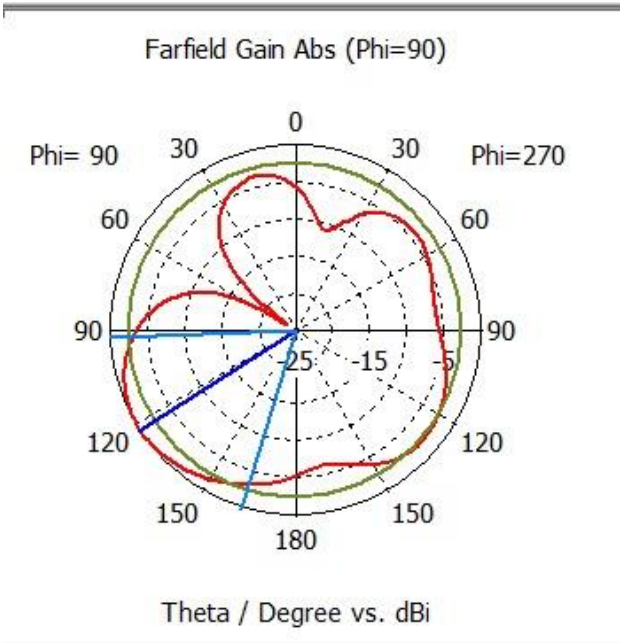

Figure 3.14 b

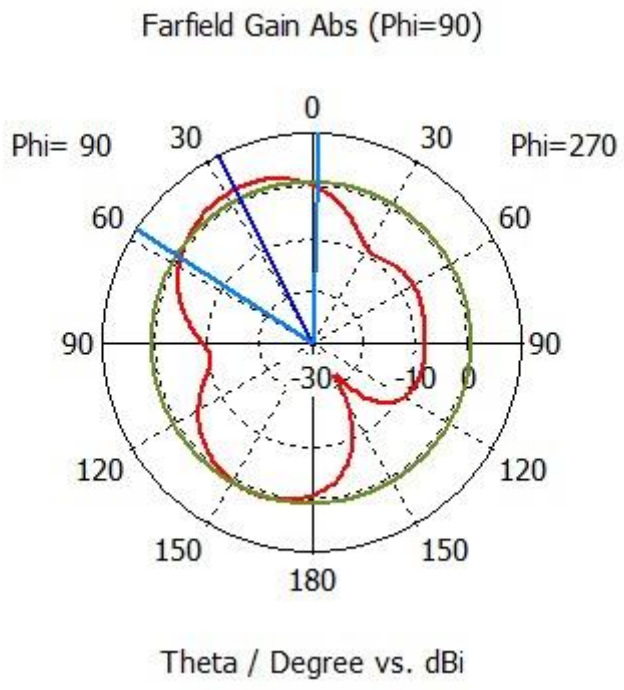

Figure 3.14 c

Now we find out the current density of the purposed antenna at two frequencies like 4.25 GHz and 6.5 GHz frequencies. Current density of antenna.

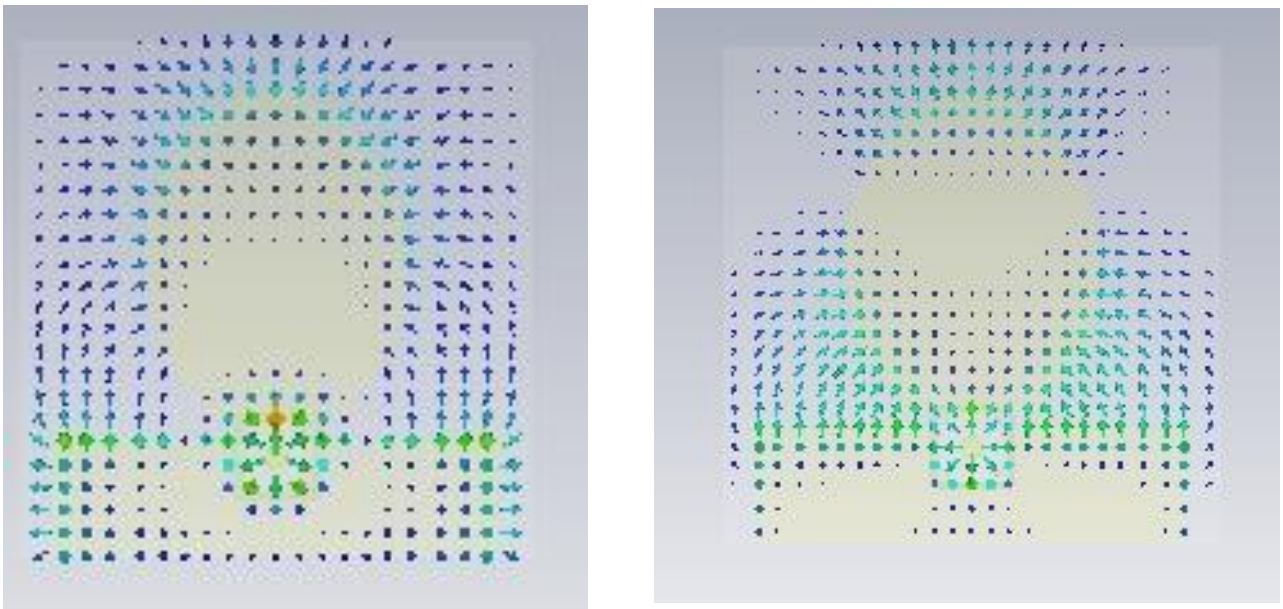

Figure 3.15 current density of antenna

3.3 Fabricated of microstrip patch antennas:

Simulated designs of different antennas were fabricated from Smart PCB, Rawalpindi, Pakistan. Fabricated antennas are shown in figure 3.15-17.

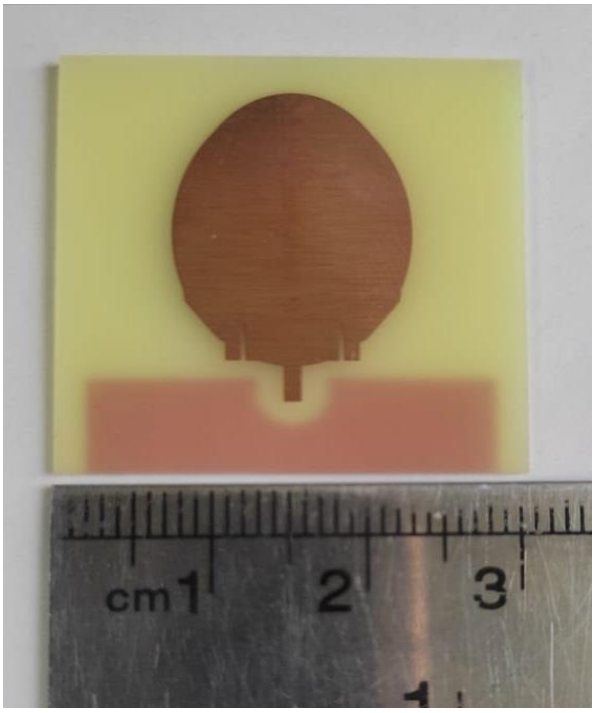

Figure 3.16 Single element antenna of microstrip patch antenna for Breast tumor Detection (Fabricated)

Figure 3.16a Back view of Single element microstrip patch antenna for breast tumor (Fabricated)

3.4 Microstrip Patch Antenna Arrays

Phased array patch antennas are being advocated for tumor detection, as stated in Chapter 1 well in advance. As a result, arrays play a crucial role in every suggested antenna for tumor detection. [7] All antennas are subjected to antenna arrays in order to improve gain and other characteristics.

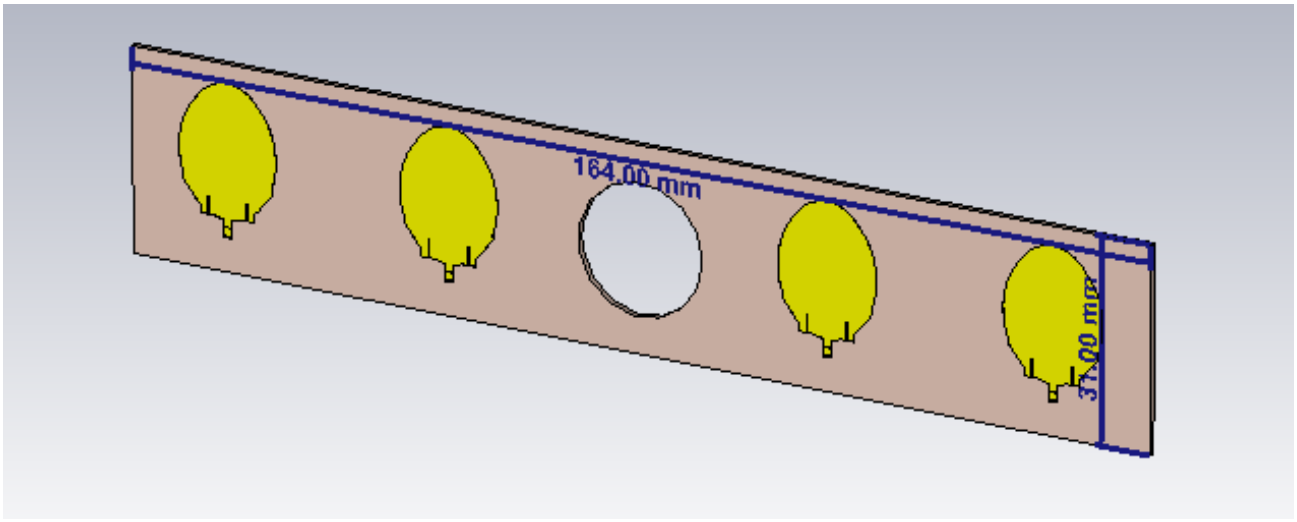

Figure 3.17 Array of final shaped of antenna Front side view

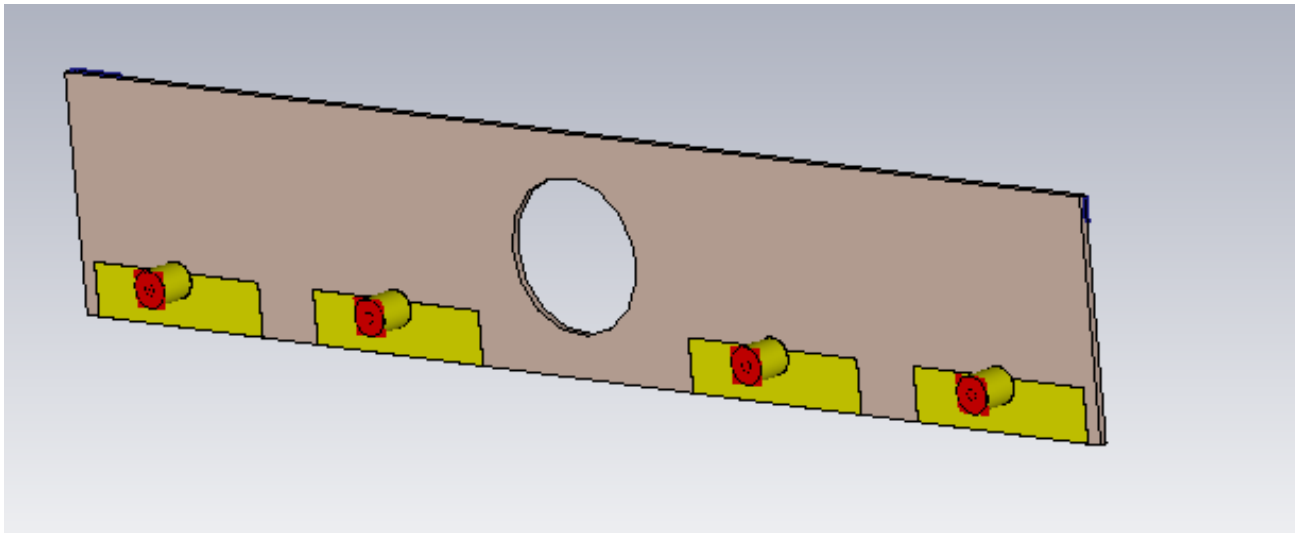

Figure 3.17a Array of final shaped of antenna back side view

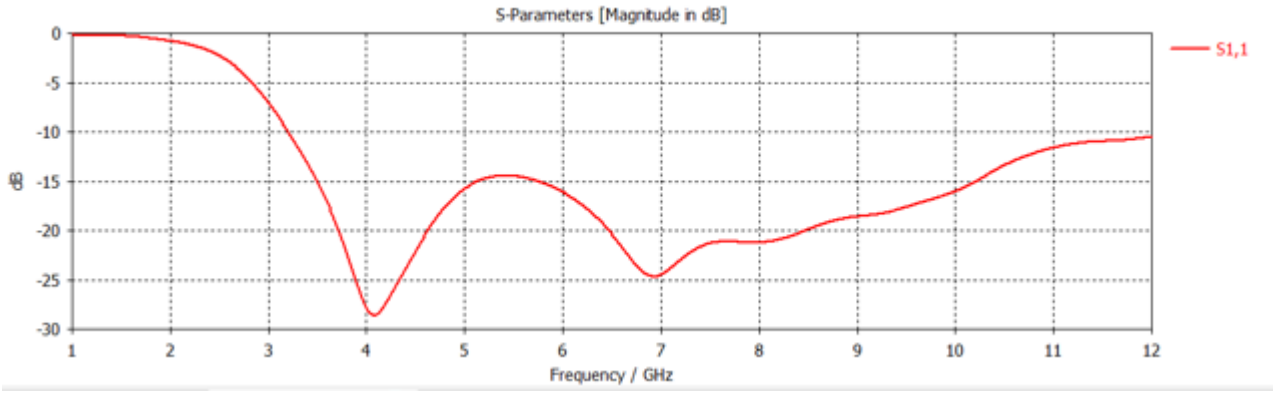

Figure 3.17b Return losses of antenna array

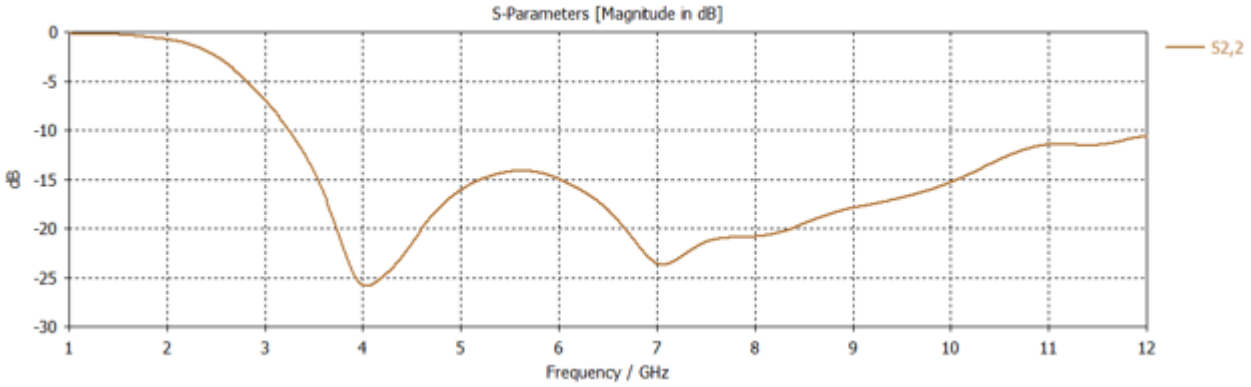

Figure 3.17c Return losses of antenna array

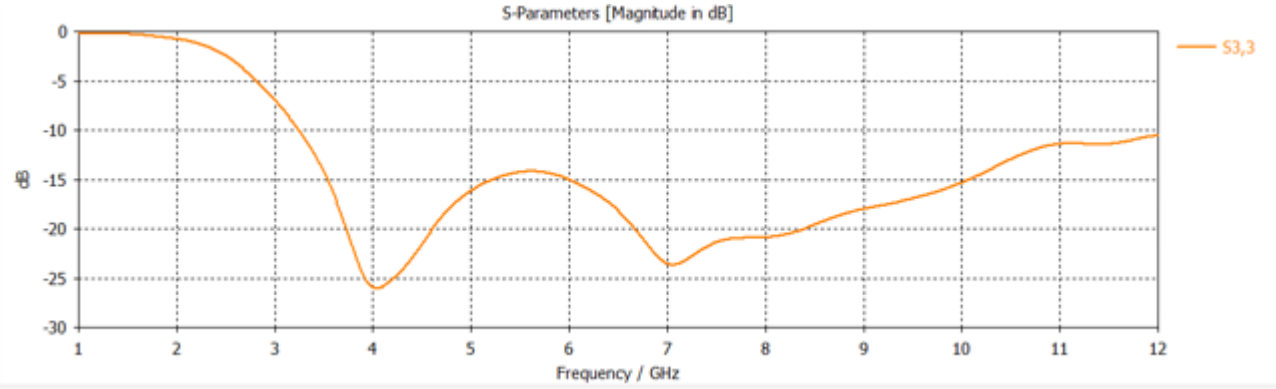

Figure 3.17d Return losses of antenna array

Here you can see that S11, s22, s33, s44 of array of antenna, its almost starts from 3.24 GHz to almost more than 12 GHz bands covers in it.

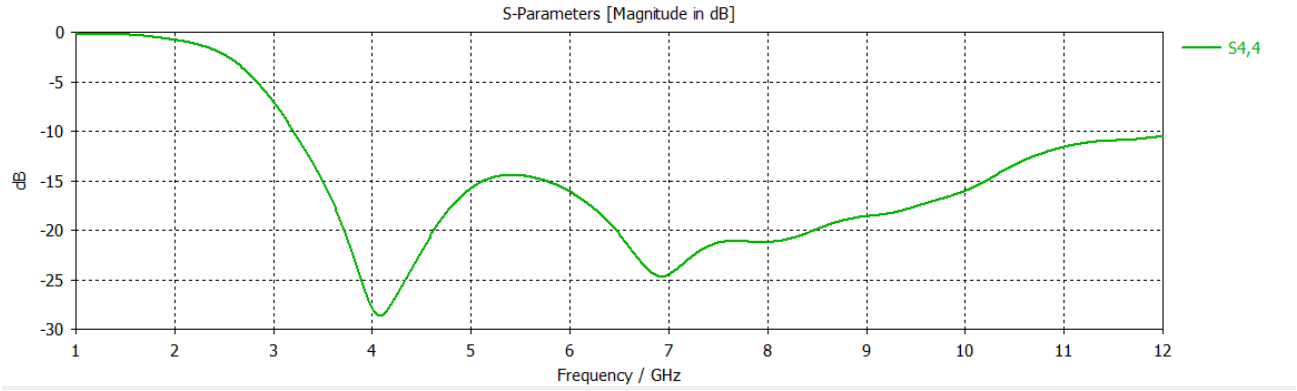

Figure 3.17e Return losses of antenna array

That's results are simulated on CST suite. The size of array is 164x31 mm^2. That size makes its more comfortable and gave us a good result and gain as well.

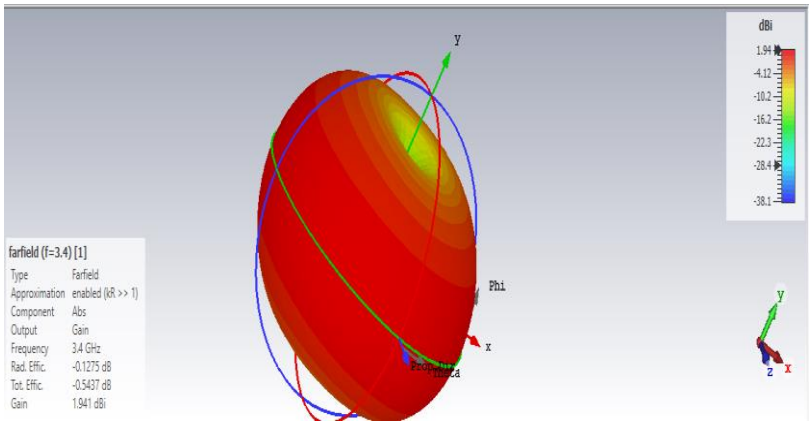

Figure 3.18 gain of antenna at frequency 4GHz

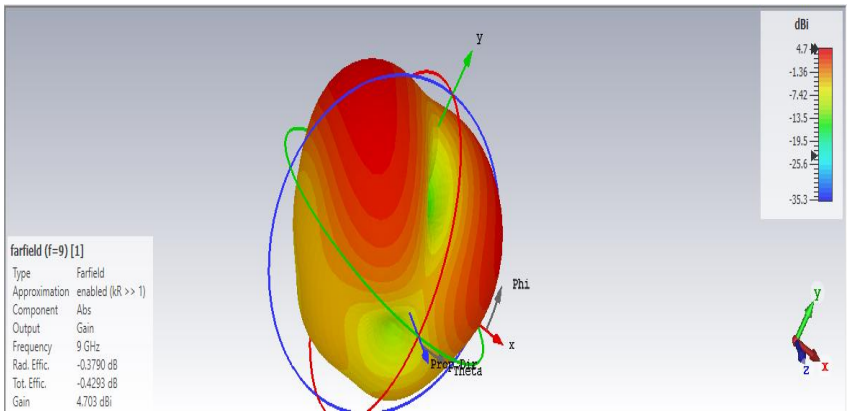

Figure 3.18a gain of antenna at frequency 9GHz

Figure 18 and 18a shows the maximum and minimum gain of the antenna at

frequency of 4 GHz and 9 GHz. Minimum gain of purposed antenna is 1.9 db and maximum gain of antenna is 4.71 dbi.

this is the final shape of array which is used for the cancer detection of breast. It's almost covers 360 angles at phantom which is created by properties of real breast cancer detection.[8]

3.5 Fabrication of Microstrip Patch Antenna Array:

After fabricating the single element of antenna, we need to fabricate the array of it to fine out the tumor at any point in phantom for localization of malicious tissue in fatty portion of breast.

Figure 3.19 Array of microstrip patch antenna (fabricated)

3.5.1 Feeding Technique:

For arrays, there are specialized feeding procedures that may be applied. The most common antenna array techniques are the company array, lambda by 4 transformer, and power divider. Thesis provides four elements array implement. Using a proper feeding mechanism, the spacing is generally dependent on $\frac{1}{2}\lambda$ (or half wavelength).

Depending on the types and specifications of antennas, the value of spacing may be increased using the constructed from three, five, and so on. using appropriate feeding technique.

3.5.1.1 Impedance Matching

Impedance of feed line near the patch or directly connected to the patch is kept 100 Ω and impedance of initial feed line or coaxial feed line within the port is kept 50 Ω for proper impedance matching. While impedance of the combined feed line, connecting feed lines of two elements is measured by using the given formula.

$$Z_o = \sqrt{Z_1 \times Z_2}$$

The natural log of the ratio of the outer diameter (D2) to the inner diameter (D1) determines the characteristic impedance of a coaxial cable (D1). Because of the additional gap between the inner and outside conductors, the impedance is larger.

The coaxial feed, often known as probe feed, is one of the most used ways for feeding Microstrip Patch antennas. As show in figure the internal conductor of the coaxial connection extends through the dielectric and is soldered to the radiating patch at the same time as the outer conductor is soldered to the floor plane.

Position of the probe is very important results varies with change the position of it. Converting the position of the feed factor may be used to alter the impedance of the feeding point for Microstrip Patch antennas. The feed probe method was utilized to enhance the patch antenna while keeping the input impedance low and the matching high. The patch antenna's input impedance is reduced when the feeding factor position is chosen correctly, and the go back loss, benefit, performance, and directivity are all improved.

Impedance is calculated from analytical line impedance calculator in CST. Impedance calculation depends upon the following three parameters:

i) Material of Substrate

ii) Height of Substrate

iii) radius of outer conductor

Once a substrate material has been chosen, it cannot be changed. Furthermore, the height of the substrate cannot be changed to accommodate alternative antenna designs. Because FR4 material with a 1mm height is readily accessible in the marketplace, it is preferred over alternative materials. As a result, the radius of the outer conductor is the only characteristic that may be changed. As a result, the radius of the outer conductor is altered to adapt different impedance values. What should be the values radius of outer conductor to obtain required impedances, are shown in table 3.5?

Table 3.4 Values of parameters for impedance calculation

Radius of outer conduction (mm)	**Permittivity of Substrate**	**Height of Substrate (mm)**	**Calculated Impedance (Ω)**
2.4	4.7 / 4.4	1	50
2.3	4.7 / 4.4	1	47.5
22	4.7 / 4.4	1	45.05
2.5	4.7/4.4	1	51

3.6 Measured Results of antenna.

Measured results of all the antennas are represented separately. Measured results of S11 parameter were measured using VNA from National Institute of Electronics (NIE), Islamabad, Pakistan.

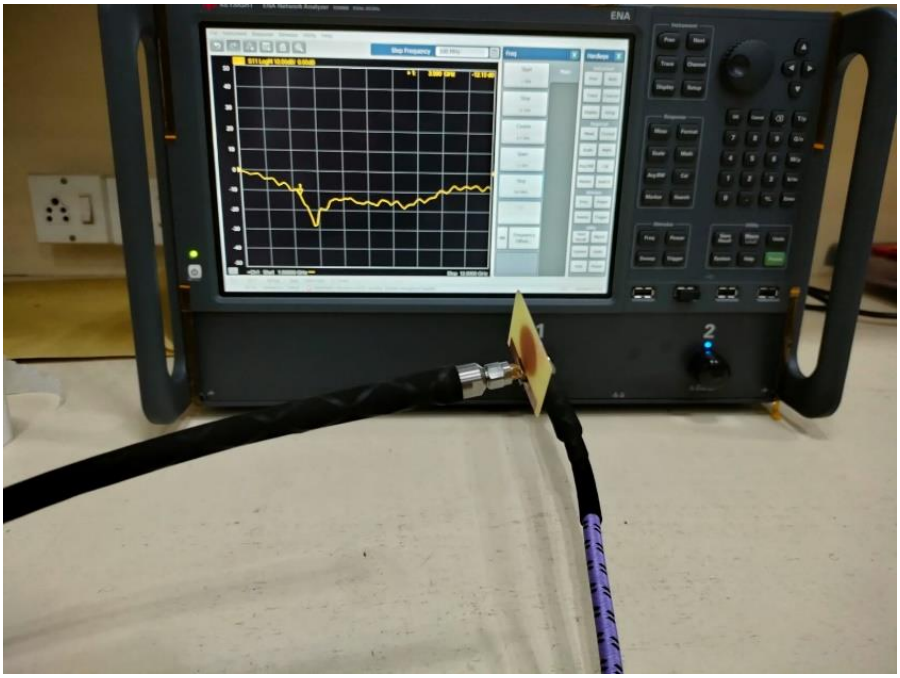

Figure 3.20 Measurement of antenna by VNA

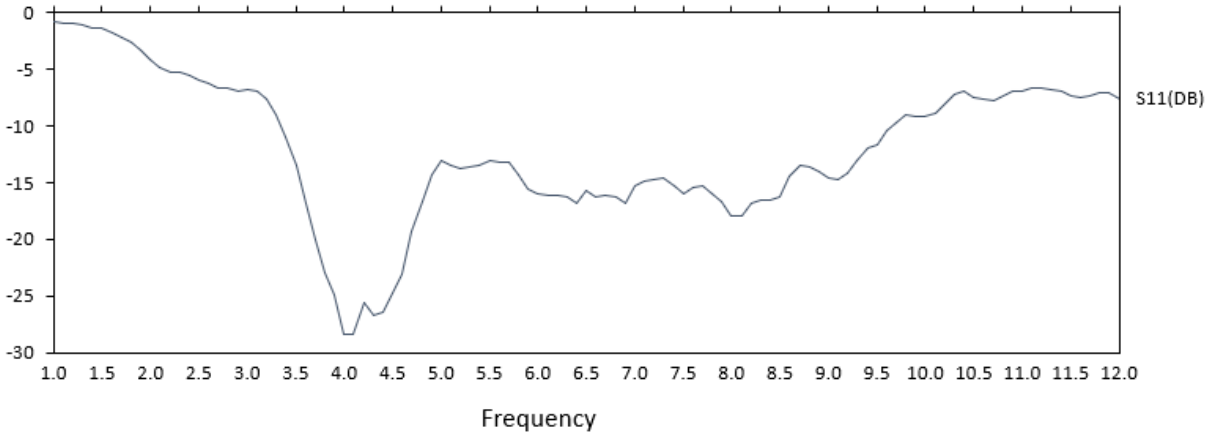

Figure 3.21 Measuring Results of antenna by VNA

You can see that Frequency band starts from 3.4 GHz to 10 GHz.

PHANTOM FABRICATION

4.1 Introductions

Breast imaging generation is crucial for the detection and treatment of breast cancer. Due to its adaptability and relatively inexpensive cost, 3-D printing has recently experienced a boom in popularity among enthusiasts in the field of scientific phantom creation. However, there is currently no established process for requiring multi-modality breast phantoms for high level of assurance testing (quality control). In this study, we aimed to develop a 3-d-revealed breast phantom that could serve as an anatomically and physiologically correct substitute for real breast tissue and be utilized for a variety of breast imaging best-manipulation applications.

Before going to real scenario, we tested our antenna of fabricated phantom which is made in lab. That phantom has the all the properties for example electrical properties permittivity, density, heat capacity, and loss tangent which are nearly match to the real breast phantom. For fabricate the phantom we have to create a skin tissue on CST, after created the skin tissue we go for the fat tissue after that we have to create the tumor with different properties from the fat.

Actually, we create the 2 type of phantom like phantom without tumor and phantom with tumor. In this way we can check the results of both phantom from our antenna and save it in library.

4.2 Modeling of breast phantom (simulated)

We can see below table 4.1 in which we see that the electrical properties of skin, fat and tumor tissue, here you can see that the permittivity of tumor is much higher than the fat tissue.

Table 4.1 Electrical properties of normal and tumor tissue.

Tissues	**Permittivity**	**Electrical Conductance**	**Density**	**Capacity of heat**	**Thermal Conductance**
Skin	36.7	2.34	1109	3391	0.37
Fat tissues	4.84	0.262	911	2348	0.21
Tumor	54.9	4	1058	-	-

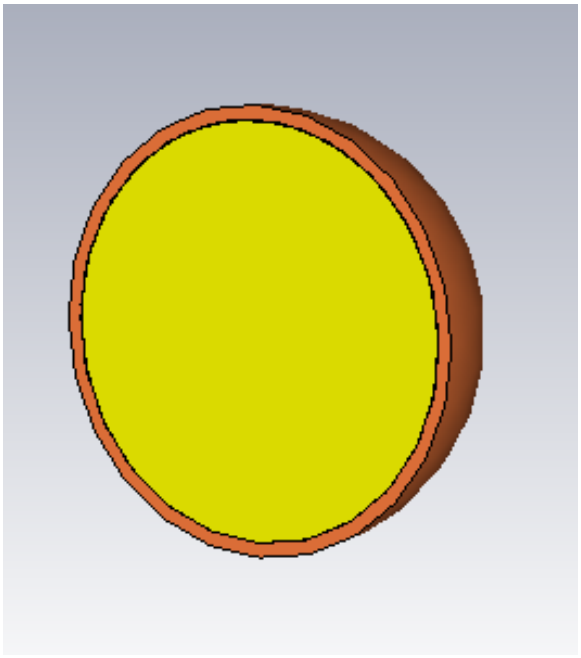

Figure 4.1 phantom without tumor

As you can see that that is the phantom which has no malicious tissues. Now I will show you the phantom with tumor.

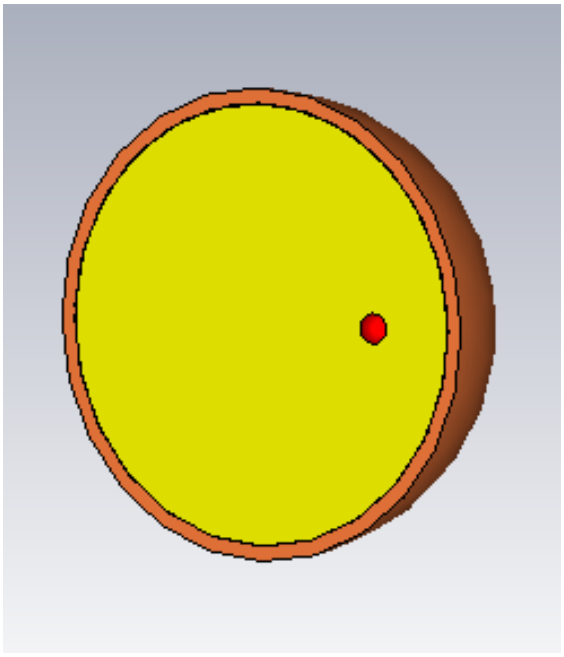

Figure 4.2 phantom with tumor

Here we can place antenna on phantom on different places to fine the location of tumor.

4.3 Analysis of phantom:

For the analysis of phantom, we have to construct the phantom in simulated software like CST, for that purpose we first create a skin tissue then fat and at the last we create the

tumor. The size of phantom should be equal to the size of fabricated phantom (which is develop in lab).

4.3.1 Skin Analysis (simulated):

For the analysis of skin, we build skin tissue in CST software and with electrical properties shown in table 4.1 place final design of antenna on it and calculate the S_{11} parameter which is shown in figures below.

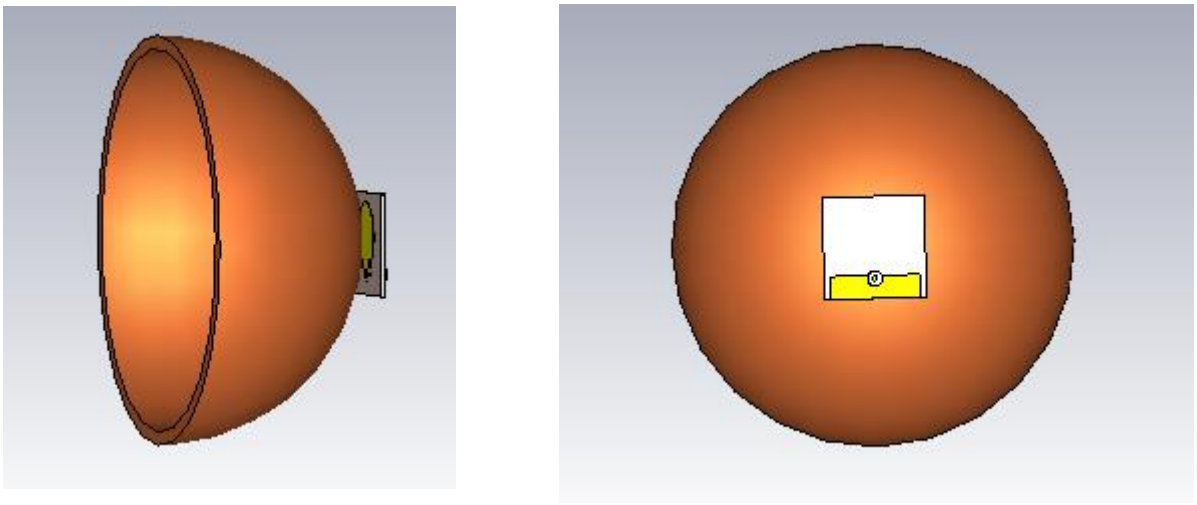

Figure 4.3 Antenna Place on skin tissue

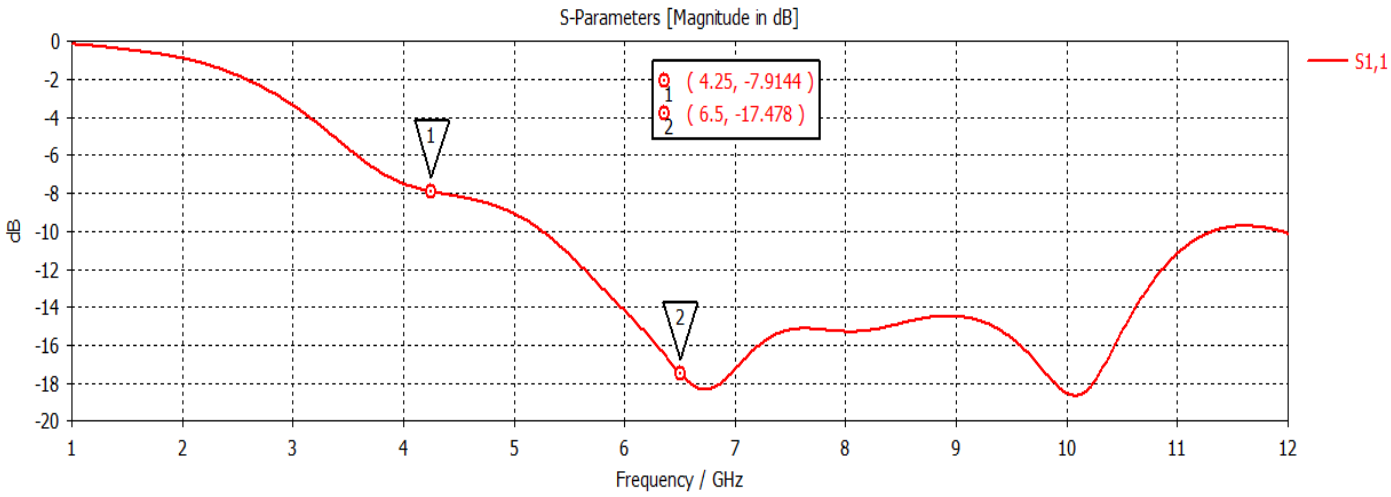

Figure 4.4 S_{11} of skin tissue

4.3.2 Fat Analysis (simulated):

For the analysis of fat, we build fat tissue in CST software with electrical properties shown in table 4.1 and place final design of antenna on it and calculate the S_{11} parameter which is shown in figure below.

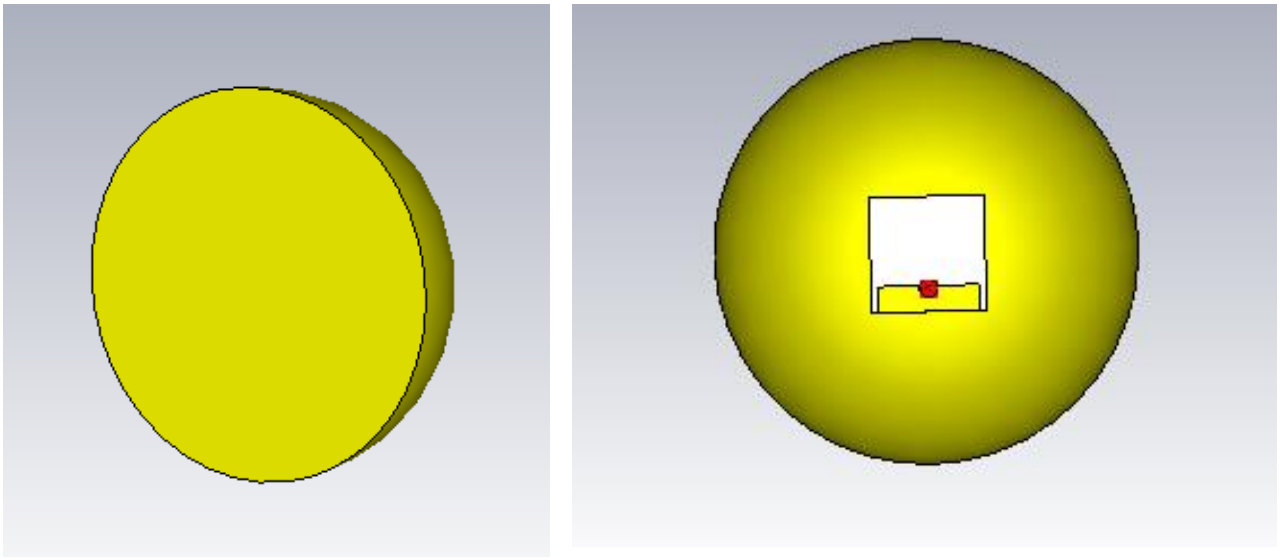

Figure 4.5 Antenna Place on Fatty tissue

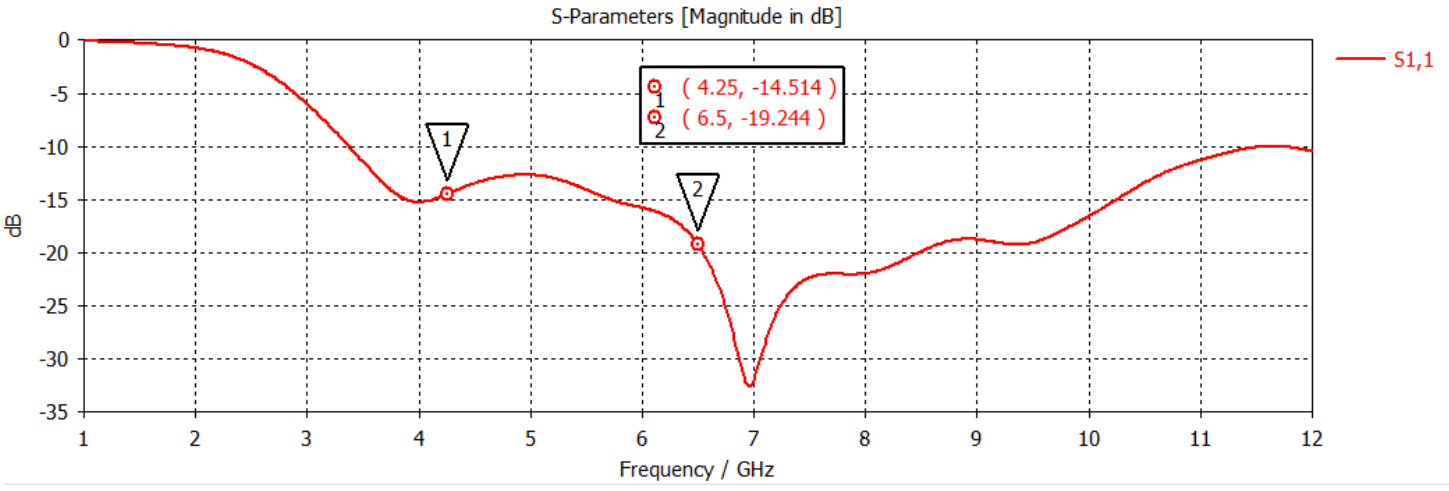

Figure 4.6 S_{11} of Fatty tissue

4.3.3 phantom Analysis (simulated):

For the analysis of Phantom, we build phantom tissue in CST software with electrical properties shown in table 4.1 and place final design of antenna on it and calculate the S_{11} parameter which is shown in figure below.

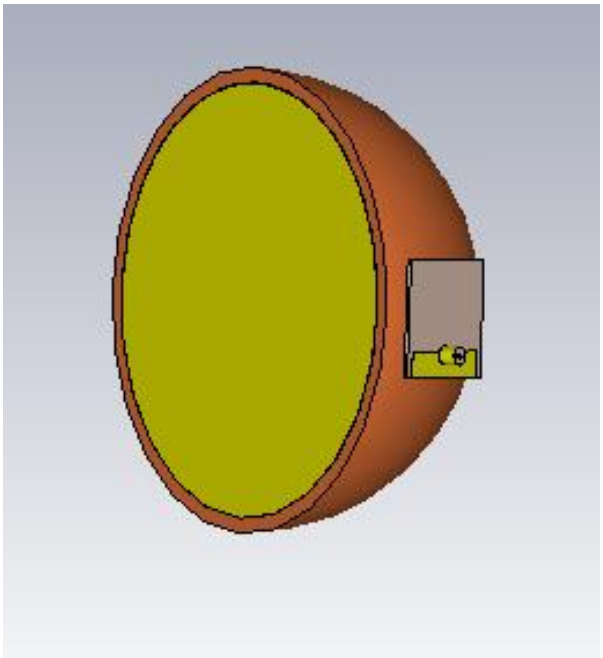

Figure 4.7 Antenna place on phantom (without tumor)

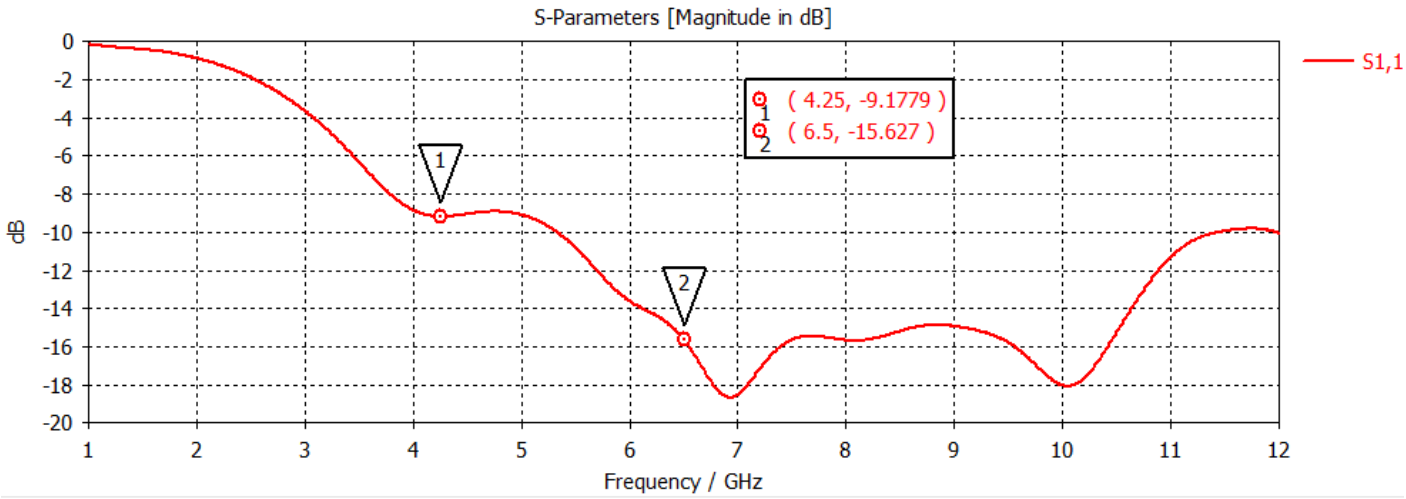

Figure 4.8 S11 of phantom (without tumor)

4.3.4 Tumor Analysis (simulated):

For the analysis of Tumor, we build malicious(tumor) tissue in CST software with electrical properties shown in table 4.1 and place final design of antenna on it and

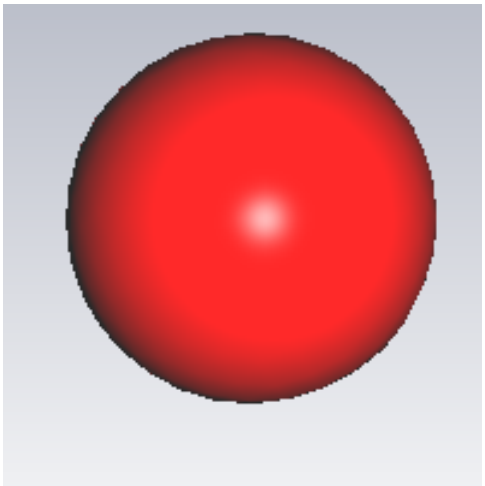

Fig 4.9 Tumor Model

calculate the S_{11} parameter which is shown in figure below.

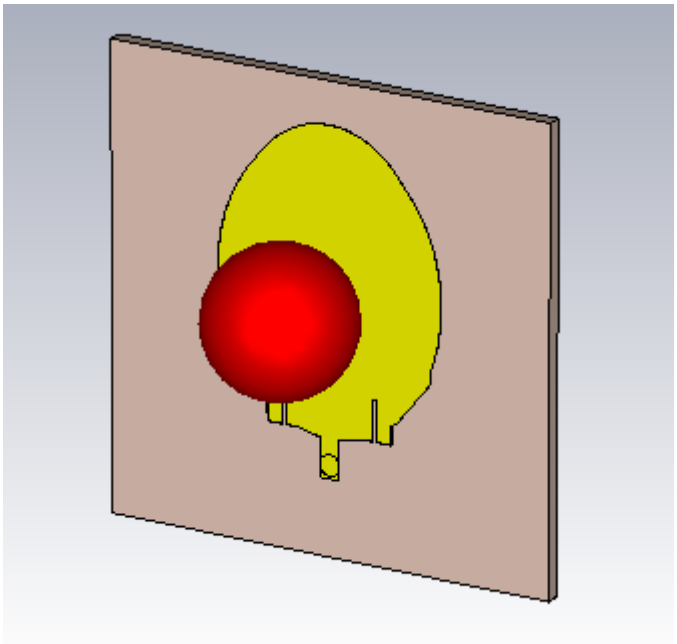

Figure 4.9a Antenna place on tumor(cancer) tissue

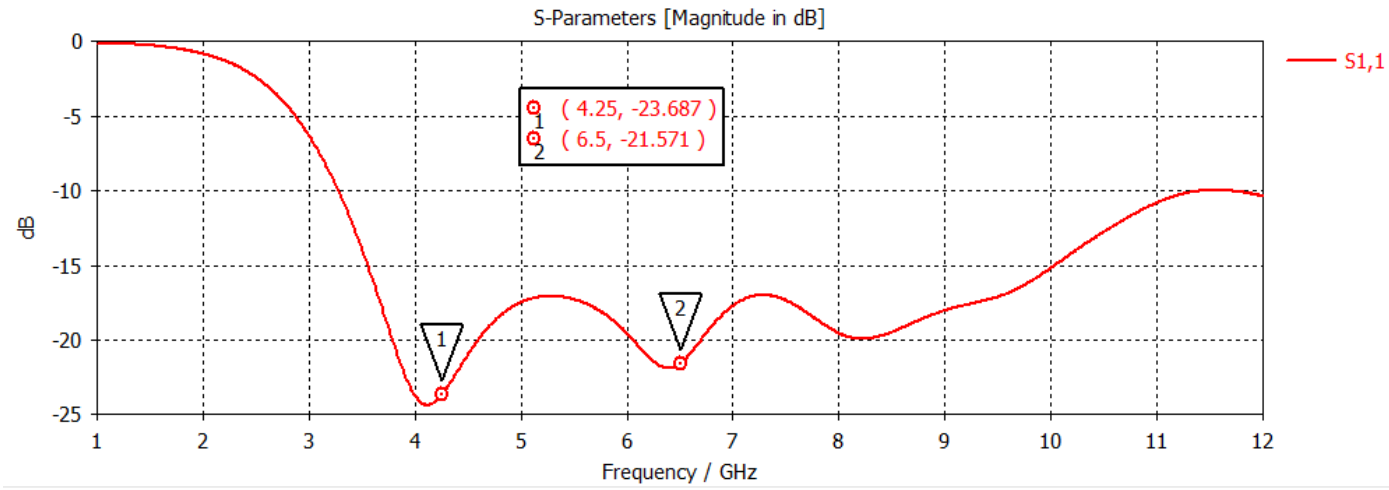

Figure 4.10 S_{11} of tumor(cancer) tissue

4.3.5 Phantom with Tumor Analysis (simulated):

For the analysis of phantom with Tumor, we build malicious(tumor) tissue in phantom which u build before in CST software with electrical properties shown in table 4.1 and place final design of antenna on it and calculate the S11 parameter which is shown in figure below.

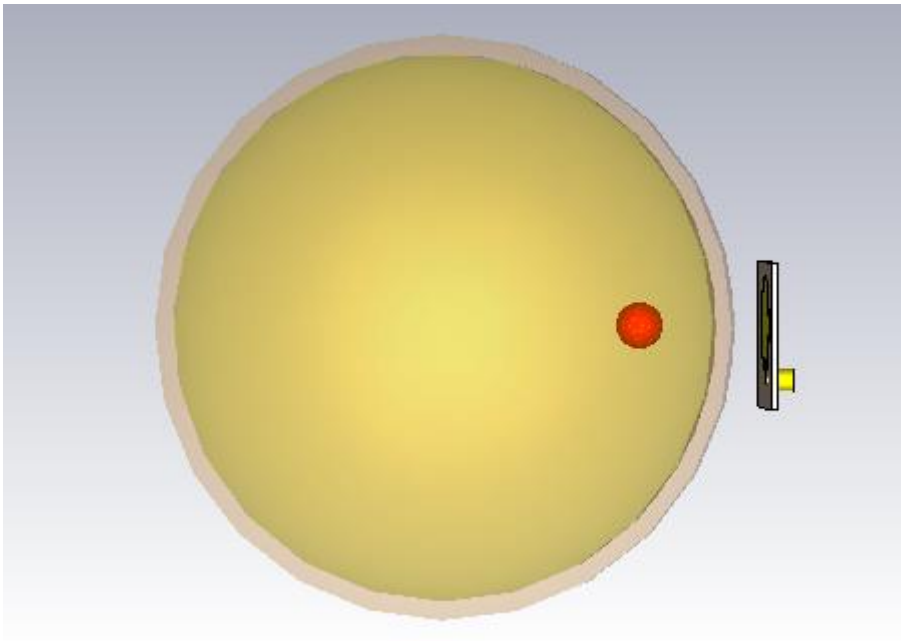

Figure 4.11 Antenna Placed on phantom (with tumor)

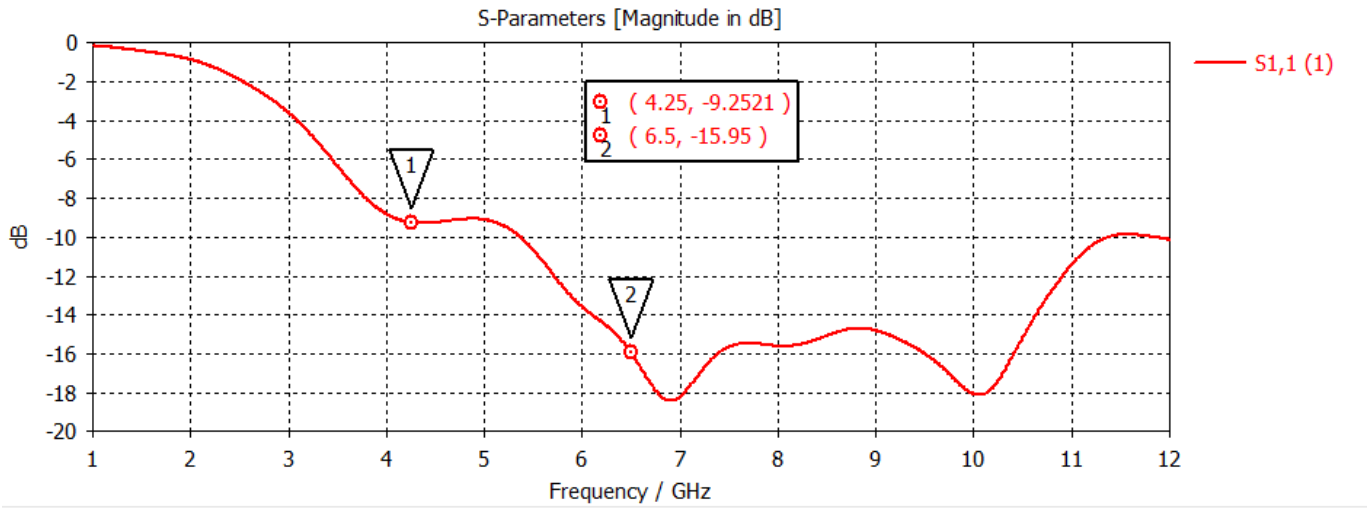

Figure 4.12 S_{11} of phantom (with tumor)

4.4 Development of phantom:

The materials used to create the breast phantoms are diverse. The permittivity and conductivity of the breast phantoms' dielectric properties must match those of real breast tissue for the experiment to be successful. According to analyses of the pertinent literature, it is common practice to produce diverse breast phantoms using less expensive and non-chemical materials such wheat flour, water, soy oil, or Vaseline (petroleum jelly). The breast phantoms employed in this observation were constructed similarly to those used in another research, as described in [20]. The breast phantom skin is shaped like a cup with measurements of 124 mm in diameter, 5.5 mm in height, and 1.9 mm in thickness. A heterogeneous breast phantasm is produced by combining petroleum jelly, soy oil, and wheat flour in equal amounts. As seen in fig. 6, it is additionally diluted with water to a concentration of 25%. At a ratio of 5.5:1, the water content of tumor growth medium is ten times more than that of wheat flour. a technique for creating test tumors of different sizes (2 mm, 3 mm, 4 mm, 5 mm, and 6 mm).

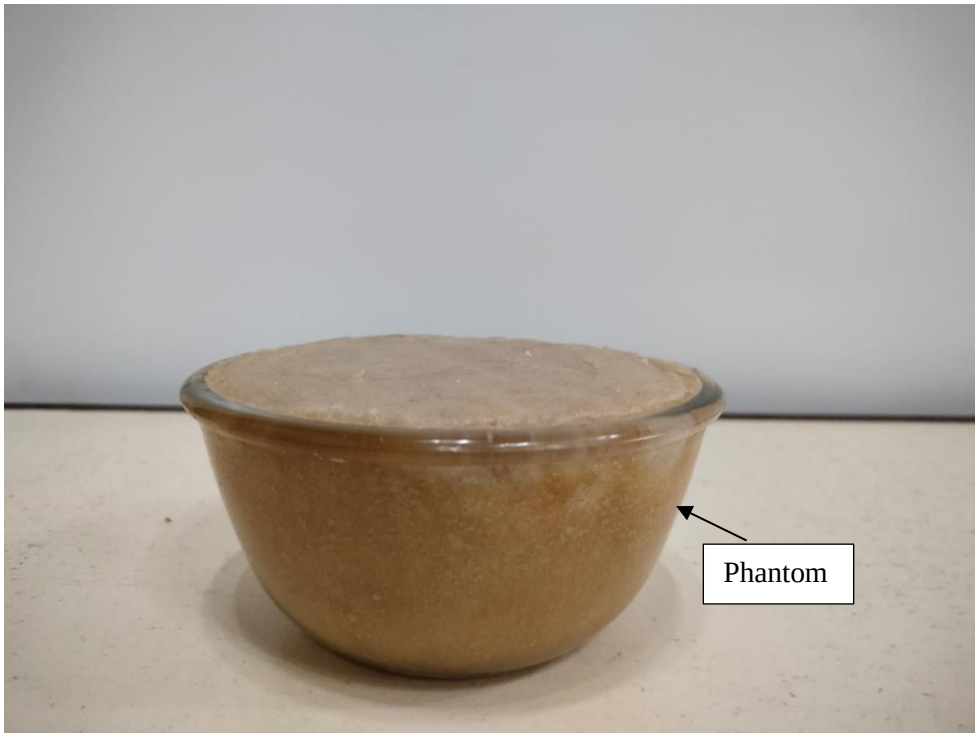

Figure 4.13 Breast phantom

Petroleum jelly, olive oil, wheat flour, and water are the materials chosen for the development of the breast phantom, as reported in the aforementioned literature. Breast phantoms can be made with a mixture of petroleum jelly, olive oil, and wheat flour (in that order) and 75% water.

There are two type of phantom one is homogeneous and other is heterogeneous breast phantom.

4.4.1 Homogeneous breast phantom:

In a cup with a 124 mm diameter and a peak height of 55 mm, breast phantoms have been created. A homogeneous breast phantom was created using 65 % oil. 800 ml-sized breast phantoms were created in order to fully fill the cup. Six hours after creation, the breast phantoms were transformed from top to bottom every half-hour. The goal of the operation is to prevent water from moving toward the phantom's bottom.

4.4.2 Heterogeneous breast phantom:

Fat and fibro glandular tissue combine to form the very diverse breast tissue. Heterogeneous materials include ingredients like water, gelatin, oil (a mixture of kerosene and safflower oil in a ratio of 1:1), and preservatives. Due to changes in oil attention, the dielectric characteristics vary. Higher oil concentrations create compounds with dielectric properties comparable to tissues with lesser water content whereas lower oil concentrations create substances that duplicate excess water-containing tissues [26]. These materials are incredibly cheap to create, can be shaped into any shape, and maintain their high dielectric properties even when in close contact with other heterogeneous materials.

4.4.3 Tumor tissue construction:

The data series procedure makes use of tumors. The following have been applied in the development of the tumors:

1) Water 2) Wheat flour

Wheat flour transforms into malignant when a 10:9 ratio of water to wheat flour is employed to produce tumors. Ninety % of wheat flour is made up of water. At exclusive probability of 55%, 75%, 88%, and 90%, we created tumors, and at 90%, we had outcomes that were almost exactly as we had hoped.

When I placed antenna of phantom, we see the different results like change in S11, gain change, radiation pattern also changes.[30] Here we can see that there is different between in antenna results with phantom and antenna results without phantom. And also, we can see different in gain and radiation pattern as well.

4.5 Measurement of phantom (fabricated)

After developed the phantom we go for the results of the fabricated phantom, skin, fat, tumor, and phantom without tumor etc.

4.5.1 Return Losses of skin.

As above we discuss how to create breast phantom and mentioned percentage of material at table shown above. After build phantom now we check the its results. First of all we measure the results of skin by placed antenna on skin. The electrical properties of skin are almost same as the real breast skin.

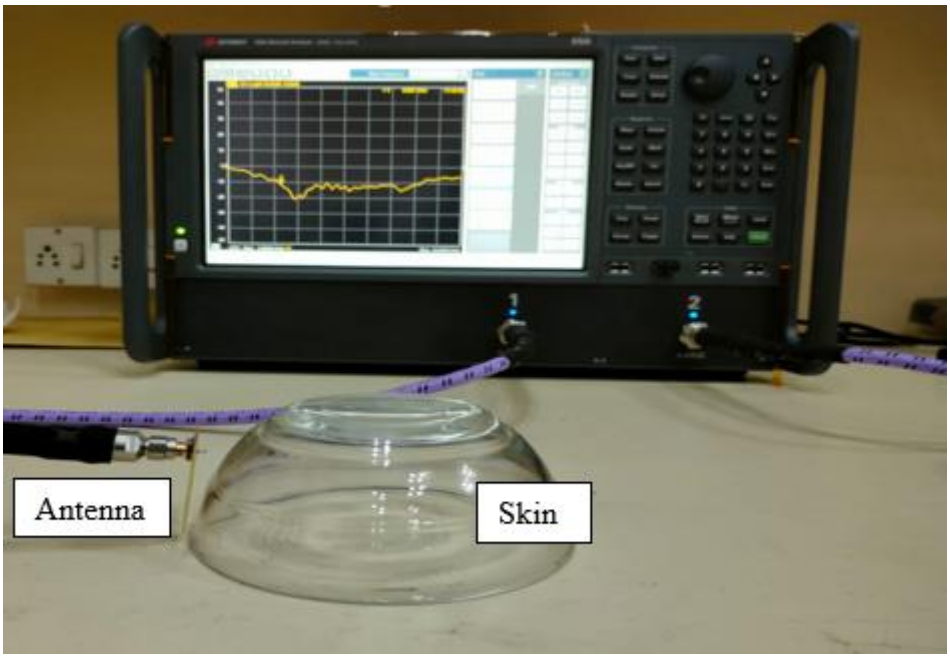

Figure 4.14 Skin tissue analysis

In this way we can calculate the S_{11} of skin tissue.

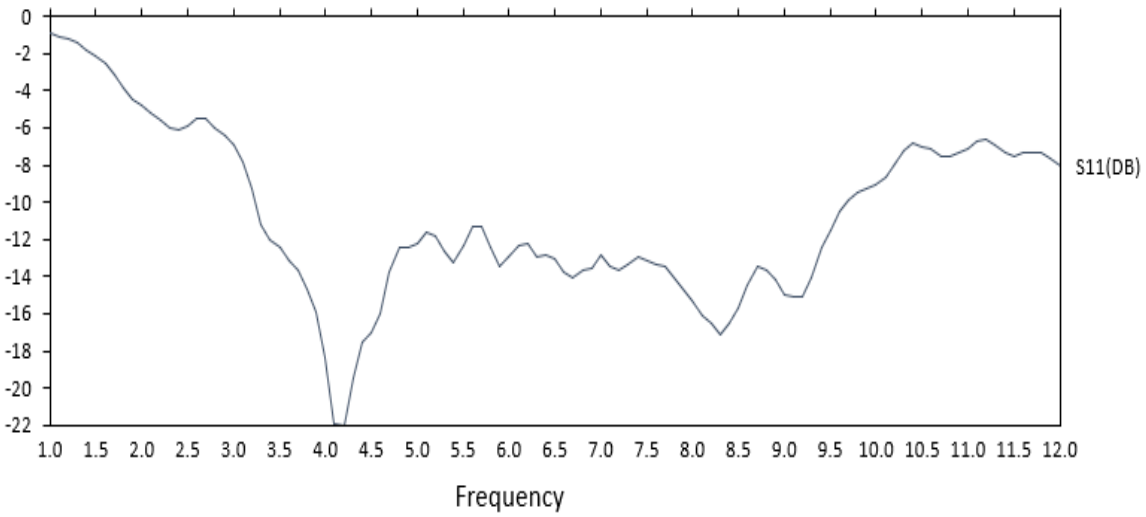

Figure 4.14a S_{11} of Skin

4.5.2 Return Losses of Fat.

As above we discuss how to create breast phantom and mentioned percentage of material at table shown above. After build phantom now we check the its results. Secondly, we measure the results of fat by placed antenna on fat. The electrical properties of fat are almost same as the real breast fat.

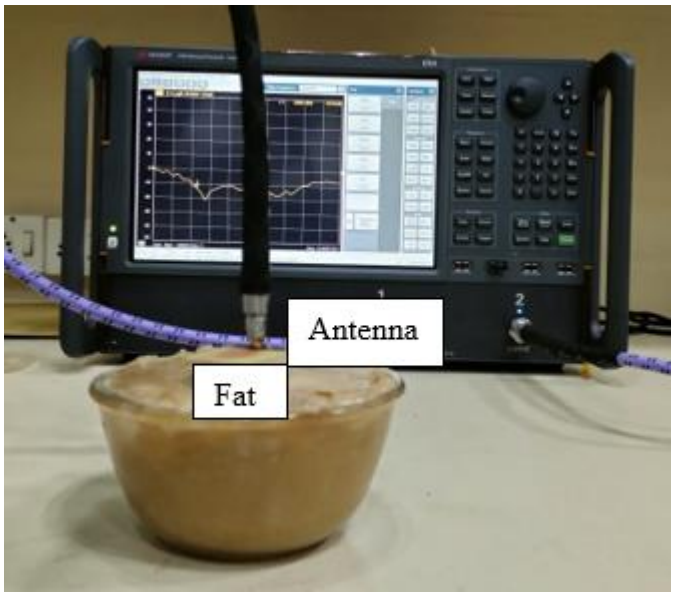

Figure 4.15 Analysis of fat

Now we calculate the return losses of developed phantom

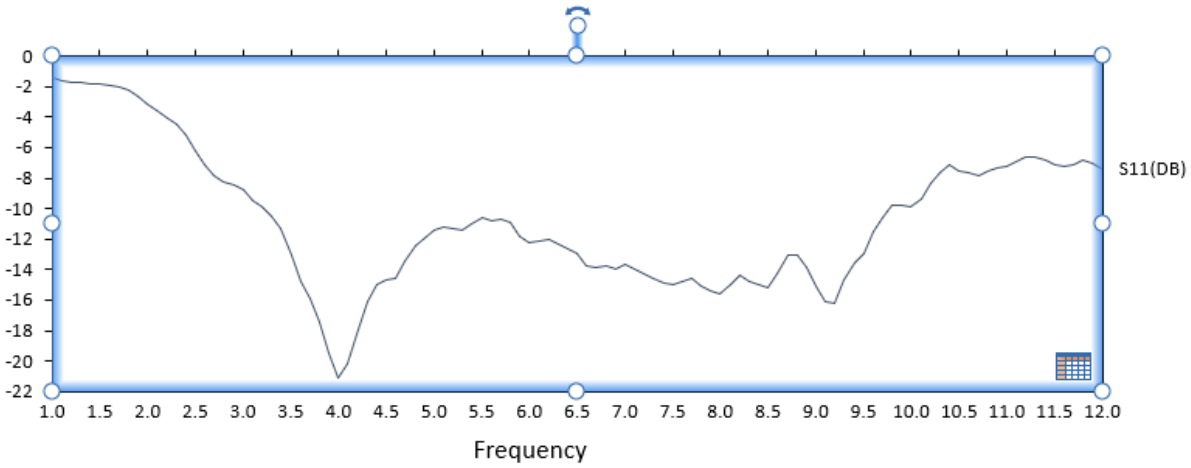

Figure 4.15a S_{11} of fat

4.5.3 Return Losses of phantom.

As above we discuss how to create breast phantom and mentioned percentage of material at table shown above. After build phantom now we check the its results. we measure the results of Phantom by placed antenna on phantom. The electrical properties of skin are almost same as the real breast phantom.

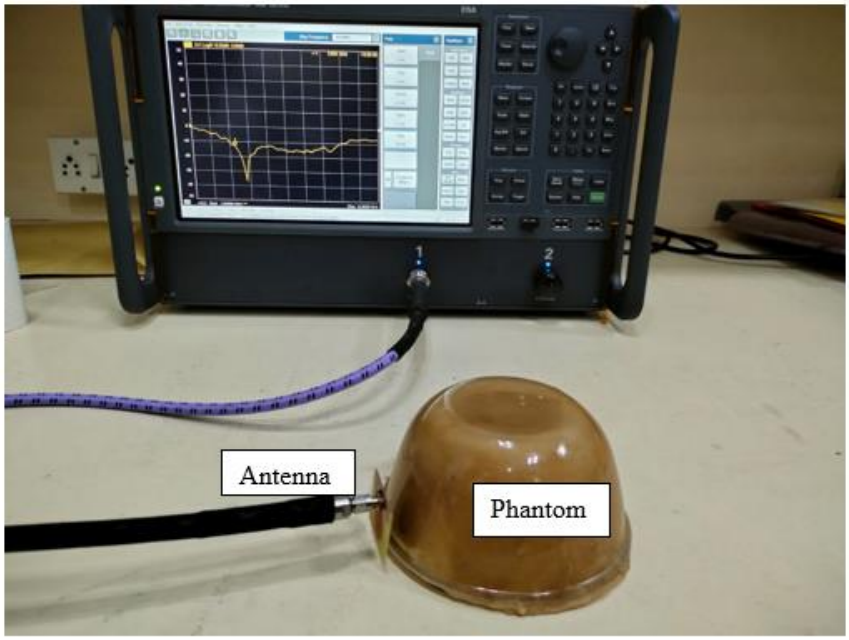

Figure 4.16 Analysis of phantom

Now we calculate the return losses of developed phantom

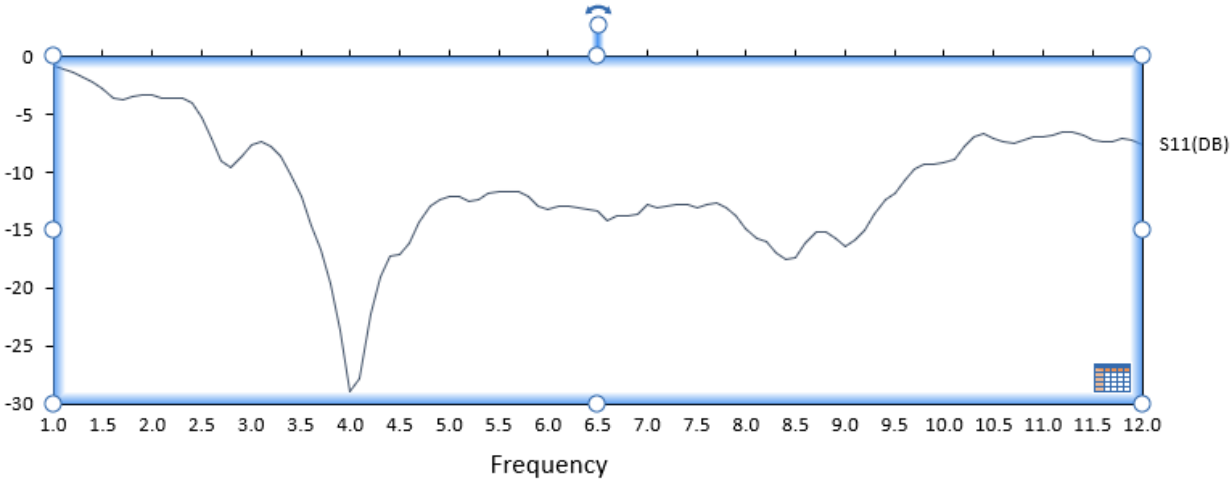

Figure 4.16a S_{11} of phantom

4.5.4 Return Losses of tumor.

As above we discuss how to build a tumor and mentioned percentage of material at table shown above. After build tumor now we check the its results. we measure the results of tumor by placed antenna on tumor. The electrical properties of skin are almost same as the real breast tumor.

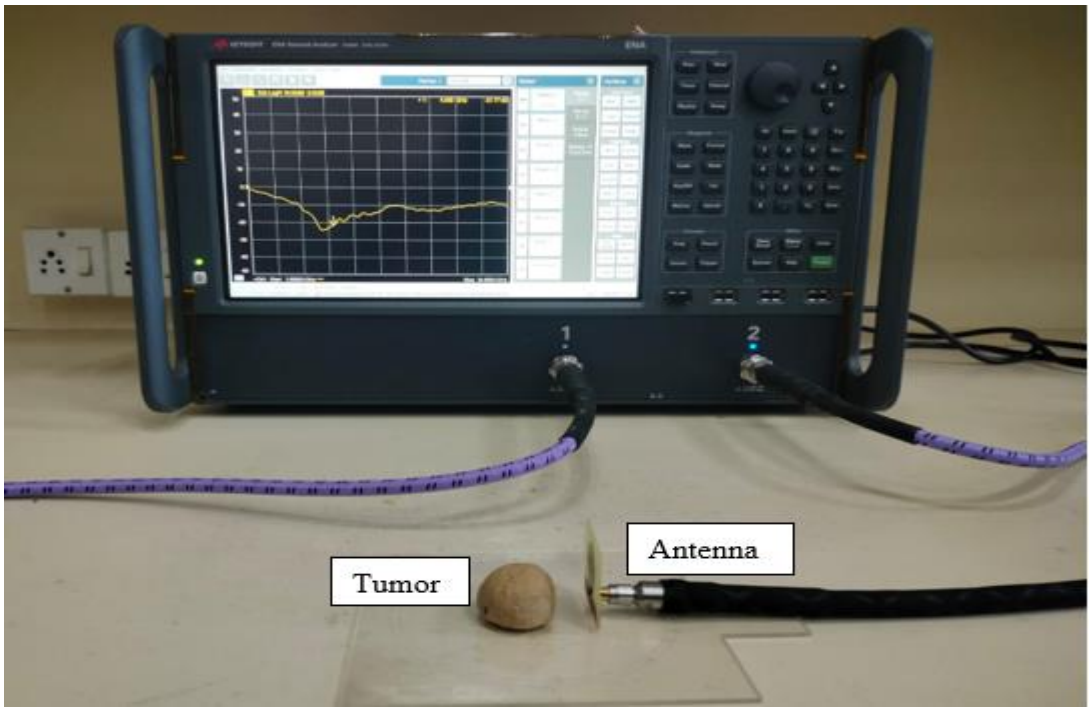

Figure 4.17 Analysis of tumor

Now we calculate the return losses of developed tumor.

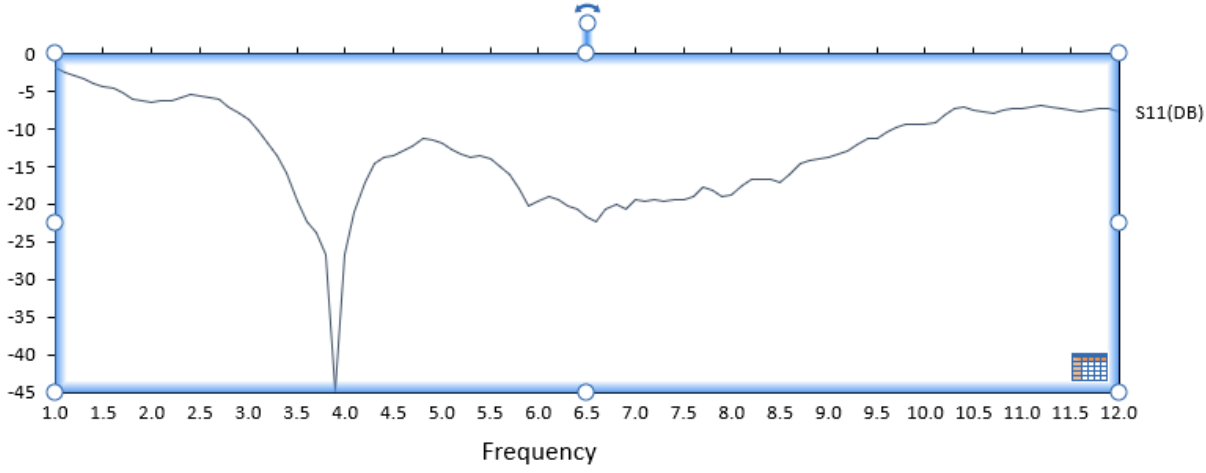

Figure 4.17a S_{11} of tumor

4.5.5 Return Losses of phantom with tumor:

After conducting the different analysis of skin, fat, tumor and simple phantom, we need the measure S_{11} of phantom with tumor that is the last analysis. After put tumor in a specific position in phantom calculate the results of S_{11} of it. You can see the figure 4.18

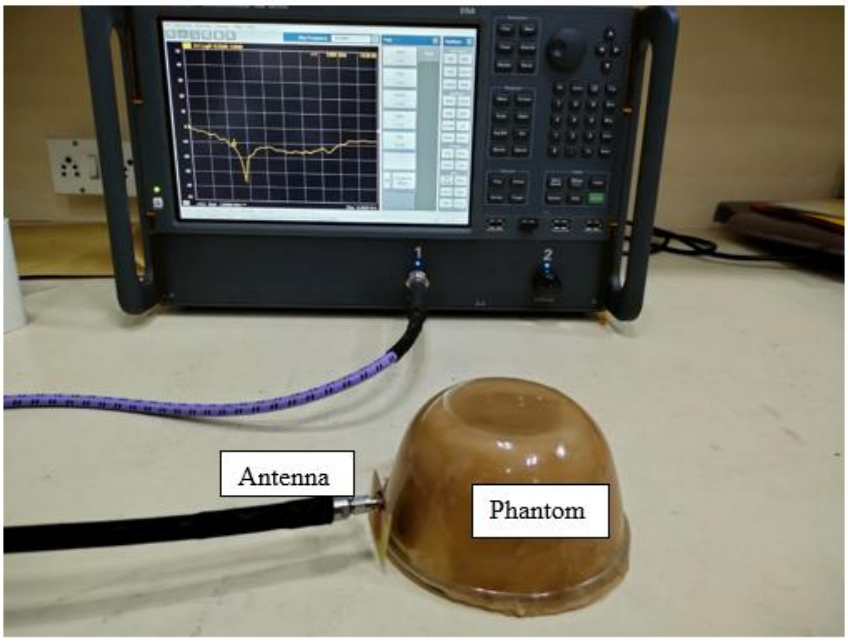

Figure 4.18 Analysis of phantom with tumor

Now we calculate the return losses of developed phantom with tumor

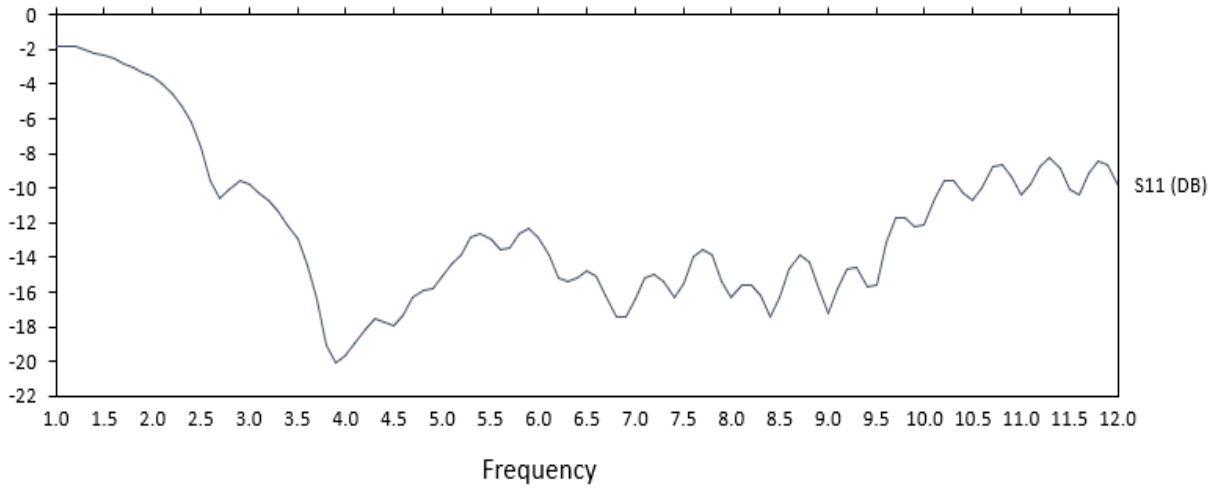

Figure 4.18a S_{11} of phantom with tumor

4.6 Measurement of dielectric constant of phantom:

The breast phantom is situated between two antennas that re facing opposite directions. The measurements in Figure 4.19 were made using an array patch antenna, where one serves as a receiver and the other as a transmitter. The two-array patch antenna that had been attached to the VNA contained the phantom. By positioning the phantom between the transmitter and receiver, the values of the scattering parameters S_{11} and S_{21} have been investigated. Phantom space between the transmitter and receiver became 10 mm and 1 mm, respectively. The dielectric constant of phantom was determined using the S_{11} and S_{21} values of the phantom obtained by VNA. The current artwork uses a series of MATLAB rules to locate the permittivity and permeability using the Nicholson-Ross-Weir approach [7].

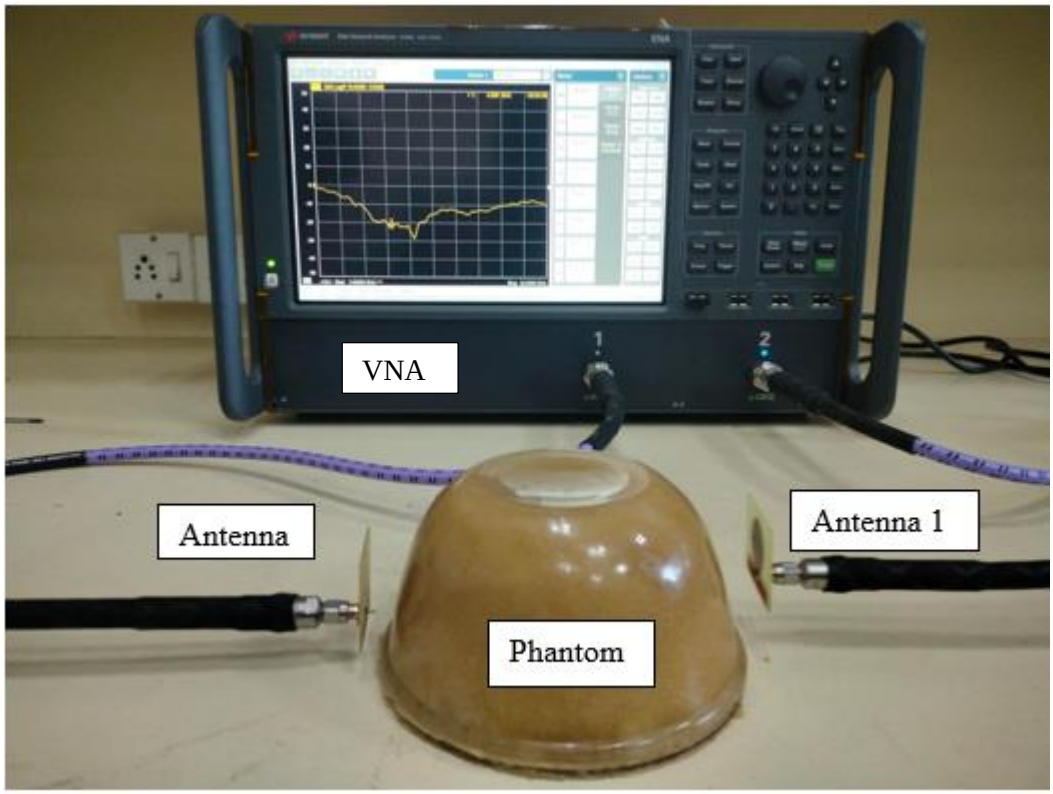

Figure 4.19 Measurement dielectric constant of phantom

When S_{11}, S_{21} values are measured, then it's converted by using the equation.

The following equations lead to the technique that the NRW method proposes:

$$S_{11} = \frac{\Gamma(1-r^2)}{(1-\Gamma^2 r^2)} \qquad \text{and} \qquad S_{21} = \frac{\Gamma(1-r^2)}{(1-\Gamma^2 r^2)}$$

These are the parameters which we obtained from the VNA. The reflection coefficient reduced to such as

$$\Gamma = x \pm \sqrt{x^2 - 1}$$

The root X can be found from

$$X = \frac{S_{11}^2 - S_{21}^2 + 1}{2S_{11}}$$

The transmission coefficients can be calculated as

$$T = \frac{S_{11} + S_{21} - \Gamma}{1 - (S_{11} + S_{21})\Gamma}$$

The permeability can be found as

$$\mu_r = \frac{1+\Gamma_1}{\lambda(1-\Gamma)\sqrt{\frac{1}{\lambda_0^2} - \frac{1}{\lambda_c^2}}}$$

$$\frac{1}{\lambda^2} = \left(\frac{\varepsilon_r * \mu_r}{\lambda_o^2} - \frac{1}{\lambda_c^2}\right) = -\left\{\frac{1}{2\pi L}\ln\left(\frac{1}{T}\right)\right\}^2$$

Where λ_c is cutoff wavelength

The permittivity can be calculated as

$$\varepsilon_r = \frac{\lambda_o^2}{\mu_r}\left[\frac{1}{\lambda_c^2} - \left\{\frac{1}{2\pi L}\ln\left(\frac{1}{T}\right)\right\}^2\right]$$

The phase of the transmission coefficient remains constant as the material's length increases [7]. To clear out this uncertainty, consider how delays through the material relates to the total length of the material. We can calculate group delay as

$$\tau_{cal} = L\frac{d}{df}\sqrt{\frac{\varepsilon_r \mu_r f^2}{c^2} - \frac{1}{\lambda_c^2}} = \frac{1 * f\varepsilon_r\mu_r + f^2 * \frac{1 * d(\varepsilon_r \mu_r)}{2\ df}}{c^2 * \sqrt{\frac{\varepsilon_r \mu_r f^2}{c^2} - \frac{1}{\lambda_c^2}}} * L$$

The measured group delay can be found

$$\tau_{meas} = -\frac{1}{2\pi}\frac{d\phi}{df}$$

4.7 Measurement the dielectric constant of tumor:

Two antennas that are placed at an angle to one another contain the tumor. Two array patch antennas were used to take the measurements; one served as a receiver and the other as a transmitter. The two-array patch antenna that was connected to the VNA when the tumor shifted location. The tumor was placed between the transmitter and receiver to test the values of the scattering parameters S11 and S21. The dielectric constant of the phantom was determined using the S11 and S21 values that were measured using a VNA. The current work uses an algorithm in MATLAB to implement the Nicholson-Ross-Weir approach [7] to determine permittivity and permeability.

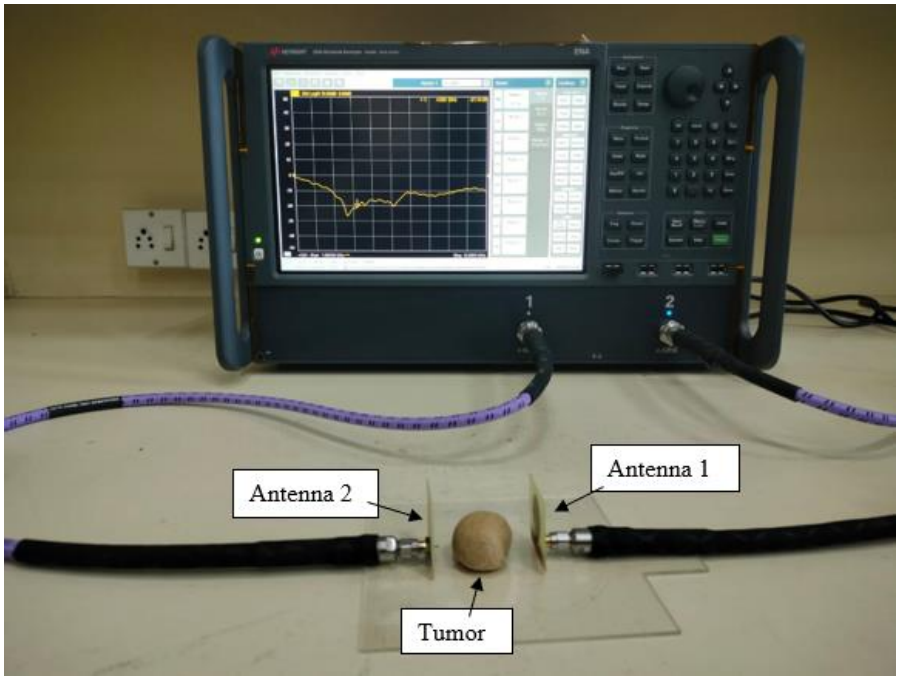

Figure 4.20 Measurement of dielectric constant of tumor

Chapter 5

DETECTION OF TUMOR

5.1 Detection of tumor using microwave imaging technique

5.1.1 Introduction:

Because of a number of benefits, including cheap cost, safe radiation, and convenience of use in comparison to current procedures, the notion of using microwaves for breast cancer screening has drawn substantial attention and examination from various research institutions. X-ray mammography, ultrasound, MRI, and positron emission tomography are current breast imaging methods. Low-power X-rays are used in X-ray mammography [2] to produce pictures of the breast [8]. For the analysis of early breast cancer, it is widely employed. Sound waves are used in ultrasound to examine inside body structure. It has frequencies that exceed 20 kHz. MRI creates images of the inside of the body using radio waves and powerful magnetic fields. This method makes use of the energy that different types of tissues can absorb. A potential new method for early-stage breast cancer diagnosis is microwave imaging. The measurement of electrical characteristics between the tumor and normal breast tissue in the microwave spectrum serves as the foundation for this. By estimating the electric differential between the benign and malignant tissues present inside the breast, microwave imaging is a challenging and successful technique for finding breast cancer tumors.[11] Medical information from reviews of the literature and studies shows that determining the depth of a tumor is crucial for determining its specific identification and the afflicted area.

Studies have shown that tissues with low water content, like fat, have lower permittivity than tissues with high water content, such muscle, skin, the heart, and most other tissues. While conductivity indicates how much of the signal is lost (dissipated) or muted (absorbed) as it goes through the tissue, permittivity assesses how well the tissue can save microwave power. It's essential to understand the electrical characteristics and

inhomogeneities of the female breast in order to construct more accurate or realistic breast phantoms that may be used to test the effectiveness of any microwave imaging technique for most cancers' prediction and detection. The two methods used in microwave imaging are microwave tomography imaging and radar-based imaging. On this thesis, we made use of tomography imaging technology.

5.1.2 GPR Technique:

A real-time technique that uses high-frequency radio waves and produces rapidly recordings with extremely high resolution. GPR uses electromagnetic waves that move at a certain speed that is defined by the material's permittivity [37]. Due to the variation in electric households, prices will vary depending on the kind of fabric and will thus respond at different times [25–26]. Series of lines are obtained along a survey line as antenna move beside it. The ground penetrating radar (GPR) set of criteria is therefore successfully applied to determine the precise depth of cancerous tissue. GPR was initially intended for archaeological studies, evaluating building conditions, finding subsurface mines, and other purposes.[13] For a growing image of the breast tissue, radar is employed. The device allows for the rapid impulse transfer from the antenna onto breast tissue. The sign processing method is utilized to acquire the backscattered signal. Essentially, it then identifies the affected element, a malignant tumor, as a highly scattering region. Here, however, there were attempts to employ GPR for radar-based breast cancer detection. [14, 29,] The suggested UWB antenna's simulated bandwidth ranges from 3.4 GHz to 10 GHz. [15] The GPR algorithm uses the reflection of electromagnetic waves caused by variations in the dielectric properties to calculate the depth of the tumor. Before to using a depth migration technique, the backscattered signal needs go through processing procedures including Artesian form transformation, Hermitian sign processing, and Inverse fast Fourier transform (IFFT) to convert positive frequency records into time-domain data. The migrated image that is created following

the migration procedure contains the intensity's specifics [37]. The outcome demonstrates that the GPR algorithm has been demonstrated to be successful in detecting tumors embedded inside the breast tissue. A combination of flour and water-petroleum jelly is used in a partner experimental assessment to determine the efficacy of this imaging subject. From 3.4 GHz to 10 GHz, the recorded electric powered resistance statistics measure the UWB antenna levels.

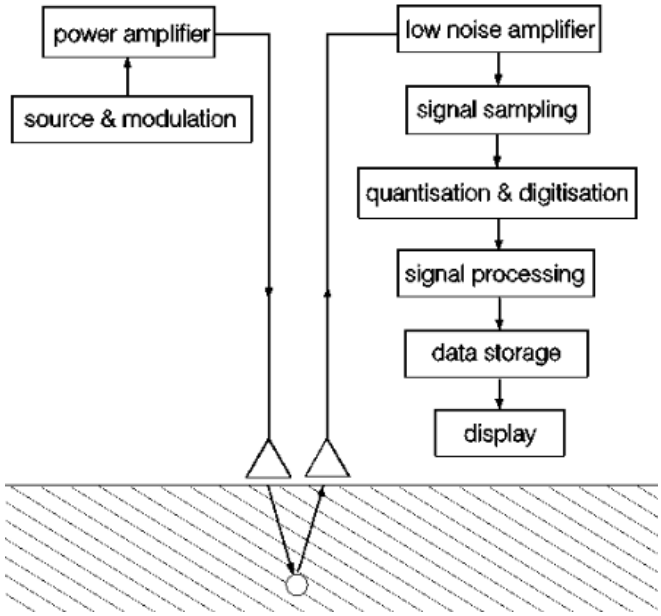

Figure 5.1 block gram of GPR Technique

The strength and expansion of the tumor are measured using a variety of imaging techniques and algorithms. To determine the tumor's intensity, scientists use a variety of techniques like the Microwave Imaging via Reference Body (MIST) beamforming rule, Parallel Plate Conductor Port approach, Time of Arrival (TOA) data fusion approach, delay, and total beamforming rule, etc. On the other side, the most effective solutions have a lot of limitations. Boom detection requires complex antenna array configuration and designing an extremely wideband (UWB) antenna is challenging.

5.1.3 Principle of Microwave Imaging:

By employing the microwave imaging technology, we will successfully locate the target tumor's location. The microwaves that were backscattered might be used to complete this. According to the straightforward concept of microwave imaging, when a microwave arrives at a point with a high dielectric constant from a position with a much lower dielectric constant, the microwaves are dispersed. Figure unquestionably illustrates the fundamental idea of microwave imaging [14]. He same antenna that broadcasts the microwaves may be used to collect them after they are spread. As a result, the antenna

serves as both a receiver and a transmitter.

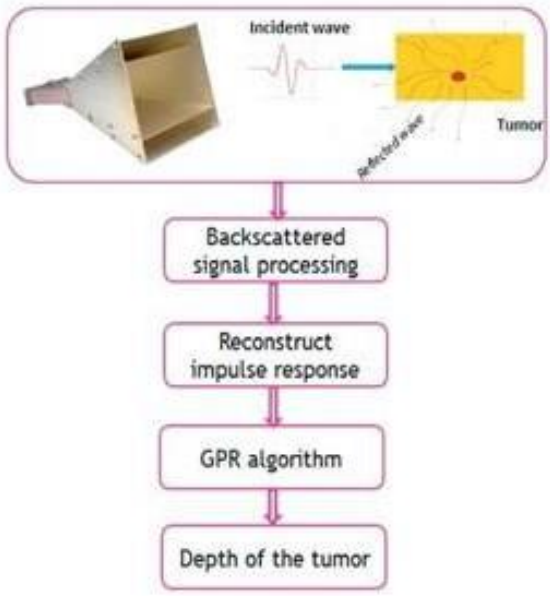

Figure 5.2 Flow chart of Microwave Brest Imaging

The processing of these microwaves leads to the creation of an image. This depiction actually makes a distinction between the location and the powerful imagined tumor tissue.

5.1.4 Hermitian approach:

According to the Hermitian technique, the real value feature's ft characteristic is symmetric. The frequency f must fulfill Hermitian symmetry since S11(t) is an actual-valued feature.

Despite the fact that the overall frequency (f) spans the range [fstop, fstop], the data from S11 better represents the narrow frequency ranges (f). The frequency ranges with low values are just as pointless as the frequency ranges with high ones. The frequency change from fstart to fstop, which is a property of S11(f) and is essential for creating the impulse feature S11(t), is shown in figure 5.1. (a).. Starting with the frequencies [0, fstart], 0 padding must be implemented as indicated in figure 5.1. (b). Acquired S11 signal, zero-padded signal, complex

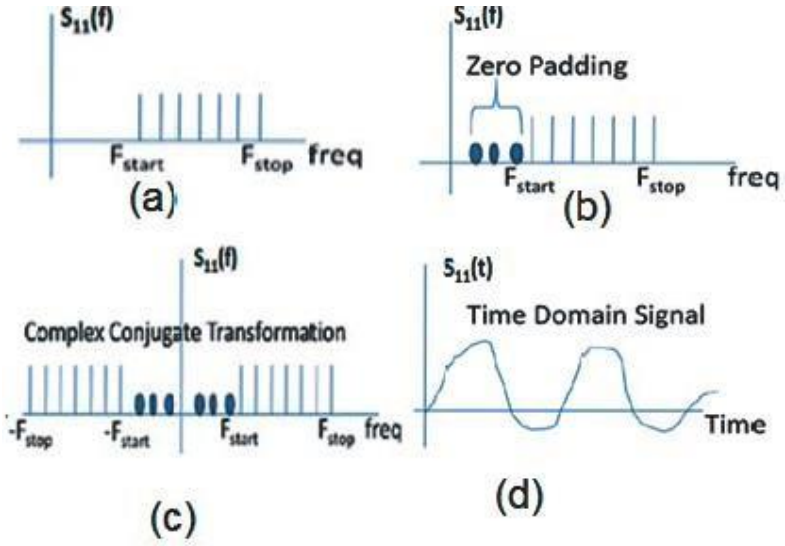

conjugate signal, and S11(t) signal are the first four steps in the pre-processing of backscattered signals. Which shown in figure 5.2 (a), (b). (c). (d) respectively.

Figure 5.2 (a), (b), (c), (d)

The quantity of leading zeros required for zero padding may be calculated using the equation below:

$$\text{Number of zeros to be padded} = \frac{fstart}{\Delta f - 1}$$

5.1.5 Restore Impulse Response:

The Inverse Fourier transform is a reliable method for transforming the time-area-stored time-frequency illustration into the frequency domain-stored backscattered signal. The purpose of this study is to determine, by analysis of the backscattered signal, where the target is located inside the breast phantom. The methods used to modify the impulse response of the reflected

signal are shown in Figure 5.3

Two different categories of meditated alarms are gathered from a breast phantom on the route to measuring the depth of a tumor. The contemplated sign is measured twice: once from a

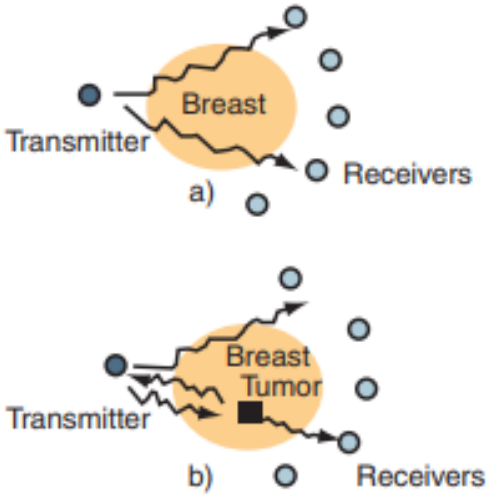

Figure 5.3 working principle

breast that is tumor-free and once from a breast that is healthy. Next, an IFFT and a Hermitian method are used to handle the two backscattered signals [7]. The impulse response of the backscattered signal is obtained by adding the impulse responses of the transmitted signal, the noise disturbance, the antenna move-coupling factors, and the tumor reaction. The tumor reaction component is minimal in relation to the other heritage response. By subtracting the impulse responses of the backscattered sign with and without the tumor, the impulse response caused by the tumor may be improved.

$$S11_d(t) = S11_{wt}(t) - S11_{wot}(t)$$

The backscattered signal with the tumor is represented by the impulse reaction factor S11wt(t), while the backscattered signal without the tumor is represented by S11wot(t) (t).

5.1.6 Backscattered Signal Processing:

Figure 5.4 shows the many stages of a signal's initial processing. A model of the pondering sign in an equal frequency domain is obtained. A temporal representation of records is required for processing radar alerts [31]. We should first do an inverse rapid fourier remodel (IFFT) on S11, which contains effective frequency data, to ascertain the impulse response of the reflected information. The route travelled before the IFFT technique was adopted is shown in figure 5.4.

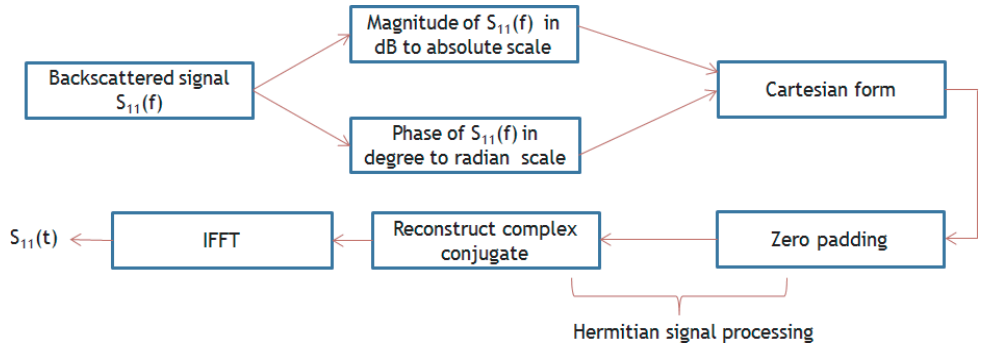

Figure 5.4 Steps for signal pre-processing

An antenna in polar configuration ((f) section (f) will capture a wave that is reflected back to it. The relative dB scale for the meditation sign strength (S_{11}) is changed to an absolute dB scale. Segment restrictions are converted from degrees to radians from the meditated signal. This indicates that the following processing step should employ the Cartesian shape of S11, z = a + bj.

5.1.7 Algorithm of GPR Technique:

A GPR method is used to forecast the depth of the tumor. To identify the target's true function, imaging migration using frequency-wavenumber techniques is performed (F-k). This migration method compares the patient's horizontal position to the windowed backscattered signal [8] to determine the depth of the tumor. As seen in figure 5.3,

[zmin, zmax] here stand for the lowest and maximum depths that must be attained in

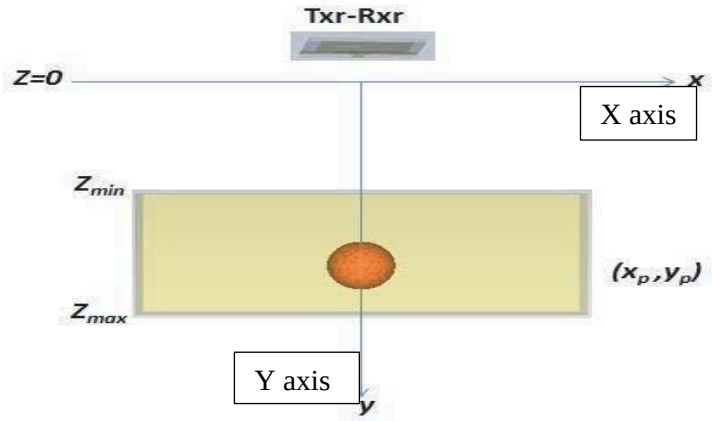

Figure 5.5 depth of tumor

order to achieve the goal. The discrete impulse response in time and depth of the backscattered signal is indicated by S11d (t).

$$\Delta t = 1/fs$$

Let's suppose that fs is the sampling frequency to be more accurate.

$$fs = 3 * fstop$$

$$\Delta d = v * \Delta t/2$$

The electromagnetic wave's velocity, v, is employed in this equation. We will employ the depth decision d to estimate the depth vector at z = (0, 4087). The application of the aforementioned formulae eventually windows the facts. We may discover the 3D architecture of the tumor when the meditated signal is shown as a function of X coordinate.

5.2 Analysis of phantom with and without tumor (experimental results):

When we go for measure the results of phantom with tumor and without tumor, we get both the are different by see the return loss of both phantom. We can clearly see different. First of all, we place antenna a position A of the phantom which does not have tumor and get result of return losses through VNA. After that we place antenna at same position A on phantom which having tumor in it. And get the results of return

losses from VNA at MCS NUST as well.Then we compare both the results then we see the different. See figure 5.6

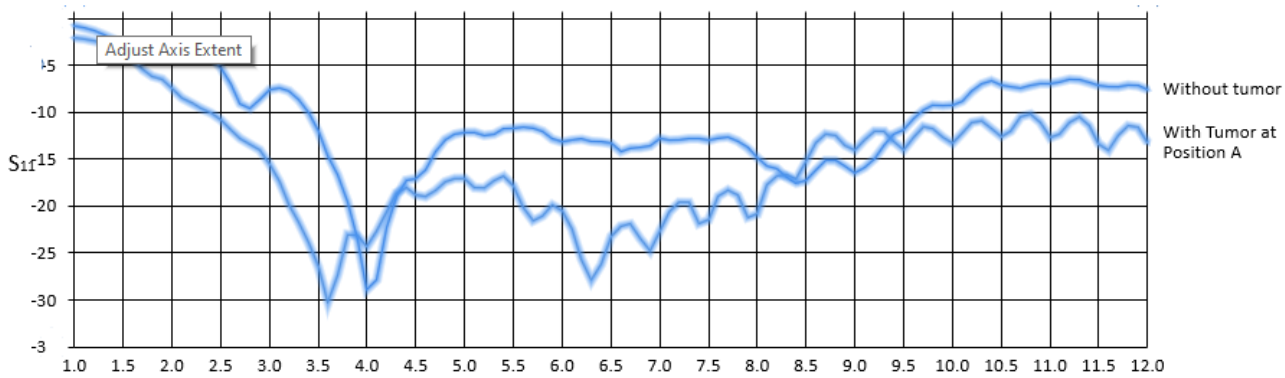

Figure 5.6 Comparison of phantom with tumor and without tumor

That return losses shows that some abnormal behaviors or tissue are present in phantom which are different from healthy one [30].

The next step covers the practical measures for locating the tumor in the phantom. The experimental configuration for the entire device for measuring the desired sign is shown in Figure 5.2. In the experimental inquiry using the breast phantom, the VNA is used to measure the return losses.

The UWB antenna place over phantom and over the location of tumor to get the return losses of tumor better. The measured impedance bandwidth of the microstrip patch antenna covers the frequency range from 3.4 GHz to 10.2 GHz. On the phantom, where it is furthest from the VNA, is the transmitting antenna. The ghost lights from the antenna's microwave signal. The S_{11} properties of the antenna were first measured using phantom. Then, using a tumor within the phantom, we assessed the S_{11} features of the antenna with the tumor. These backscattered parameters are then kept in storage. In addition, we had MATLAB code for a floor penetrating radar (GPR) imaging approach that would produce a picture in MATLAB and help us locate the tumor's precise X and Y coordinates.

5.3 Experimental Analysis of phantom:

For getting results of phantom with tumor and without tumor we place antennas at different positions. Position A, Position B, Position C, Position D, Position E, Position F, and Position G, then we calculate the results of return losses. We gave power to the antennas individually then calculate the results. That results are nearly equal to the simulated one. In this way we can find out the depth of the tumor, if there is tumor is place in it.

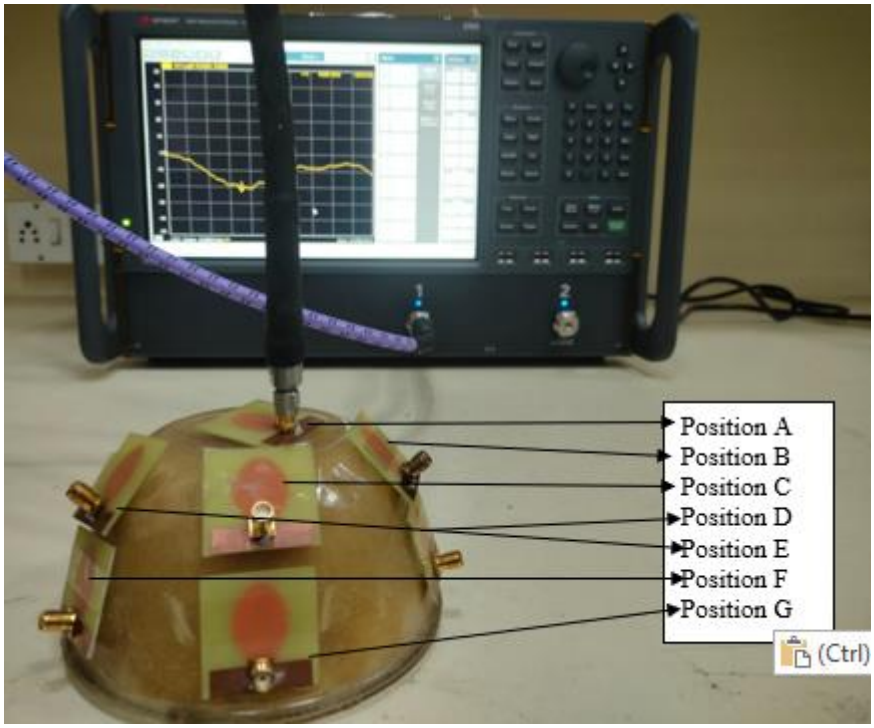

Figure 5.7 Experimental Analysis of Phantom

Then we put these (S_{11}) in mat-lab code which gave us the position of tumor.

5.3 Tumor at position A:

The tumor is first positioned in the phantom in the area seen in fig. 5.7. The antenna that is detecting this tumor is then positioned where it is indicated in the illustration.

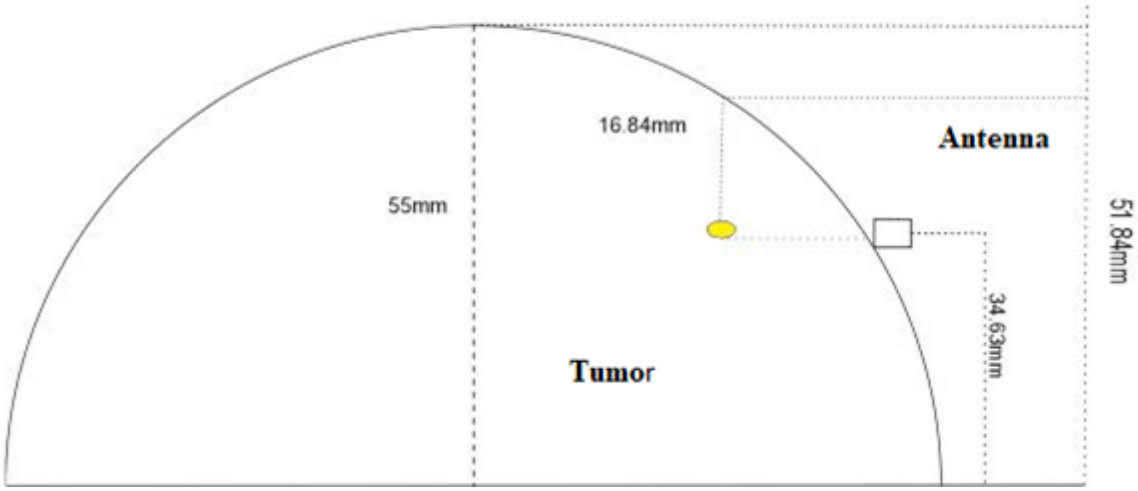

Figure 5.7 Tumor A analysis

Then, at the same position, the go returns losses of the antenna with and without a tumor had been simulated and measured. Figure contrasts the measured and simulated results without the phantom tumor, whereas Figure shows the antenna return losses when the phantom tumor is present.

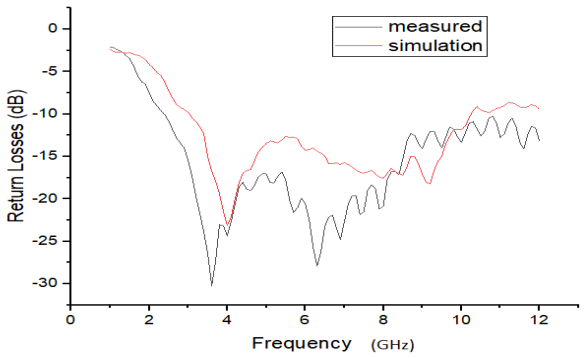

Figure 5.8 Return loss with tumor

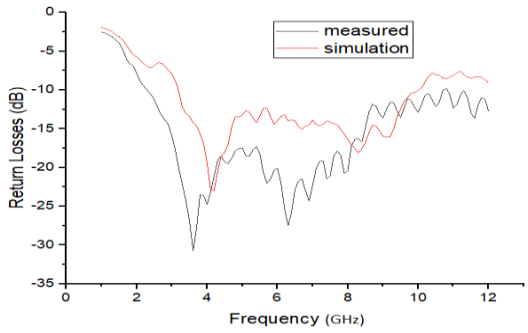

Fig. 5.9 Return loss without tumor

The location of the tumor was then determined by using the GPR Imaging set of rules in MATLAB.Then using MATLAB, we can find the location of the tumor as shown in fig 5.10

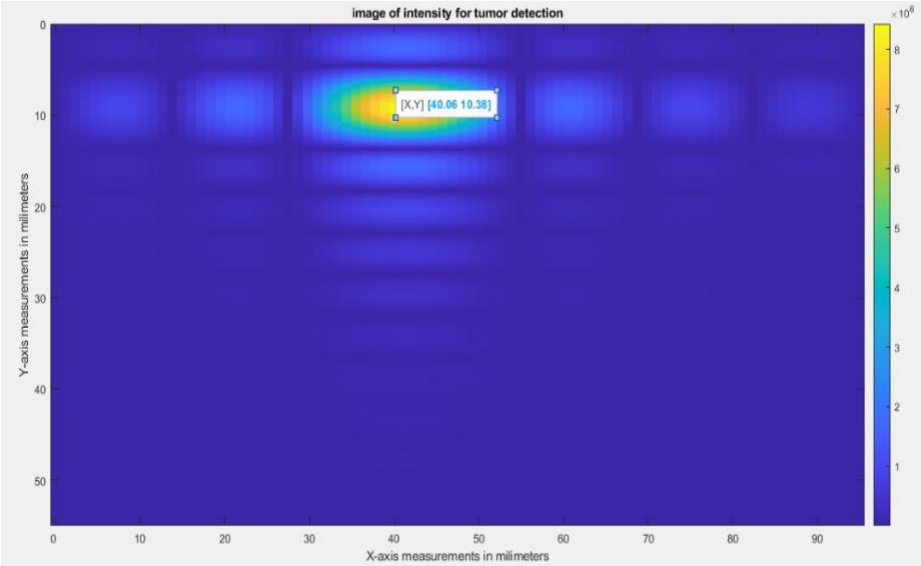

Fig 5.10 Tumor A location

5.2.2 Tumor at position B:

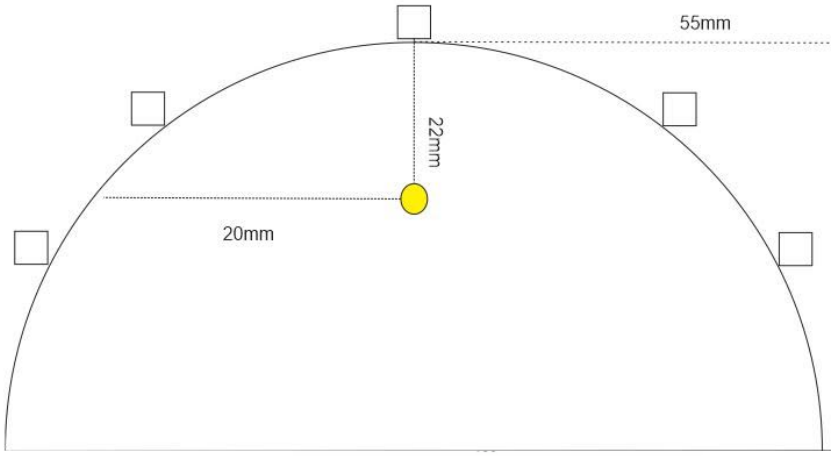

Fig. 5.11 Tumor B analysis

The tumor is positioned in this study at the site depicted in fig. 5.12, and the antenna that will find the tumor is situated there.

The antenna is activated and its simulated and measured return losses of the antenna with and without tumor have been noted. This is done at the same place. Figure 5.14

shows the return losses of the antenna without a tumor in the phantom, and Figure 5.13 compares the measured and simulated values with a tumor.

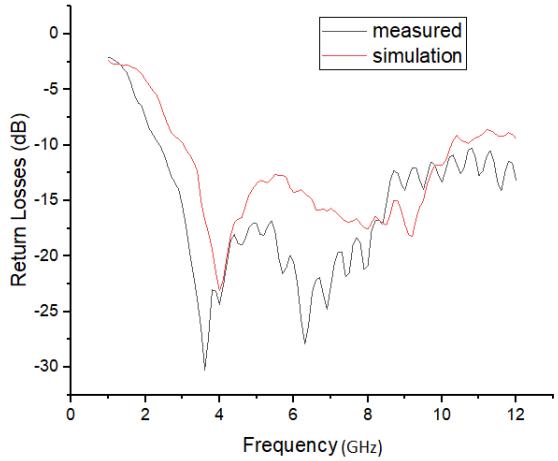

Fig 5.12 Return loss with tumor

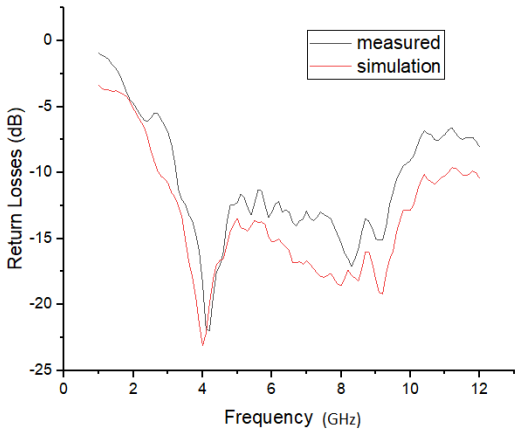

Fig 5.13 Return loss without tumor

Then using GPR Imaging Algorithm, we detected the location of the tumor used in the phantom as shown in fig 5.14.

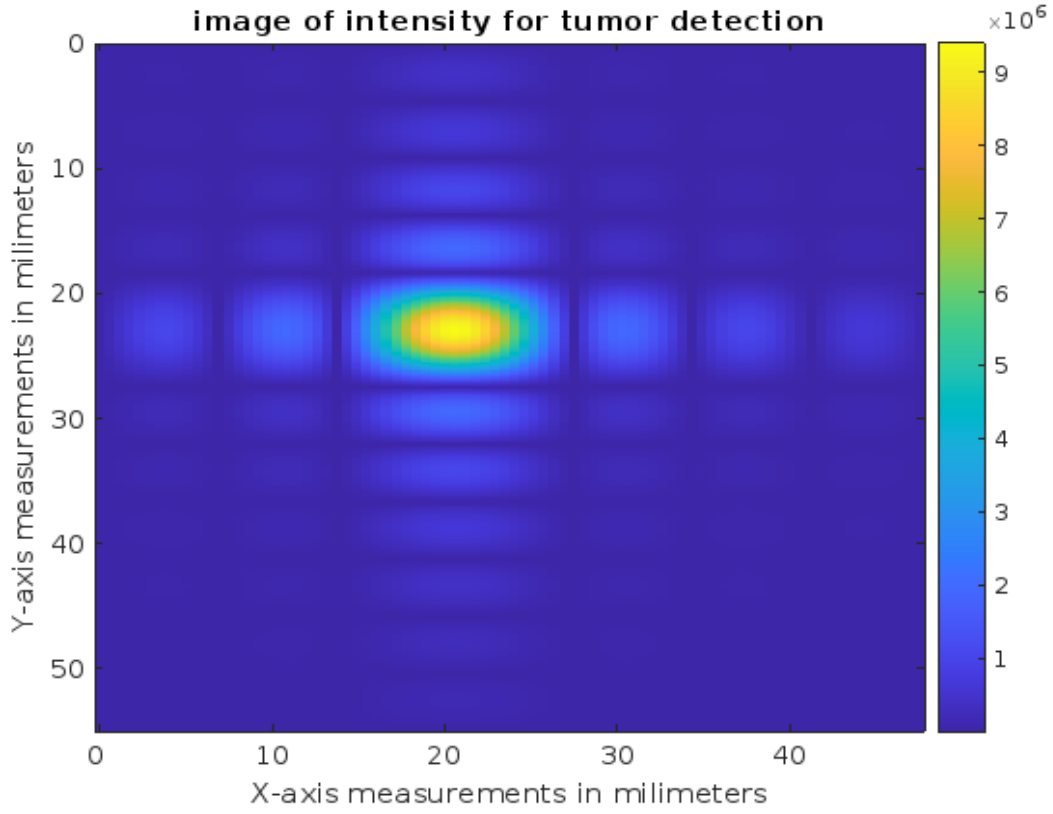

Fig 5.14 Tumor B location

5.3.3 Tumor at position C:

The tumor is positioned in this study at the site depicted in fig. 5.16, and the antenna that will find the tumor is situated there.

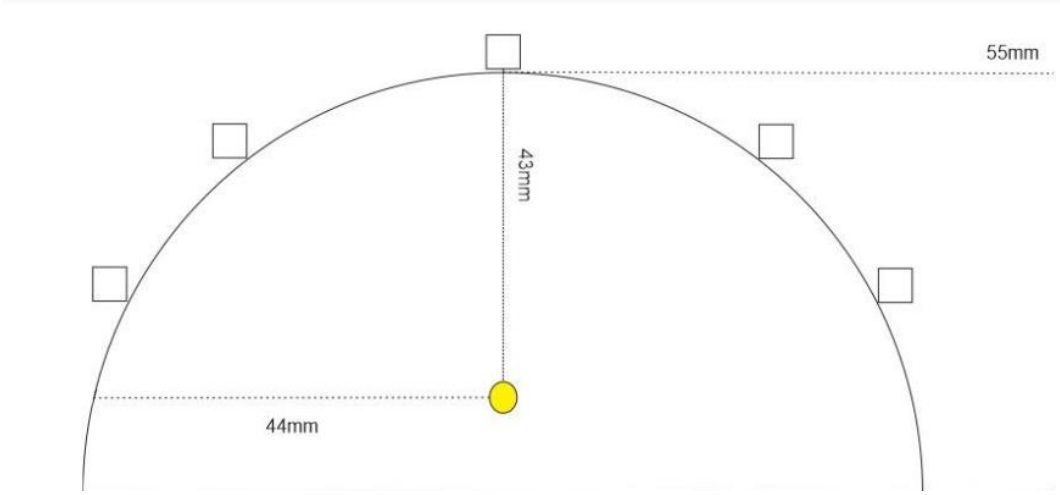

Fig 5.15 Tumor C Analysis

Then, at this site, the antenna's modelled and measured return losses for both the tumor and for the antenna were noted. The return losses of the antenna without a tumor in the phantom are depicted in fig. 5.16, and the measured and simulated results have been contrasted with a tumor in the figure 5.17.

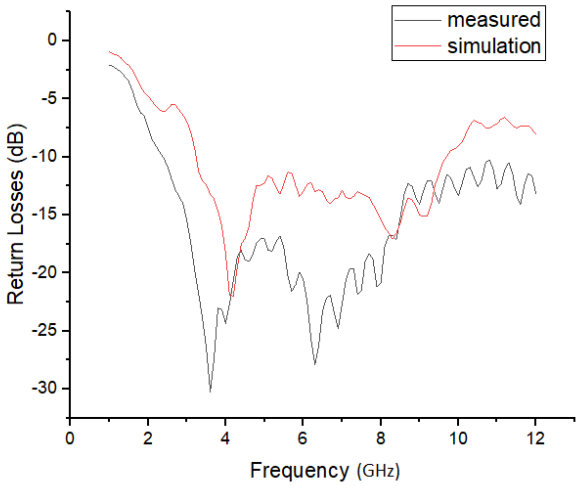

Fig 5.16 Return loss with tumor

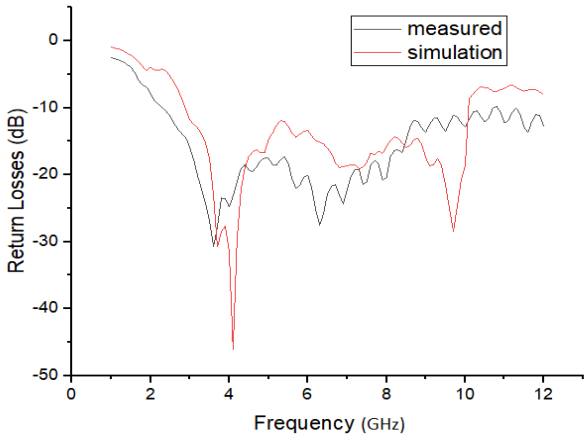

Fig 5.17 Return loss without tumor

Then by MATLAB, we detected the location of the tumor which is shown in fig 5.18

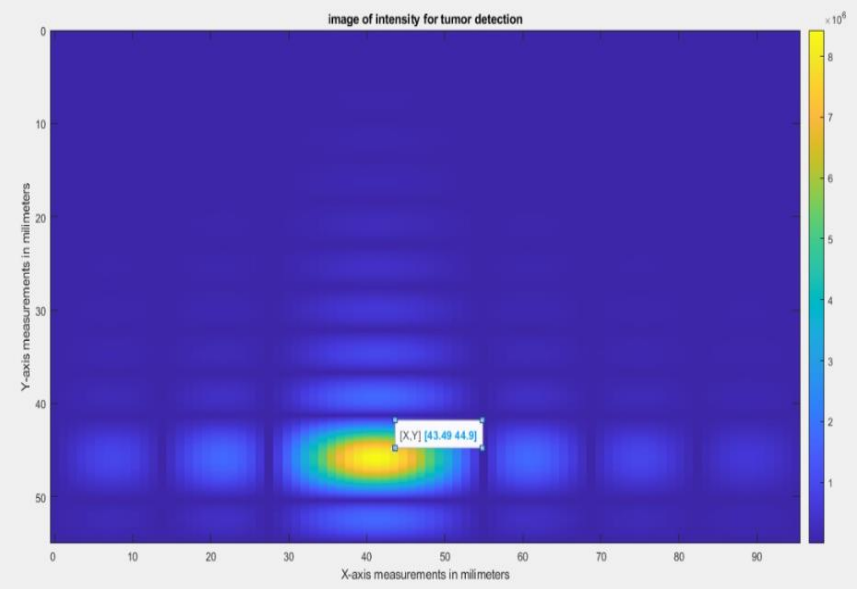

Fig 5.18 Tumor C location

5.5.4 tumor at position D:

The tumor is positioned in this study at the site depicted in figure 5.19, and an antenna with power and a detector for the tumor has been installed at that location.

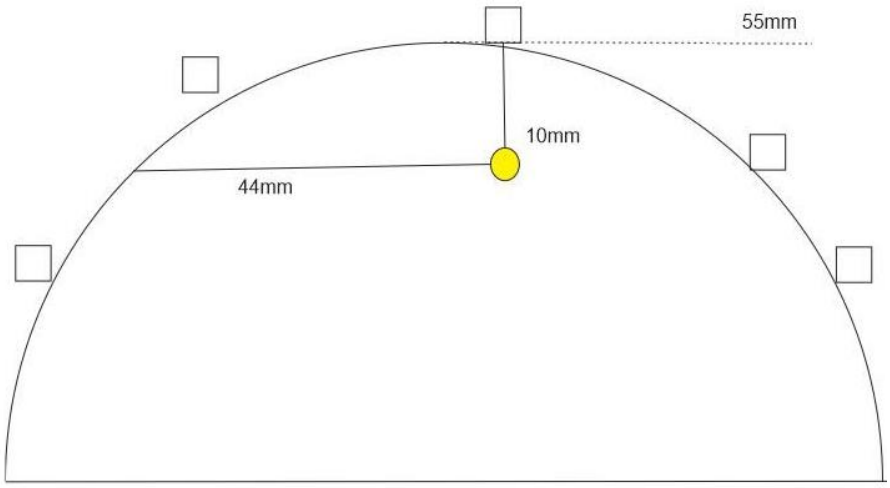

Fig 5.19 Tumor D analysis

Then simulated and measured return losses have been compared with and without

tumor as shown in fig5.20 and 5.21.

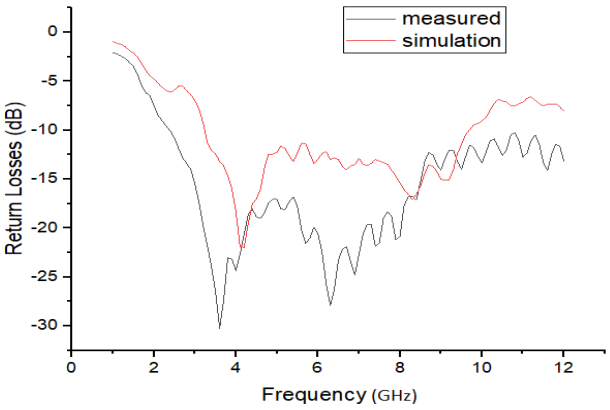

Fig 5.20 Return loss with tumor

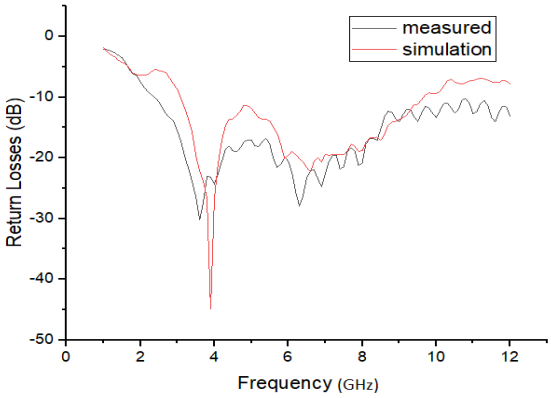

Fig 5.21 Return loss without tumor

Using MATLAB, the location of tumor D obtained is as shown in fig 5.22

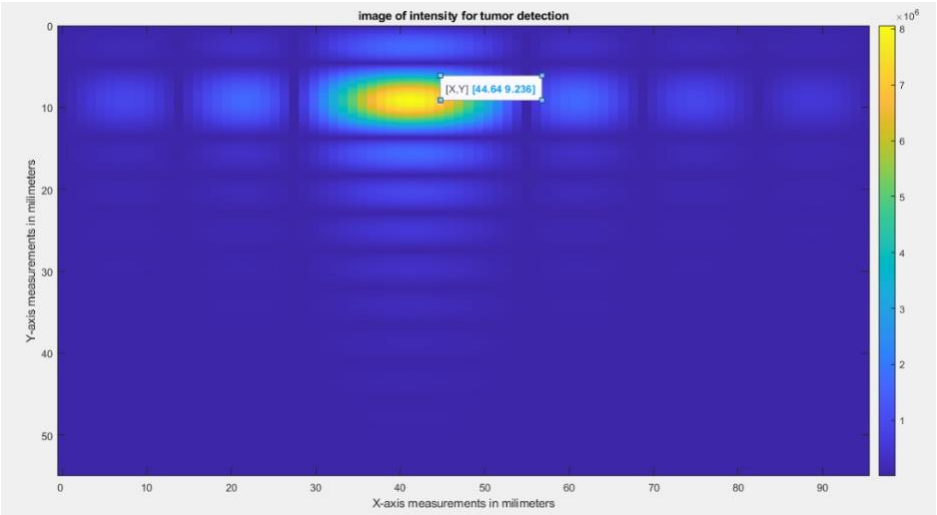

Fig 5.22 Tumor D location

5.5.5 tumor at position E:

Again. The tumor is positioned in this study at the site depicted in figure 5.23, and an antenna with power and a detector for the tumor has been installed at that location. T hen as shown in figs.5.24 and 5.25, measured and simulated return losses were compared with and without tumors in the phantom.

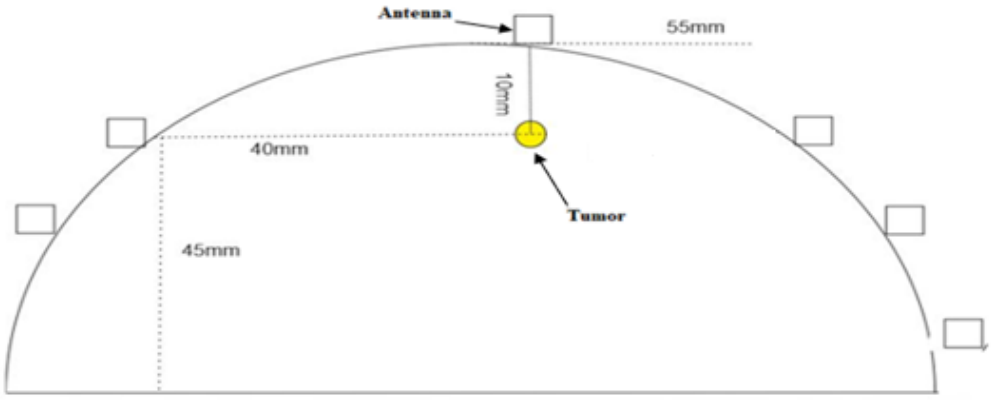

Figure 5.23 tumor at location E

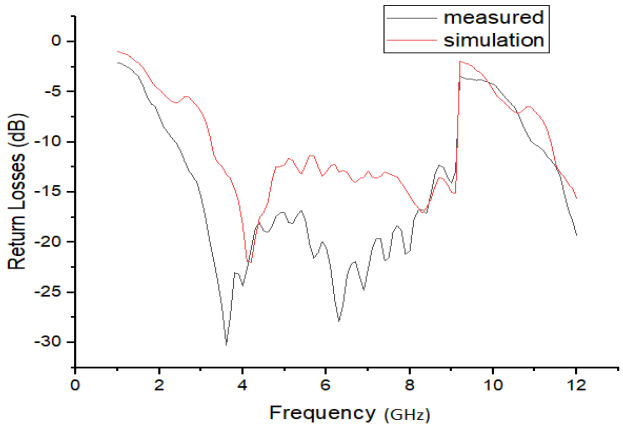

Fig 5.24 Return loss with tumor

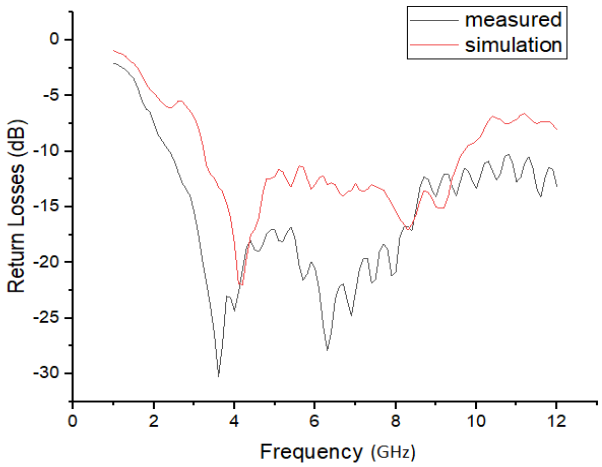

Fig 5.25 Return loss without tumor

The location of tumor G as determined by MATLAB is displayed in figure. 5.26.

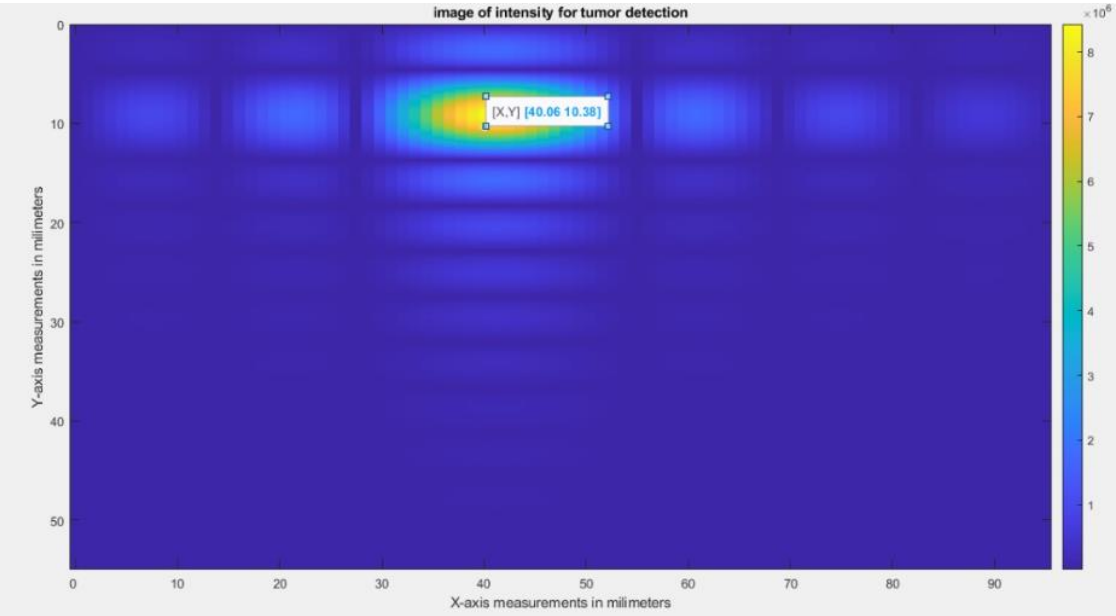

Fig 5.26 Tumor E location

By using GPR technique we can find-out the location of tumor.

Chapter 6

CONCLUSION AND FUTURE WORKS

6.1 Conclusion

Single element UWB antenna on FR-4 lossy substrate material with dielectric constant of 4.4 and thickness of 1mm for the detection of breast cancer tumor has been developed. Frequency band from 3.34 GHz to 10 GHz has been achieved. Four element array antennas have all been develop for the detection of breast cancer tumor. Reflection coefficient of -30dB for the 4-element array at 4.25 GHz has also been achieve. Phantom has been fabricated with the material of wheat flour, water, soy oil and petroleum jelly and similarly the tumor has also been developed with wheat flour and water. The dielectric constant of phantom and tumor has also been measured and is found to be exactly same as published in the literature. Simulation of the phantom and tumor has been achieved on CST and the simulated results are compared with the measured results. Both the simulated and measured results are exactly in accordance with each other. Finally, the Ground Penetrating Radar (GPR) imaging technique has been implemented for the detection of the tumor. Code of GPR for our scenario has been developed. After developing the code for GPR technique, the technique has been implemented for the detection of breast cancer tumor in phantom. The image has been located and been tested by placing the tumor at different location within the phantom. All the measured results of the imaging technique are found to be in accordance with the simulated results.

6.2 Future Works:

The Ultrawide band flexible antenna is being suggested for the future work. The UWB antenna can be designed on the flexible substrate and can be used for the detection of cancer tumor applying the same GPR imaging Technique.

REFERENCES

[1] Yahya Rahmat-Samii, Fellow, IEEE, and Arthur C. Densmore Member, IEEE "Technology Trends and Challenges of Antennas for Breast Cancer detectionSystems" IEEE Transactions on Antennas and Propagation, Feb. 2014.

[2]. Heywang-Köbrunner, Sylvia H., Astrid Hacker, and Stefan Sedlacek. "Advantages and disadvantages of mammography screening." *Breast care* 6, no. 3 (2011):

[3]. Song, H., Kubota, S., Xiao, X. and Kikkawa, T., Design of UWB antennas for breast Cancer detection. IEEE, International Conference on Electromagnetic in Advanced Applications (ICEAA), 978–1–4673-9810-7, 2016.

[4]. Morrow, Monica, Janet Waters, and Elizabeth Morris. "MRI for breast cancer screening, diagnosis, and treatment." 1804-1811." International Journal of Electronics, Electrical and Computational System, Volume 7, pp 1804-1811; February - 2011.

[5] Kavitha, A., and J. N. Swaminathan. "Design of flexible textile antenna using FR4, jeans cotton, and Teflon substrates." Microsystem Technologies, Volume 25, pp 1311-1320, Dec 2019.

[6] F. Alsharif, S. Safi, T. AbouFoul, M. Abu Nasr, S. S. Abu Naser, "Mechanical Reconfigurable Microstrip Antenna", International Journal of Microwave and Optical Technology, vol.11, no.3, pp.153-160, 2016.

[7] S. K. Davis, B. D. Van Veen, S. C.Hagness, and F. Kelcz, "Breast tumor characterization based on ultrawideband microwave backscatter," IEEE Transactions on Biomedical Engineering, vol. 55, no. 1, pp. 237–246, 2008.

[8] W. T. Joines, Y. Zhang, C. Li, and R. L. Jirtle, ''The measured electrical properties of normal and malignant human tissues from 50 to 900 MHz,'' Med. Phys., vol. 21, no. 4, pp. 547–550, 1994.

[9]. El Fatimi, Aziz, Seddik Bri, and Adil Saadi. "UWB antenna with circular patch for early breast

cancer detection." *TELKOMNIKA (Telecommunication Computing Electronics and Control)* 17, no. 5 (2019).

[10] Hammouch, Nirmine, and Hassan Ammor. "Smart UWB antenna for early breast cancer detection." *ARPN journal of engineering and applied sciences* 13, no. 11 (2018).

[11] Amdaouch, Ibtisam, Otman Aghzout, Azzeddin Naghar, Ana Vazquez Alejos, and Francisco J. Falcone. "Breast tumor detection system based on a compact UWB antenna design." *Progress In Electromagnetics Research M* 64 (2018): 123-133.

[12]. A. Eesuola, Y. Chen, G. Y. Tian, "Novel ultra-wideband directional antennas for microwave breast cancer detection", 2011 IEEE International Symposium on Antennas and Propagation (APSURSI), pp.90-93, 2011.

[13] Jamlos, Mohd Aminudin, et al. "Tumor detection via specific absorption rate technique using ultra-wideband antenna." *IOP Conference Series: Materials Science and Engineering*. Vol. 557. No. 1. IOP Publishing, 2019.

[14] C. Kissi, M. Särestöniemi, T. Kumpuniemi, M. Sonkki, S. Myllymäki, M. N. Scrifi, et al., "Directive low-band UWB antenna for in-body medical communications", *IEEE Access*, vol. 7, pp. 149026-149038, 2019.

[15] F. Alsharif and C. Kurnaz, "Wearable Microstrip Patch Ultra Wide Band Antenna for Breast Cancer Detection", *2018 41st Int. Conf Telecommun. Signal Process. TSP 2018*, pp. 456-459, 2018.

[16] Lazebnik, Mariya, Leah McCartney, Dijana Popovic, Cynthia B. Watkins, Mary J. Lindstrom, Josephine Harter, Sarah Sewall et al. "A large-scale study of the ultrawideband microwave dielectric properties of normal breast tissue obtained from reduction surgeries." *Physics in medicine & biology* 52, no. 10 (2007):

[17]. Bahrami, H., E. Porter, A. Santorelli, B. Gosselin, M. Popović, and L. A. Rusch. "Flexible sixteen antenna array for microwave breast cancer detection." *IEEE Transactions on biomedical engineering* 62, no. 10 (2015).

[18]. Porter, Emily, Hadi Bahrami, Adam Santorelli, Benoit Gosselin, Leslie A. Rusch, and Milica

Popović. "A wearable microwave antenna array for time-domain breast tumor screening." *IEEE transactions on medical imaging* 35, no. 6 (2016):

[19]. Craddock, I. J., M. Klemm, J. Leendertz, A. W. Preece, and R. Benjamin. "Development and application of a UWB radar system for breast imaging." In *2008 Loughborough Antennas and Propagation Conference*, pp. 24-27. IEEE, 2008.

[20]. Kuwahara, Yoshihiko, and A. M. Malik. "Microwave imaging for early breast cancer detection." *New Perspect. Breast Imaging* (2017).

[21]. Fernández, María García, Yuri Álvarez López, Ana Arboleya Arboleya, Borja González Valdés, Yolanda Rodríguez Vaqueiro, Fernando Las-Heras Andrés, and Antonio Pino García. "Synthetic aperture radar imaging system for landmine detection using a ground penetrating radar on board a unmanned aerial vehicle." *IEEE Access* 6 (2018).

[22]. . Chen, Y., E. Gunawan, K. S. Low, S. C. Wang, C. B. Soh, and L. L. Thi, "Time of arrival data fusion method for two-dimensional ultrawideband breast cancer detection," IEEE Transactions on Antennas and Propagation, Vol. 55, No. 10, 2852–2865, 2007.

[23]. Mendat, C. C., D. Mislan, and L. Hession-Kunz, "Patient comfort from the technologist perspective: Factors to consider in mammographic imaging," International Journal of Women's Health, Vol. 9, 359, 2017.

[24]. Lazebnik, Mariya, Dijana Popovic, Leah McCartney, Cynthia B. Watkins, Mary J. Lindstrom, Josephine Harter, Sarah Sewall et al. "A large-scale study of the ultrawideband microwave dielectric properties of normal, benign and malignant breast tissues obtained from cancer surgeries." *Physics in medicine & biology* 52, no. 20 (2007).

[25]. Susila, J. Joyselin, and H. Riyaz Fathima. "A slot loaded rectangular microstrip patch antenna for breast Cancer detection." *International Research Journal of Engineering and Technology (IRJET)* 4, no. 4 (2017).

[26]. Sill, Jeff M., and Elise C. Fear. "Tissue sensing adaptive radar for breast cancer detection—Experimental investigation of simple tumor models." *IEEE Transactions on Microwave theory and Techniques* 53, no. 11 (2005).

[27]. Y. Q. Zhang, S. T. Qin, and L. X. Guo, “Novel broadband bow-tie antenna with high-gain performance using electromagnetic coupling feed,” International Journal of RF and Microwave Computer-Aided Engineering, vol. 29, no. 1, Article ID e21478, 2019.

[28]. O'Halloran, M., M. Glavin, and E. Jones, "Rotating antenna microwave imaging system for breast cancer detection," Progress In Electromagnetic Research, Vol. 107, 203-217, 2010.

[29] Ghassemi, Pejman, T. Joshua Pfefer, Jon P. Casamento, Rob Simpson, and Quanzeng Wang. "Best practices for standardized performance testing of infrared thermographs intended for fever screening." *PloS one* 13, no. 9 (2018).

[30] Köşüş, Nermin, Aydın Köşüş, Müzeyyen Duran, Serap Simavlı, and Nilgün Turhan. "Comparison of standard mammography with digital mammography and digital infrared thermal imaging for breast cancer screening." *Journal of the Turkish German Gynecological Association* 11, no. 3 (2010):

[31] Lai, J. C., C. B. Soh, E. Gunawan, and K. S. Low, “Homogeneous and heterogeneous breast phantom for ultra-wideband microwave imaging applications,” Progress In Electromagnetic Research, Vol. 100, pp. 377–415, 2010

[32] Craddock I.J, Preece A Leendertz, J Klemm, M Nilavalan and Benjamin R. “Development of a hemispherical wideband antenna array for breast cancer imaging”. European Conference on Antennas and Propagation, pp. 1-5, 2006.

[33] Aziz, Abdul, Dhrubo Ahmad, Taslima Akter Shila, Sohel Rana, Raja Rashidul Hasan, and Md Abdur Rahman. "On-body circular patch antenna for breast cancer detection." In 2019 IEEE international electromagnetics and antenna conference (IEMANTENNA), Volume 7, pp. 029-034, 2019.

[34] M. Ur Rashid, A. Rahman, L. Chandra Paul, J. Rafa, B. Podder and A. K. Sarkar, "Breast Cancer Detection & Tumor Localization Using Four Flexible Microstrip Patch Antennas", in International Conference on Computer, Communication,

Chemical, Material and Electronic Engineering (IC4ME2-2019), Rajshahi, Bangladesh, 2019

[35] Ortega-Palacios Rocío, Lorenzo Leija, Arturo Vera, and M. F. J. Cepeda. "Measurement of breast-tumor phantom dielectric properties for microwave breast cancer treatment evaluation." International conference on electrical engineering computing science and automatic control, pp. 216-219, 2010.

[36] Lazaro, Antonio, David Girbau, and Ramon Villarino. "Wavelet-based breast tumor localization technique using a UWB radar." *Progress In Electromagnetics Research* 98 (2009).

[37] Lestari, A. A., D. Yulian, L. A. B. Suksmono, E. Bharata, A. G. Yarovoy, and L. P. Ligthart, Improved bow-tie antenna for pulse radiation and its implementation in a GPR survey, 2007 4th International Workshop on Advanced Ground Penetrating Radar, 197-202, June 2007.

Appendix – A: Matlab Code for dielectric constant of phantom

```
clear all; clc;
close all;
S21_amp = [ -15.59, -15.59];
S21_phase = [ -125.05, -125.05];
S11_amp = [ -36.79, -36.79];
S11_phase = [ -56.79, -56.79];
C = 3e10;  % Velocity of light in free space in m/s Freq_vec
=2e9:0.5e9:6e9;  % Frequency zone of Operation

for k = 1: length (Freq_vec)
  Freq = Freq_vec(k)
    lamda0 = C./Freq;  % Free Space Wavelength
%lamda0 = C./Freq;              % Free Space Wavelength
lamdaC =30 ;
    L = 0.4e-3;  % Sample length in centimeter
  % Starting of the calculation...
% Stage - 1 : Calculation of S11 & S21 S11
    = -15.59*exp(1j*-125.50*pi/180);
    S21 = -36.79*exp(-1j*56.79*pi/180);
% Stage - 2 : Calculation of various relevant parametersX
    = ((S11.^2)-(S21.^2)+1.0)./(2.*S11);
    Y1 = X + sqrt((X.^2)-1.0);
      Y2 = X - sqrt((X.^2)-1.0);
for ii = 1:length(Y1)if
abs(Y1(ii)) >= 1
```

```
        Y(ii) = Y2(ii);
else
        Y(ii) = Y1(ii);
end
   T = (S11+S21-Y.')./(1.0-((S11+S21).*Y.'));
   Z=  log(1./T)
```

Appendix – B: Matlab code of dielectric constant of tumor

```
%% Calculation of Mu & Epsilon from Data file
% Development Date : 18.04.2020
clear all; clc;
close all;
S21_amp = [ -21.64,-21.64];
S21_phase = [ 158.05,158.05];
S11_amp = [ -19.36, -19.36];
S11_phase = [ -151.64, -151.64];
C = 3e10;   % Velocity of light in free space in m/s Freq_vec
=2e9:0.5e9:6e9;  % Frequency zone of Operationfor k =
1:length(Freq_vec)
   Freq = Freq_vec(k)
   lamda0 = C./Freq;  % Free Space Wavelength
%lamda0 = C./Freq;              % Free Space Wavelength
lamdaC =30 ;
   L = 0.4e-3;  % Sample length in centimeter
% Starting of the calculation...
% Stage - 1 : Calculation of S11 & S21 S11
```

```
    = -21.64*exp(1j*158.05*pi/180); S21 = -
    19.36*exp(-1j*151.64*pi/180);
% Stage - 2 : Calculation of various relevant parametersX
    = ((S11.^2)-(S21.^2)+1.0)./(2.*S11);
    Y1 = X + sqrt((X.^2)-1.0);
    Y2 = X - sqrt((X.^2)-1.0);
for ii = 1:length(Y1)if
abs(Y1(ii)) >= 1
            Y(ii) = Y2(ii);
%           disp(ii)
else
            Y(ii) = Y1(ii);
end
end
    T = (S11+S21-Y.')./(1.0-((S11+S21).*Y.'));
    Z=  log(1./T)
    Q =-(((Z)./(2*pi*0.5)).^2);
    R = sqrt(Q);
    O=((1+Y.')/(1-Y.'))
    I = sqrt((1./lamda0.^2)-(1./lamdaC.^2));
Mu_eff(k) = (R.*O)./(I)
Eps_eff(k) = (((Q+(1./(lamdaC).^2))).*((lamda0).^2))./(Mu_eff(k))
end
plot(Freq_vec,real(Mu_eff))
xlabel('Frequency');
ylabel('real. Mu');
```

```
figure
plot(Freq_vec,imag(Mu_eff))
xlabel('Frequency');
ylabel('Imag. Mu');
figure
plot(Freq_vec,real(Eps_eff))
xlabel('Frequency');
ylabel('real. Eps');
figure
plot(Freq_vec,imag(Eps_eff))
xlabel('Frequency');
ylabel('Imag. Eps');
    Q =-(((Z)./(2*pi*0.5)).^2);
    R = sqrt(Q);
    O=((1+Y.')/(1-Y.'))
    I = sqrt((1./lamda0.^2)-(1./lamdaC.^2));
Mu_eff(k) = (R.*O)./(I)
Eps_eff(k) = (((Q+(1./(lamdaC).^2))).*((lamda0).^2))./(Mu_eff(k))
end
plot(Freq_vec, real(Mu_eff))
xlabel('Frequency');
ylabel('real. Mu');
figure
plot(Freq_vec,imag(Mu_eff))
xlabel('Frequency');
ylabel('Imag. Mu');
```

```
figure
plot(Freq_vec,real(Eps_eff))
xlabel('Frequency');
ylabel('real. Eps');
figure
plot(Freq_vec,imag(Eps_eff))
xlabel('Frequency');
ylabel('Imag. Eps');
```

Appendix – C: Matlab code of imaging.

```
%%
% loading data of sparameters in Matlab and extracting parameters
Data1=sparameters('WOT1.s1p'); % s1p parameters without tumor
Data1_1=Data1.Parameters; % extracting parameters from s1p file of tumor
Data1_1=ifft(Data1_1); % converting frequency domain into time domain
Data2=sparameters('WT.s1p'); % s1p parameters with tumor
Data2_1=Data2.Parameters;   % extracting parameters from s1p file of without tumor
Data2_1=ifft(Data2_1); % converting frequency domain parameters into time domain
Frequency=Data1.Frequencies; % getting out the frequency from parameters which is
      eventually same for both
% tumor data and without tumor data
%%
% * |converting sparameters into tables| *
options = delimitedTextImportOptions("NumVariables", 3);
options.DataLines = [13, Inf];
options.Delimiter = "\t";
options.VariableNames = ["Frequency", "Magnitude", "Phase"];
```

```
options.VariableTypes = ["double", "double", "double"];
Data1 = readtable("WOT1.s1p", options);
Data2 = readtable("WT.s1p", options);
Data1_1=Data1.Frequency; %freq
Data1_1=[Data1_1,Data1.Magnitude]; % Mag
Data1_2=[Data1.Frequency,Data1.Phase]; %phase
Data2_1=Data2.Frequency; %freq
Data2_1=[Data1_1,Data2.Magnitude]; % Meg
Data2_2=[Data2.Frequency,Data2.Phase]; % phase
writematrix(Data1_1,"Data1_1.txt",'Delimiter','\t')
writematrix(Data1_2,"Data1_2.txt",'Delimiter','\t')
writematrix(Data2_1,"Data2_1.txt",'Delimiter','\t')
writematrix(Data2_2,"Data2_2.txt",'Delimiter','\t')

%% _ | Windowning -Hamming window| _


 %reducing the level of side lobe using    Windowing
number_rows = 201;
number_columns = 2; % number of antennas
%Window option % Hamming window
% in the prescene of hamming window
W=hamming(201);
% with presence of hamming window
W1 = zeros(number_rows,number_columns);
% without presence of hamming window
W2 = zeros(number_rows,number_columns);
```

```
%%
% * _ |finding without tumor signal strenth| _ *
W1=load('Data1_2.txt');
w1_1=W1(:,1);
[a1,b1]= size(w1_1);
Distance_A = 10;
Locations_x = b1(:)';
Locations_y = a1(:)';
w1_1=w1_1(1:a1,end);
w1_2=W1(:,2);
w1_2=db2mag(w1_2);
w1_2=w1_2(1:a1,end);
w1_3=load('Data2_1.txt');
w1_3=w1_3(:,2);
w1_3=deg2rad(w1_3);
w1_3=w1_3(1:a1,end);
% deleting environmental signals // CALIBRATION
response=w1_1(2)-w1_1(1);
sample_freq=3*w1_1(end);
time=1/sample_freq;
lowfre=fliplr((w1_1(1)-response):-response:0);
signal_1=w1_2.*exp(i*w1_3); lowzeros=length(lowfre);
sig1_2=[zeros(lowzeros,1);signal_1];
sig1_3=flipud(conj(sig1_2(2:end,:)));
signal1=[sig1_2;sig1_3];
%frequency domain to time domain
final1=(ifft(signal1));
```

```
t=(0:length(signal1)-1)*time; t=t';
%%
% * _ |finding with tumor signal strength| _ *
W1=load('Data2_1.txt');
w1_1=W1(:,1);
mag2=W1(:,2);
mag2=db2mag(mag2);
w1_3=load('Data2_2.txt');
w1_3=w1_3(:,2);
w1_3=deg2rad(w1_3);
signal_1=mag2.*exp(1i*w1_3);
sig1_2=[zeros(lowzeros,1);signal_1];
sig1_3=flipud(conj(sig1_2(2:end,:)));
signal2=[sig1_2;sig1_3];
% removing signal with tumor from signals without tumor
final2=(ifft(signal2));
%%
% * _ |removing signal with tumor from signals without tumor to remove clutter| _ *
% of environmenta; factors
%CLUTTER REMOVEL
intensity1=(final2-final1);
 t=t(4:15,:);
intensity1(1:3,:)=0;
intensity1=intensity1(4:15,:); intensity1(4,1)=0;
% creating grid
[X,Y]=size(intensity1);
diff2=zeros(X,1);
```

```
diff3=zeros(X,1);
diff4=zeros(X,1);
%%
% * _ |finding intensity of only tumor signal strength| _ *
for i=1:X
   if intensity1(i)== max(intensity1)
      intensity1(i) = intensity1(i);
   else
      intensity1(i) = 0;
   end
end
intensity=[diff4,diff3,diff2,intensity1,diff2,diff3,diff4];
%intensity is coming from many antennas and also from environmental factors
%in order to make intenisty foucs on one focal point , resampling is
%required
intensity=intensity'; intensity=resample(intensity,12,1);
intensity=intensity'; intensity=resample(intensity,12,1);
%   DISTANCE OF ANtenna FROM EACH  POINT
E = 8;
v = 3e2/sqrt(E);
dx=v*time/2;
%y=0:dx:(length(intensity1)-1)*dx;

%%
% averaging intesnity to focus on one point // SYNTHETIC FOCUSING
intensity=resample(intensity,12,1);
Extracted=abs(intensity)
```

```
%x=linspace(-5,15,10);
y=[0 55]
b = fliplr(y)
x=[0 95]
figure,
imagesc(x,b,Extracted);
set(gca,'XTicklabel',[0, 10, 20, 30, 40, 50, 60, 70, 80, 90])
%set(gca,'YTicklabel',[55, 47.1426, 39.2855, 31.8571, 23.5713, 15.7142, 7.8571, 0])
%p = plot(15,8);
%p.DataTipTemplate.DataTipRows(1).Format = '%g'; % x
%p.DataTipTemplate.DataTipRows(2).Format = '%g'; % y
colorbar;
title('image of intensity for tumor detection')
xlabel('X-axis measurements in milimeters')
ylabel('Y-axis measurements in milimeters')
```